DEPARTMENT OF SCIENCE AND TECHNOLOGICAL INNOVATION,
ALESSANDRIA

PHD IN ENVIRONMENTAL SCIENCES
(INTERNAL WATERS AND AGROECOSYSTEMS)

XXVII CICLE

PhD Thesis

Lagrangian stochastic modelling of the fluctuations of active and passive scalars in turbulent flows.

Author:
Andrea BISIGNANO

Supervisor:
Prof. Enrico FERRERO
Co-Supervisor:
Dr. Luca MORTARINI

January 23, 2015

This thesis is dedicated to my parents Manuela and Raffaele and my girlfriend Valentina who have patiently tolerated me.

”The next great era of awakening of human intellect may well produce a method of understanding the qualitative content of equations. Today we cannot. Today we cannot see that the water flow equations contains such things as the barber pole structure of turbulence that one sees between rotating cylinders. Today we cannot see whether Schrodinger’s equation contains frogs, musical composers, or morality–or whether it does not. We cannot say whether something beyond it like God is needed, or not. And so we can all hold strong opinions either way.”

Richard Feynman in Volume II, Section 41, page 12 of ”The Feynman Lectures on Physics”, 1964.

Abstract

Dynamical systems in nature such as turbulent atmospheric flows exhibit irregular space-time fluctuations on different scales as can be readily noticed in a casual observation of, for example, a plume emanating from a fire or power-station chimney. It is the chaotic nature of turbulence that influences may aspects of our lives, operating at many scales, from the vast to the small. There is a clear need for the ability to make quantitative predictions. Such predictions are, however, extremely difficult. No theory will ever able to predict the exact concentration of a scalar at a particular location and time. All theories of turbulence are statistical theories. Hence the science of turbulence is largely about making statistical predictions of chaotic solutions of the non-liner partial equations (known as Navier-Stokes equations).
The transport of scalar fields by turbulent flows is a common physical phenomenon. The quantification of the fluctuations patterns and their influence on the turbulent mixing of a contaminant for predictability purposes has not yet been achieved. There are many case in which one is interested in the influence of a turbulent velocity field on the distribution of some scalar quantity, say the distribution of temperature, smoke, dye or concentration of a contaminant. If the scalar has no dynamic influence on the flow then it can be referred to as a passive scalar. The scalar is active if the dynamics of the advecting velocity field depends on the transported field. That is, for instance, the case of temperature, affecting the velocity via buoyancy forces.
Models of turbulent dispersion often take a Lagrangian form which provides a natural framework for modelling, for example, dispersion from a point source which is harder to model with an Eulerian approach. Typically, thousands of model particles are followed through a given flow field and statistics such as the mean concentration are calculated from the ensemble of particles. The resolved part of the flow field would, for realistic applications, normally be taken from a numerical weather prediction model while the unresolved part of the motion is modelled by means of random increments to the velocity of the particles. These models, which are known

as Lagrangian stochastic models (LSMs), can be rigorously formulated [Thomson (1987)] have been very successful at reproducing observations. I investigate two different aspects of the scalars fluctuations focused on passive and attive scalars respectively.The major aspects that distinguish buoyant and passive dispersion are that buoyant fluid particles create their own turbulent field in a turbulent environment and the exchange processes should be included in the dynamics. In both the cases, active and passive, I considered the scalar fluctuations in term of the statistical properties of particle trajectories, i.e. using LSMs, from which the field characteristics, i.e the Eulerian description, can be readily obtained.

For the case of active scalar fluctuations, I present a hybrid Lagrangian stochastic model for buoyant plume rise from an isolated source that includes the effects of temperature fluctuations. The model is based on that of [Webster and Thomson (2002)] in that it is a coupling of a classical plume model in a crossflow with stochastic differential equations (SDEs) for the vertical velocity and temperature (which are themselves coupled). The novelty lies in the addition of the latter SDE. The root-mean-square temperature is assumed to be proportional to the temperature difference between the centreline temperature of the plume and the ambient temperature. The constant of proportionality is tuned by comparison with equivalent statistics from large-eddy simulations (LES) of buoyant plumes in a uniform crossflow and constant stratification. The scalar concentration computed from the model is compared with the equivalent LES results and generally compares well both in terms of the height reached by the plumes and their spread. The exception to this occurs when the crossflow velocity becomes very weak. The model is extended to allow for realistic profiles of ambient wind and temperature and the results are compared with LES of the plume that emanated from the explosion and fire at the Buncefield oil depot in 2005.

For the passive case, the prediction of concentration fluctuations of a dilute tracer is considered. Whereas the evaluation of mean concentration field is considered an almost closed matter, concentration fluctuations modelling is still an open argument, especially for models devoted to real turbulence. Modelling concentration fluctuations is fundamental to a great number of practical applications and play an essential role in a great number of environmental issues, such as prediction of air pollution, determination of reaction rates in turbulent chemical reactors, estimation of odour threshold and analysis of turbulent combustion. Only a few models are available to calculate at least the second moment, such as direct numerical simulations (DNSs), large eddy simulation (LES), two particles Lagrangian stochastic models and proba-

bility density function (PDF) models. The available models are subject to limitations such as applicability only in strongly idealised conditions (e.g. two-particles models), very elaborate numerical implementation (e.g. PDF models)and expensive computation (e.g. DNS), reduction of reliability for small-scale turbulence (e.g. LES).
A simple and effective method for predicting higher moments of concentration for stationary release of contaminant is the fluctuating plume model (hereinafter FPM). I use an offline approach of a FPM able to evaluate all the higher order moments of the passive scalars only requiring the knowledge of the first one. In the fluctuationg plume approach the total plume dispersion can be split into two independent components, the meandering barycentre and the relative dispersion. While the meandering motion of the plume centroid has to be modelled, the relative dispersion, taking into account the turbulent mixing and scalar dissipation, can be simply parameterised. Being independent of the method used to obtain the mean concentration field, this approach is an ideal offline tool to predict second and higher order concentration moments. The model adaptability to different kinds of turbulence is shown by comparing its results first with analytical predictions present in the literature for homogeneous turbulence and then with two dispersion experiments in the neutral boundary layers generated by a water and a wind tunnel simulations respectively. The simplicity of the numerical algorithm used to calculate the meandering centroid component makes the model very fast and thus especially suitable for practical applications.

Acknowledgements

A special thank goes to the Institute of Atmospheric Sciences and Climate (ISAC - CNR) of Turin, and expecially to Dr.Domenico Anfossi and Dr.Silvia Trini Castelli for their hospitality. It is a pleasure to thank Dr. Ben Devenish for having hosted me at Metoffice, for his explanations and for his many important suggestions. I offer my sincere appreciation for the learning opportunities provided by the Dispersion Group of the Metoffice and in particular I would like to thank David Thomson and Gabriel Rooney for their useful advices. Finally the most important thanks go to my supervisor Prof. Enrico Ferrero and my co-supervisor Dr. Luca Mortarini. I would never have been able to produce this work without their guidance, I cannot express enough thanks to them for their continued support and encouragement.

Contents

List of Figures

Introduction

The purpose of thesis is the application and the development of Lagrangian stochastic models (LSMs hereinfater) to investigate active and passive scalars fluctuations in a turbulent flow both in idealised (homogenous,) and real (inhomogeneous) conditions. In chapter §I, I introduce the mathematical tools used in the statistical description of turbulence, as mean values, correlation function and spectral functions in chapter 1 and the Lagrangian description of turbulence in chapter 2. Then I introduce a theoretical framework for the turbulence focused on inhomogeneous turbulent flows since they represent the real conditions of the atmosphere. Equations for velocity and temperature correlations, spectra and structure functions are considered in chapter 3 and section 3.3 for isotropic turbulence, and in chapter 4 locally isotropic turbulence along with the Kolmogorov similarity hyphoteses. In chapter 5 I describe the Lagrangian modelling and in particular the Lagrangian single particle model (hereinafter SPM). For phenomena such as the turbulent transport or the material surface deformation in a turbulent flow the Lagrangian framework is almost a natural choice. The Lagrangian approach consists in following the motion of fixed fluid particles from a certain initial time. With fluid particle a fluid volume whose linear dimensions are far bigger than the mean distances between the molecules is meant. In other words a fluid particle is a point of the fluid volume that is moving inside of it following the equations of fluid mechanics. The Lagrangian description is related to individual fluid elements whose summation produces the total turbulent flow. Typically, thousands of model particles are followed through a given flow field and statistics such as the mean concentration are calculated from the ensemble of particles. The resolved part of the flow field would, for realistic applications, normally be taken from a numerical weather prediction model while the unresolved part of the motion is modelled by means of random increments to the velocity of the particles. The most exhaustive work about LSMs is due to [Thomson (1987)] who proposed a complete theory for the one-particle dispersion in 3D turbulence based on

the concept of Markovian stochastic process. i.e. a process were present is correlated to past and future to present, but past and future are statistically independent. In this frame, the dynamics of a passive tracer particle is described by a couple of stochastic differential equation: the turbulent increments velocity the Langevin equation and the Fokker-Planck equation, which determines the Eulerian probability density function (PDF) of the stochastic process. In particular [Thomson (1987)] applies the well-mixed constraint to determine the drift term in the Langevin equations from a prescribed form for the Eulerian two-point velocity PDF. The so called well-mixed condition is fundamental constraint that a LSM has to satisfy [Thomson (1987)]. This constraint physically implies that if the particles are initially well-mixed they will remain so during the flow evolution, that the solution of the Fokker- Planck equation are compatible with the Eulerian equations and that direct and inverse diffusion are equivalent. In section 5.2 I analise the previous theories in the context of a rise of a buoyant plume.

In part §II I discuss the application of Lagragian modelling to the active and passive scalars I developed. In chapter 6 I present a hybrid Lagrangian stochastic model for buoyant plume rise. Models of buoyant plumes have a long and successful history originating with the work of [Morton et al. (1956)] and [Priestley (1956)]. These models describe the mean flow of the plume but do not take account of fluctuations in the velocity and buoyancy of the plume. In most realistic dispersion models that are used for operational purposes, as the LSMs, the Lagrangian particles move independently of each other through the flow field. There is then an inherent difficulty in modelling a coherent process such as buoyant plume rise using single-particle LSMs: the motion of individual particles or fluid elements depends on the buoyancy of all the fluid elements. Moreover, there is nothing to constrain two neighbouring model particles to be moving upwards with similar velocities. Several authors have attempted to model buoyant plume rise using a Lagrangian approach (e.g. [Luhar and Britter (1992)], [Anfossi et al. 1993], [Weil (1994)], [Heinz and van Dop (1999)], [Alessandrini et al. (2013)], [Marro et al. (2014)]). Here I consider a hybrid model introduced by [Webster and Thomson (2002)] in which the mean flow is calculated from a simple plume model (as will be described in section 6.1) and the fluctuations are calculated using an LSM. [Webster and Thomson (2002)] only considered fluctuations in the velocity and not the temperature; here I treat both fluctuations of the velocity and temperature. As a buoyant plume rises through a stratified environment, its temperature decreases and will eventually equal the ambient temperature. The momentum of the plume forces the plume to continue rising above

this level until it is eventually brought to rest by the action of the negative buoyancy forces. Accounting for fluctuations in temperature means that the Lagrangian particles will experience different levels of neutral buoyancy. I thus anticipate that the final spread of the plume will be greater than that of a plume in the absence of temperature fluctuations. The stochastic differential equation I consider in section 6.1 is similar to that considered by [van Dop (1992)]. I compare the results of the model with the large-eddy simulations (LES) of [Devenish et al. (2010b)] in section 6.4. I then apply the model to the case of a buoyant plume in a realistic atmosphere in section 6.5 and compare the results with observations.

The prediction of concentration fluctuations in the framework of one-particle Lagrangian stochastic models is an open question. Knowledge of the concentration fluctuations is often required. This is the case, for example, in olfactory research, the chemistry of naturally emitted volatile organic compounds (VOC), as for example anthropogenic VOC, ozone and NOx and the modelling of areleases of toxic, flammable and explosive materials. If the dispersed scalar can be considered non-reactive the methods that account for fluctuations are: the two-particle approach [Thomson (1990)], the meandering plume approach (e.g. [Luhar et al. (2000)], [Cassiani and Giostra (2002)]) and Lagrangian probability density function transport methods (e.g. [Cassiani et al (2005a)]). Among these methods, the two-particle approach seems currently confined to theoretical studies due to the difficulties in parametrizing, or more generally, providing the necessary two-point correlation statistics. The Lagrangian PDF method is more flexible and theoretically allows for the computation of one-point concentration moments of any order. The main shortcoming of this approach, frequently also referred to as the micromixing method [Cassiani et al (2005a)], lies in the demand for every grid element to contain a large number of particles throughout the whole simulation. Recently, very sophisticated new models for concentration fluctuations has been developed. The volumetric particle model proposed by [Cassiani (2012)] does not consider the presence of particles not passing through the source and the micromixing is simulated as a change in volume of the particles originally marked by the source. This approach considerably minimizes the computational simulation time which is the same as a standard one-particle Lagrangian dispersion model. [Kaplan (2013)] introduce an additional particle variable, the conditional average scalar concentration, over the particle's trajectory of a LSM. In contrast to the particle's scalar concentration which is conserved, the conditional average scalar concentration evolves in time. Following past success in modelling the dynamics of concentration variance as a diffusion-advection process, [Manor

(2014)] calculate the concentration variance by assuming an appropriate distribution of effective variance sources for a given mean concentration field.
Nevertheless, all the mentioned models has to be (even easily and naturally) simultaneously implemented as an extension to an existing LS model. In chapter 7 I present a simple and fast offline version of the fluctuating plume model (hereinfater FPM) that does not require any Lagragian simulations. Hence the model is especially suitable for pratical application.
The basic idea of a FPM is that absolute dispersion can be divided into two independent parts: the meandering motion of the barycentre and the relative diffusion around it (see section 7.1). The meandering plume centroid is usually simulated in a fixed coordinate system relative to the source; the internal mixing of the plume, i.e. the relative concentration PDF, can be parameterized on a relative coordinate system around the barycentre as it is evaluated on a local reference frame. The first technique providing the basis of a number of modelling studies on higher order concentration statistics is [Gifford (1959)] Gaussian meandering (or fluctuating) plume model that assumes the fluctuations are produced solely by the meandering of the ensemble-mean instantaneous plume. This model has been particularly successful for predictions close to the source where meandering is the primary mechanism responsible for generating fluctuations, but it ignores the in-plume fluctuations that dominate the overall fluctuation statistics in the far field. [Yee et al. (1994)] and [Yee and Wilson (2000)] extended [Gifford (1959)] model to include the in-plume fluctuations by specifying them in terms of a Gamma PDF. Their model can very well simulate the rich structure of concentration statistics observed in field and laboratory experiments. Many meandering plume model applications have been restricted to neutral, near-neutral or stable flow conditions because of the difficulty of incorporating the inhomogeneous and skewed characteristics of the convective boundary layer or a canopy layer vertical turbulence in the analytical framework of the meandering plume approach. [Luhar et al. (2000)] significantly improved the FPM ability of describing less-idealized turbulence using a single particle model (hereinafter SPM) to evaluate the PDF of the plume centroid for a contaminant in the convective boundary layer. [Luhar et al. (2000)] evaluated the instantaneous plume meandering applying a linear relation to the one-particle trajectories. Hence the [Luhar et al. (2000)] model needs the trajectories of the centroids of each instantaneous plume to compute the high order concentration fields. [Franzese (2003)] developed a new version of FPM where the equations of the centroid are derived from the single particle stochastic equations filtering out the turbulent kinetic energy (TKE). This model

does not require an analytical form for the turbulent velocity PDF, because the acceleration of the centroid is approximated by a simple quadratic functional. [Mortarini et al. (2009)] extended the [Franzese (2003)] approach, applying the FPM model to the turbulent flow generated by a simulated canopy. [Cassiani and Giostra (2002)] proposed a linear contraction to derive the centroid position PDF from the mean concentration field derived from measurements or numerically evaluated and thus relaxing the need for Lagrangian modelling. In [Cassiani and Giostra (2002)] approach the same linear transformation of [Luhar et al. (2000)] is applied to a calculation grid instead of trajectories, causing a compression of the PDF. After calculating the centroid PDF, the concentration field is evaluated by parameterizing the dispersion of the cloud relative to its instantaneous centroid. Hence it is necessary to provide an analytical expression for the relative position and concentration PDFs and the relative position variance. [Luhar et al. (2000)] parameterize the relative vertical position and concentration PDFs respectively as a skewed distribution obtained as the linear combination of two reflected Gaussian PDFs and a gamma distribution, whereas [Franzese (2003)] used a simple reflected Gaussian and a lognormal distribution. [Cassiani and Giostra (2002)] assumed that the skewness of the single particle was equal to the skewness of the barycentre, however [Dosio and de Arellano (2006)] showed that this approximation is valid only close to the source when dispersion is dominated by the meandering, but it is not true elsewhere. Hence they gave a new expression for the relative skewness in order to improve the comparison with the measured data. Both in [Franzese (2003)] and [Luhar et al. (2000)] models the relative variance is written to be consistent with inertial range form at small time and with [Taylor (1921)] limit at large time (in the vertical direction a further interpolate expansion is considered including boundary reflections). The relative concentration PDF requires the parameterisation of the relative fluctuations intensity; the form used by [Gailis et al. (2007)] is the only one dependent on height and shows the best agreement with experimental data. In the FPM version that I propose the centroid PDF is calculated applying the [Cassiani and Giostra (2002)] approach (see section 7.3), choosing each time the input mean field most suitable for the class of turbulence considered; the relative component is parameterized as in [Luhar et al. (2000)] although the simple Gaussian relative vertical position PDF of [Franzese (2003)] including multiple reflections at the boundaries is used here, see section 7.1. The model is first applied in homogeneous and stationary turbulence focusing the attention on the second moment of concentration; to this end, the model is compared with the Lagrangian two analytical solutions for concentration variance

found by [Thomson (1990)] and [Ferrero and Mortarini (2005)]; [Thomson (1990)] chooses a Gaussian distribution for the relative separation PDF, whereas [Ferrero and Mortarini (2005)] choose a Richardson PDF more appropriate at very short times. Then inhomogeneous turbulence is considered: first the model is applied to simulate the water tunnel experiments of dispersion from a continuous point source in urban canopy turbulence performed by [Huq and Franzese (2013)] and then to simulate the new data-set of [Nironi (2013)] and [Nironi et al. (2013)] describing the evolution of a fluctuating pollutant plume within a wind tunnel simulation of a neutral boundary layer (in section 7.4). I underline that the FPM introduced here worjs offlice, i.e. has the capability for evaluating the concentration PDF without a simultaneous LSM, given only a mean concentration field. The model is independent of the method used for calculating the mean field. Three different evaluations of the mean field is considered to test the flexibility of the model: a simple SPM in homogenoeus turbulence, a Gaussian model in the water boundary layer and an experimental data in the wind tunnel bounday layer.

The dispersion of scalar in a turbulent boundary layer is a very important process since it is of interest for both urban and agriculturalforest applications. Most of the research in this field has been devoted to understanding the behaviour of the mean concentration of natural and anthropogenic substances. The same can be said for the atmospheric scalar fields, e.g. the temperature field. In this frame the behaviour of the mean values is relatively well understood while the fluctuating behaviour of the scalar is an open question especially for the buoyant scalars . The central thread which run through all this thesis is Lagrangian modelling. It is the natural and most powerful means to describe many interesting atmospheric processes and with the aid of such models better strategies for many environmental issues can be developed.

Part I

Theoretical framework for inhomogeneous turbulent flows.

Chapter 1

Mathematical description of turbulence

Both the spatial and temporale dependence of the instantaneous values of the fluid dynamic fields habe a very compelx and confused nature. Moreover, if turbulent flow is set up repeatdly under the same conditions, the exact values of these fields will be different each time. The dependence on time of these fields consists of a set of fluctations of diverse periods and amplitudes, superimposed upon each other without any obvious regularity. The distributions of instantaneous values of the fluid dynamic variables in space have a similar nature; they constitute a disordered set of 3D fluctuations of diverse amplitude, wavelength and orientation. Due to this extreme disorder and the sharp variation in time and space of the fields pf fluid dynamic quantities, in the study of turbulence it is necessary to use some method of averaging which will enable to pass from the initial fluid dynamic fields to smoother, more regular mean values of the flow variables. These variables may then be investigated by means of the usual methods of mathematical analysis.
The question of the definition of mean values is delicate one in the theory of turbulence, and has a long history. In practice to determine the mean values, a most generally use of time and space averaging over some interval of time or region of space is needed. Also a more general space-time averaging of the function $f(x_1, x_2, x_3, t) = f(\vec{x}, t)$ has to be considered, and it is given by the equation

$$\overline{f(x_1, x_2, x_3, t)} = \int\int\int\int_{-\infty}^{\infty} f(x_1-\zeta_1, x_2-\zeta_2, x_3-\zeta_,t-\tau)\omega(\zeta_1, \zeta_2, \zeta_3, \tau)\mathrm{d}\zeta_1\mathrm{d}\zeta_2\mathrm{d}\zeta_3\mathrm{d}\tau \tag{1.0.1}$$

here the overbar indicates averaging and $\omega(\zeta_1, \zeta_2, \zeta_3)$ is some weighting nonnegative function which satisfies the normalisation condition:

$$\overline{f(x_1, x_2, x_3, t)} = \int\int\int\int_{-\infty}^{\infty} f\omega(\zeta_1, \zeta_2, \zeta_3, \tau)\mathrm{d}\zeta_1\mathrm{d}\zeta_2\mathrm{d}\zeta_3\mathrm{d}\tau \tag{1.0.2}$$

If the functions ω is equal to 0 outside of 4D region and takes a constant value within it, then 1.0.1 is simple average over a given region of space-time. It is clear that 1.0.1 will depend on the form of ω. Thus 1.0.1 gives rises to many different mean values and it is necessary to discover which of these is the best.

1.1 Mean values and correlation function.

The use of time, space or space-time averaging defined by some equations of the form 1.0.1, is very convenient from a practical viewpoints, but leads to a great nuember of unavoidable difficulties in theoretical calculations. This type of averaging has the great disadvantage that the question of the form of ω most suitable for the given problem must be resolved each time before use. Hence it is desiderable in theory of turbulence to avoid the use of this type of averaging altogether, and to adopt instead some other method of defining mean value, a method that has simpler properties and is more general. A convenient definiton of this type is found in the probability theory treatment of the fields of fluid dynamic variables in a turbulent flow as random fields. The basic feature of probability theory approach to the turbulence is the transition from the consideration of a single turbulent flow to the consideration of a the statistical ensemble of all similar flows created by some set of fixed external conditions. For turbulent folw, the effect of small uncontrollable dusturbances in the flow and in initial condition leads to a situation in which, when an experiment is performed two times under the same conditions I shal obtain two different value of the velocity $u(\vec{x}, t)$ and the other turbulent variables. If I now fix the external conditions and repeat the experiemtn may times, then the arithmetic means of the values obtained will be fairly stable. In this case the value about which the mean of $\underline{u(\vec{x}, t)}$ oscillates is called probability mean of velocity and is denoted by the simbol $\overline{u(\vec{x}, t)}$. Le te me call $p(u', u")$ the probability that $u(\vec{x}, t)$ will take the value in the range between u' and $u"$. Usually this number $p(u', u")$ may be represented as an integral from u' to $u"$ of some non-negative function $p(u)$ called probability density function (PDF of u. Therefore the set of all u for which $p(u) \neq 0$ will give the set of possibile values

of $u(\vec{x},t)$. I shall call the actual value $u(\vec{x},t)$ observed in one of the experiments a sample value, or realisation. The fact of the existence of the PDF is sometimes expressed as:

$$P\{u < u(\vec{x},t) < u+du\} = p(u)du \tag{1.1.1}$$

where the symbol P denote the probabilty of the conditions specified in the braces being satisfied. The probability mean is:

$$\overline{u(\vec{x},t)} = \int_{-\infty}^{\infty} up(u)du \tag{1.1.2}$$

At the same time the probabilty mean of arbitrary functions of $u(\vec{x},t)$ is:

$$\overline{F[u(\vec{x},t)]} = \int_{-\infty}^{\infty} F(u)p(u)du \tag{1.1.3}$$

Thus I may conclude that from a probabilistic viewpoint the value of velocity at a point of a turbulent flow is a random variables described by a definite probabilty distribution.

So far I have discussed only the value of velocity at a fixed point $\vec{x}$ and at a fixed instant t. However, I may apply a similar approach to the whole field, i.e. to the function $u(x_1,x_2,x_3,t)$ of the four variables. Repeating the experiment several times under the same initial conditions, I shall obtain a new field every time. Here also I may speak of the ensemble of possible fields $u(\vec{x},t)$. Morevoer each individual field is considered as representative chosen at random from this ensemble.

For the field $u(\vec{x},t)$ to be random it is necessary that, first, the value $u(\vec{x},t) = u(M)$ of this field at a fixed space-time point $M = (\vec{x},t)$ be a random variable. If I choose two values $u_1(M_1)$ and $u_2(M_2)$ the arithmetic mean of any function of these two values should be also statistically stable. This means that for the values $u_1(M_1)$ and $u_2(M_2)$ there must exist a two-dimensional PDF defined by:

$$P\{u_1 < u_1(M) < u_1+du_1, u_2 < u_2(M) < u_2+du_2\} = p_{M_1M_2}(u_1,u_2)du_1du_2 \tag{1.1.4}$$

Moreover if $M_1, M_2, ..., M_N$ are N arbitrary space-time points there must exist a corresponding function of N variables $p_{M_1.....M_N}(u_1,.....,u_N)$. This function is the N-dimensional PDF of the values of the N random variables $u_i(M_1)$. This function clearly must be non-negative and such taht the integral of each over all variables is equal to unity.

It is natural to assimw that in a turbulent flow also the fields of pressure, density and temperature will be also random fields. In this case each of this fields will have a

correpsonding multidimensional PDF. Moreover the different fluid dynamic fields in a turbulent flow are statistically interconnected and account must be taken that for thse fields there also exist a joint PDF of the values of one of the fields at some given points of space-time, values of a sceond field at given point, values of third field, etc. This it follows that if I have any function of hte fluid dynamic variables of a turbulent flow, i may determine its mean value as the integral of product of this function with the joint probability densities of all its arguments.
The mean value is understood as the mean taken over all the possible values of the quantity under discussion. Thus to determine empirically mean values I should need results of a large number of measurements carried out in a long series of repeated similar experiments. In practice I generally do not have such a series of experiments and thus I am obliged to determine the mean from data of a single experiment. Then normally simplified averaging over space interval or time are used. This I see that the assumption of the existence of PDF does not eliminate by itself the problem of the validity of using ordinary time or space mean values in the theory of turbulence, but only alters the formulation of the problem. Instead of investigating the special poroperties of particular methods of averaging, I must now discover how close the empirical mean values obtained by these methods lie to the probability mean value. The position is completely analogous to that in ordinary statistical mechanics where the theoretical mean over all possible states of the system (the ensemble mean) may also be replaced by the directly observed time-mean. I statistical mechanics it is well known that such a change in generally made of the basis assumption that as the averaging interval becomes infinetely great, the times means converge to the corresponding ensemble mean. In certan special cases, the validity of this assumption may be proved strictly and in all other cases it is adopted as an additional, highly likely, hyphotesis, the ergodic hyphotesis. In theory of turbulence the concept of convergence of time means to the corresponding probability mean is introduced also as ergodic hyphotesis.

1.1.1 Moments of random variables

If I have a system with N random variables $u_1, ..., u_N$ with a N-dimensional PDF $p(u_1, ..., u_N)$ then the moments of thse variables are defined by:

$$B_{k_1....k_N} = \overline{u_1^{k_1}.....u_N^{k_N}} = \int ... \int_{-\infty}^{\infty} u_1^{k_1}.....u_N^{k_N} p(u_1, ..., u_N) du_1.....du_N \qquad (1.1.5)$$

where $k_1, ..., k_N$ are non-negative integers, the sum of which gives the order of the moments. The moments of first order are the mean values. In addition I often use the central moment, i.e. the moments of the deviations of $u_1, ..., u_N$ from their mean values:

$$b_{k_1....k_N} = \overline{(u_1 - \overline{u_1})^{k_1}.....(u_N - \overline{u_N})^{k_N}} \tag{1.1.6}$$

Opening the brackets in the right side of 1.1.6 it is easy to express $b_{k_1....k_N}$ in terms of $B_{k_1....k_N}$. In particular fo $N = 1$ I have:

$$\begin{aligned} b_1 &= 0 \\ b_2 &= B_2 - B_1^2 \\ b_3 &= B_3 - 3B_1B_2 + 2B_1^3 \\ b_4 &= B_4 - 4B_1B_3 + 6B_1^2B_2 - 3B_1^4 \\ &..... \end{aligned} \tag{1.1.7}$$

The moment $b_2 = \sigma_u^2$ is called variance of u and $\sigma_u = \sqrt{\sigma_u^2}$ os the standard deviation of u. Similarly the general second central moment $b_{11} = \overline{(u_1 - \overline{u_1})(u_2 - \overline{u_2})}$ is called covariance of u_1 and u_2. If u_i has some definite dimension, then the corresponding moments (and central moments) will also have the same dimension. However adimensional ratios as $s = \frac{b_3}{b_2^{3/2}}$ and $\delta = \frac{b_4}{b_2^2}$ are often used and called respectively skewness and kurtosis.
Other combinations pf the moments of special interest are the cumulants that are obtained by subtracting from the moments a special polynomial in the lower-order moments. For $N = 1$:

$$\begin{aligned} S_1 &= B_1 \\ S_2 &= B_2 - B_1^2 = b_2 \\ S_3 &= B_3 - 3B_1B_2 + 2B_1^3 = b_3 \\ S_4 &= B_4 - 4B_1B_3 - 3B_2^2 + 12B_1^2B_2 - 6B_1^4 = b_4 - 3b_2^2 \\ &..... \end{aligned} \tag{1.1.8}$$

1.1.2 Moments of random fields

In the theory of turbulence I am concerned with random fields, i.e. random functions $u(M)$ of a space-time point M. The kth order moments of such a field are the mean

values of product of k values of the field

$$B_{u...u}(M_1, ..., M_k) = \overline{u(M_1)....u(M_k)} \tag{1.1.9}$$

These moments depend of the coordinates of the points at which the values are taken. However some of the points may coincide with each other; the number of different points among them defines the type of the moments. In this frame, I shall distinguish moments of one point, two points, etc, tupes. If the type of the moment is less than its order, then the corresponding moments $\overline{[u(M_1)]^{k_1}....[u(M_N)]^{k_N}}$ will be denoted by the symbol $B_{u..u,...,u...u}(M_1, ..., M_N)$ where the subscript groups referring to different points of space-time are separated by commas.
The mean values of the products of values of several random fields are called joint moments of these fields.
When the arguments $M_1, ..., M_k$ are arbitrary points of space.time I shall call the moments, space-time moments. Very frequently, in theory of turbuelnce, one considers only moments in which the values refer to same instant; these are called space moments. Sometimes, I deal with time moments, i.e. mean values of product of the fluid dynamic field at the same point. Hereforth when I speak simply of moments I shall always mean space moments. In this thesis I shall often be dealing with correlation functions, i.e. one-point, two-point, second order moments. For instance two-point moment $B_{uv}(M_1, M_2) = \overline{u(M_1)vM_2}$ is called cross-correlation function of u and v. Two-points moments of order greater than two will rpresent correlation functions of some new fields which are products of the original fields; such two-points moments are called higher-order correlation functions. The corresponding differences between a moment of order k and a specially chosen combination of lower order moments will coincide exactly with the cumulants of the random variables discussed in subsection 1.1.1. Therefore they are called the cumulants of order k of these fields.
The general concept of a random field was discussed and the main statistical characteristic of such fields. i.e. the mean values and the correlation function were introduced. For a full treatment of these functions I refer to [Monin and Yaglom (1975)]. However when I consider the finer properties of turbulence, I find that this requires a new mathematical tool, the application of harmonic analysis, i.e. the representation of functions by Fourier series or integrals. In application however I frequently encounter non-periodic function which do not vanish at infinity nd which, strictly speaking, cannot be represented by Fourier series or integrals. The point is that a Fourier expansion, or spectral representation, of a special form, and with a clear physical interpretation, is possible for any stationary processes and homogeneous random fields which, by definition, do not vanish at infinity. Again I do not aim to

exaustively present the spectral representation of stationary and homogenoeus fields in this thesis, and again I refer to [Monin and Yaglom (1975)] for the full dissertation.

Chapter 2

Particle dispersion in a turbulent flow: the Lagrangian description of turbulence

2.1 Definition of the variables.

In the Eulerian framework the motion of an incompressible fluid is characterized at time t by the velocity field $\vec{u}(\vec{X}, t)$, i.e. by the values of the velocity vector in all the points $\vec{X} = (X_1, X_2, X_3)$. In principle, known the initial condition $\vec{u}(\vec{X}, t) = \vec{u}(\vec{X}, 0)$X), it is possible to determine the Eulerian variables $\vec{u}(\vec{X}, t)$ at each time $t > t_0$. Nevertheless it is not suitable to use Eulerian variable to describe phenomena as the turbulent transport or the material surface deformation in a turbulent flow. For such phenomena the Lagrangian framework is almost a natural choice.
The Lagrangian approach consists in following the motion of fixed fluid particles from a certain initial time t0. With fluid particle a fluid volume whose linear dimensions are far bigger than the mean distances between the molecules is meant. In other words a fluid particle is a point of the fluid volume that is moving inside of it following the equations of fluid mechanics. The Lagrangian description is related to individual fluid elements whose summation produces the total turbulent flow.
In a Lagrangian framework for an incompressible flow the function $\vec{X} = (\vec{x}, t)$ which for each time t gives the coordinate $\vec{X}$ of every fluid particle, is identified by the value of the parameter $\vec{x}$. The equations of fluid dynamics allow to determine the values of $\vec{X} = (\vec{x}, t)$ for every $t > t_0$ in terms of the fluid particles initial velocity values

$\vec{V}(\vec{X},t) = \frac{\partial \vec{V}(\vec{x},t)}{\partial t}$, i.e.:

$$\vec{V}(\vec{X},t_0) = \left[\frac{\partial \vec{V}(\vec{x},t)}{\partial t}\right]_{t=t_0} \tag{2.1.1}$$

The relation between Eulerian and Lagrangian variables is given by the expression:

$$\frac{\partial \vec{X}(\vec{x},t)}{\partial t} = \vec{u}\left[\vec{X}(\vec{x},t),t\right] \tag{2.1.2}$$

The initial values of the spacial coordinates $\vec{X}$ at time $t = t_0$ will be used as the fluid particle Lagrangian parameters, $\vec{x}$: $\vec{x}(\vec{X},t_0)$.
In this description the two variable function $\vec{X}(\vec{x},t)$ describes a family of fluid particles trajectories that at time $t = t_0$ are in all the possible points $\vec{x}$ of the volume of the fluid. Thus the Lagrangian framework consists in assigning a family of trajectories that differs one from the other for the value of $\vec{x}$ and where t is the parameter.

$$\frac{\partial \vec{X}(\vec{x},t)}{\partial t} = \vec{u}\left[\vec{X}(\vec{x},t),t\right] \tag{2.1.3}$$

2.2 Statistics of the motion of a fluid particle.

A general method, suggested by [Kolmogorov (1941)], to obtain the statistics of the motion of a fluid particle is based on changing the reference frame passing from a fixed inertial set of coordinates S_0 to a moving inertial reference frame S whose velocity (different for each realization) is $\vec{u}(\vec{x},t_0)$ and whose origin at $t = t_0$ is in $\vec{x}$. The coordinates $\vec{Y}^{(S)}$ and the velocity $\vec{V}^{(S)}$ in the new set are connected to the coordinate $\vec{x}$ and to the velocity $\vec{u}$ in the old frame S_0 by the following simple relations:

$$\vec{Y}^{(s)} = \vec{X} - \vec{x} - \vec{u}(\vec{x},t_0)\tau \vec{V}^{(s)} = \vec{u} - \vec{u}(\vec{x},t_0) \tag{2.2.1}$$

with $\tau = t - t_0$.In the set S the macroscopical effects due (for example) to the mean wind or to large scale factors do not exist, but only small scale phenomena due to turbulence are considered, in S it is always possible to consider the field as locally isotropic. The small scale properties of turbulence are studied through the relative motion of a single particle in small region of space and in short time ranges. Moreover these are not correlated to the absolute motion of the fluid that is mainly

determined by large scale perturbations. Let consider a fluid particle that leaves $\vec{x}$ at time t_0 and reaches $\vec{Y}^{(s)}(\tau) = \vec{X} - \vec{x} - \vec{u}(\vec{x}, t_0)\tau$ at the time $t_0 + \tau$ and has the velocity $\vec{V}^{(s)}(\tau) = \vec{V}(\vec{x}, t_o + \tau) - \vec{u}(\vec{x}, t_0) = \Delta_\tau \vec{V}$.
In the S reference frame it is always possible considering, at least locally, the field as isotropic and then the $\Delta_\tau \vec{V}$ statistics has to obey to the Kolmogorov similarity hypothesis ([Monin and Yaglom (1975)]). Thus the motion of the fluid particle has an universal form governed by the parameters ϵ, the dissipation of kinetic energy, and ν, the fluid viscosity, (this is true only for time $\tau \ll T_0$, with $T : 0$ large enough, and for $Re > Re_{critical}$ where Re is the Reynolds number) and and it is possile to write [Monin and Yaglom (1975)]:

$$\langle {V^{(S)}}_l(\tau) {V^{(S)}}_j(\tau) \rangle = D^{(L)}(\tau)\delta_{ij} \tag{2.2.2}$$

and considering that $\vec{Y}^{(S)}(\tau) = \int_0^\tau \vec{V}^{(S)}(\tau)d\tau$:

$$\langle {Y^{(S)}}_l(\tau) {Y^{(S)}}_j(\tau) \rangle = \int_0^\tau \int_0^\tau \langle V_l^{(S)}(\tau_1) V_j^{(S)}(\tau_2) \rangle d\tau_1 d\tau_2 = \delta_{ij} \int_0^\tau \tau' D^L(\tau') d\tau' \tag{2.2.3}$$

where $D^L(\tau)$ is the Lagrangian velocity structure function. According to Kolmogorov hypotheses (see 4.1.2) and remembering that the Kolmogorov microscales η, v_η and τ_η for $\tau \ll T_0$ simply are:

$$\eta = \left(\frac{\nu^3}{\epsilon}\right)^{1/4} \tag{2.2.4}$$

$$v_\eta = (\nu\epsilon)^{1/4} \tag{2.2.5}$$

$$\tau_\eta = \left(\frac{\nu}{\epsilon}\right)^{1/2} \tag{2.2.6}$$

2.2.2 can be expressed as:

$$D^L(\tau) = {v_\eta}^2 \beta(\frac{\tau}{\tau_\eta}) \quad \tau \ll T_0 \tag{2.2.7}$$

In the inertial subrange, $\tau_\eta \ll \tau \ll T_0$, equation 2.2.7 becomes:

$$D^L(\tau) = C_0 \epsilon \tau \quad \tau_\eta \ll \tau \ll T_0 \tag{2.2.8}$$

with C_0 universal constant. In the inertial subrange the Lagrangian velocity structure function is linear in τ. Substituting equation 2.2.8 inside equation 2.2.6 the inertial range behaviour for the particle position is obtained ([Monin and Yaglom (1975)]):

$$\langle {Y^{(S)}}_l(\tau) {Y^{(S)}}_j(\tau) \rangle = \frac{1}{3} C_0 \epsilon \tau^3 \delta_{lj} \tag{2.2.9}$$

2.3 Spatial velocity difference statistics.

Let consider the statistics of the velocity difference between the point $\vec{x}$ and $\vec{x}+\vec{r}$ at time t:

$$\Delta_r \vec{u} = \vec{u}(\vec{x}+\vec{r},t) - \vec{u}(\vec{x},t) \tag{2.3.1}$$

For sufficiently small $\vec{r}$ the PDF of $\Delta_r \vec{u}$ can be considered as homogeneous, isotropic and stationary, furthermore, for locally homogeneous turbulence, $\overline{\Delta_r \vec{u}} = 0$ and the second order moment tensor can be expressed in all the quasi-equilibrium range through two scalar functions: the longitudinal structure function, $D_{LL}(r)$, and the lateral structure function, $D_{NN}(r)$:

$$D_{ij}(r,t) = \frac{D_{LL}(r) - D_{NN}(r)}{r^2} r_i r_j + D_{NN}(r)\delta ij \tag{2.3.2}$$

These two structure functions can be defined as:

$$D_{LL}(r) = \overline{(\Delta_r u_L)^2} \tag{2.3.3}$$

$$D_{NN}(r) = \overline{(\Delta_r u_N)^2} \tag{2.3.4}$$

and are related (as a consequence of the continuity equation) by the formula:

$$D_{NN}(r) = D_{LL}(r) + \frac{r}{2}\frac{dD_{LL}(r)}{dr}. \tag{2.3.5}$$

Following the first Kolmogorov hypothesis:

$$D_{LL}(r) = {v_\eta}^2 \beta_{LL}\left(\frac{r}{\eta}\right) \tag{2.3.6}$$

$$D_{NN}(r) = {v_\eta}^2 \beta_{NN}\left(\frac{r}{\eta}\right) \tag{2.3.7}$$

In a small region of diameter $r \ll \eta$ friction will play a dominant role in the system dynamics and the velocity components will only have a slight dependence on the spatial coordinates. In this limit it is possible to expand $u_l(\vec{x}+\vec{r})$ in Taylor series, i.e. $u_L(\vec{x}+\vec{r}) = u_L(\vec{x}) + \nabla u_L \cdot \vec{r} + ...$, to obtain the following behaviour of the structure functions ([Monin and Yaglom (1975)]):

$$D_{LL}(\mathbf{r}) \approx Ar^2, \qquad D_{NN}(\mathbf{r}) \approx A'r^2 \quad r \ll \eta \tag{2.3.8}$$

with A and A' are non-dimensional constants. On the contrary in the inertial subrange, $\eta \ll r \ll L$, the second Kolmogorov similarity hypothesis ensures that equations (2.3.7 and 2.3.7) do not depend on ν:

$$D_{LL}(\mathbf{r}) \approx C\epsilon^{2/3}r^{2/3} \quad D_{NN}(\mathbf{r}) \approx C'\epsilon^{2/3}r^{2/3} \quad \eta \ll r \ll L \tag{2.3.9}$$

Here the statistics of particle pairs are not treated and I refer to [Monin and Yaglom (1975)] for their description.

2.4 Concentration fluctuations statistics.

Consider parcels of a passive contaminants released in a turbulent flow. In the absence of molecular diffusion the parcel concentration is conserved. Hence, neglecting dissipation, the mean concentration of a passive contaminant observed in any point of the flow can be evaluated integrating the concentration assigned to each particle at the source times the particle probability of reaching the observation point ([Monin and Yaglom (1975)]):

$$\overline{C(z,t)} = \int \int_{-\infty}^{\infty} P_1\left(z,t|z',t'\right) S\left(z',t'\right) dz'dt', \tag{2.4.1}$$

where $S\left(z',t'\right)$ is the source distribution, and $P_1\left(z,t|z',t'\right)$ is the probability density function that a particle starting from position z' at time t' reaches position z at time t. For the concentration covariance an analogous expression can be found:

$$\begin{aligned}\overline{C(z_1,t_1)C(z_2,t_2)} = \int \int \int_{-\infty}^{\infty} \int_{-\infty}^{\infty} P_2\left(z_1,z_2,t,t|z_1',z_2',t_1',t_2'\right) \\ S(z_1',t_1')S(z_2',t_2')dz_1'dz_2'dt_1'dt_2'\end{aligned} \tag{2.4.2}$$

where $P_2\left(z_1,z_2,t,t|z_1',z_2',t_1',t_2'\right)$ is the two-particle PDF that depends on the simultaneous motion of the particle pair [Monin and Yaglom (1975)]. For equations 2.4.1 and 2.4.2 to be consistent it is necessary that:

$$P_1(z_1,t|z_1',t_1') = \int \int_{-\infty}^{\infty} P_2(z_1,z_2,t|z_1',z_2',t_1',t_2')dz_2'dt_2' \tag{2.4.3}$$

and

$$\int \int_{-\infty}^{\infty} P_1(z,t|z',t')dz'dt' = 1 \tag{2.4.4}$$

Equation 2.4.3 ensures that integrating the two-particle PDF on all the possible position of the second particle the single particle PDF is obtained.
I am now interested in dividing the inertial contributes to the dynamics from the viscous one. It is useful to consider an inner region with eddies of the Kolmogorov lenghtscale η size and an outer region with eddies of the inertial range size or larger. If the separation between two particles, $r = |z1z2|$, is larger than η, then $P2$ is mainly determined by the outer region dynamics, i.e. by eddies larger than the integral lenght scale L. In order to define the concentration variance, $\overline{C^2(z,t)}$, I have to evaluate the $lim_{z1,z2\to z}$ of equation 2.4.2 but this limit is discontinous. As a matter of fact $|z1z2| \to 0$ in the inner region means $\frac{|z1z2|}{\eta} \to 0$, in the outer region means $\frac{|z1z2|}{L} \to 0$, but the separation behaves in different ways in these two limits and so a distinction has to be made. In realistic situations the smearing by molecular action or finite measurement probe size make the definition of $\overline{C^2(z,t)}$ in terms of the outer limit more appropriate. It is then possible to define the concentration variance averaging the concentracion covariance. This definition links the theoretical one with the instrumental smoothing:

$$\begin{aligned} \overline{C^2} &\equiv V_\eta^{-2} \int\int_{V_\eta} \overline{C(z_1)C(z_2)} dz_1 dz_2 = \\ = V_\eta^{-2} \int\int_{-\infty}^{\infty} \int\int_{V_\eta} P_2(z_1, z_2|z_1', z_2') S(z_1') S(z_2') dz_1 dz_2 dz_1' dz_2' &\approx \\ \approx \int\int_{-\infty}^{\infty} \lim_{|z_1-z_2|/L\to 0} P_2(z_1, z_2|z_1', z_2') S(z_1') S(z_2') dz_1' dz_2' & \end{aligned} \tag{2.4.5}$$

where for simplicity the time dependence was dropped. The last step in equation 2.4.5 assumes that the limit in the outer region is a good approximation of the inner region averaging process. Thus the concentration variance can be defined as:

$$\overline{C^2} = \int\int_{-\infty}^{\infty} P_2(z|z_1', z_2') S(z_1') S(z_2') dz_1' dz_2' \tag{2.4.6}$$

Equation 2.4.6 takes into account the effects of diffusion even if it has been derived for a passive scalare with null diffusivity. The results obtained in this limit can be extended to fluid particles whose molecular diffusivity has a finite value. The following hypotheses have been assumed:
i) a volume V_η tale che $L \gg V_\eta$ exists;
ii) diffusion makes $\langle C(z)C(z+\Delta)\rangle$ less peaked near $\Delta = 0$;
iii) the Peclet number ($Pe = \frac{UL}{\kappa}$ determines the importance of inertial terms in

respect to the molecular diffusivity) is large; if this is not true κ can not be neglected; iv) the Schmidt number ($Sc = \frac{Pe}{Re} = \frac{\nu}{\kappa}$) is $O(1)$, only if this constraint is satisfied viscosity does not prevail on diffusivity and the ii) can be true, in other words this hypothesis ensures that the volume V_η is larger than the peak width.
the peak width. If the diffusivity smearing process were ignored, the concentration variance would be defined in the inner limit, where:

$$\lim_{\frac{\Delta}{\eta}\to 0} P_2(z_1, z_2|z_1', z_2') = P_1(z_1|z_1')\delta(z_1' - z_2') \tag{2.4.7}$$

that states that if two particles are coincident they have the same PDF. Thus the concentration variance can be defined as:

$$\overline{C_*^2} = \int_{-\infty}^{\infty} P_1(z|z')S^2(z')dz' \tag{2.4.8}$$

Equation 2.4.8 does not include turbulent mixing processes associated with relative dispersion, while equation 2.4.6 does. [Durbin (1980)] showed that:

$$\overline{C^2} \leq \overline{C_*^2} \tag{2.4.9}$$

as long as equation 2.4.8 correponds to neglect the interaction between the particles and to evaluate the concentration fluctuations considering the motion of two indipendent particles, the inequality 2.4.9 states that the correlation between the particles reduces the concentration fluctuations. In the study of turbulence through Lagrangian stochastic particle models the interest is focused on the inertial range where viscosity and molecular diffusivity can be neglected. In the atmosphere the turbulent fluxes are characterized by large Reynolds and Peclet numbers that ensure that the mean concentration field is not influenced by ν and κ (unless very close to the source), nevertheless this can not be exetend to the concentration fluctuations. Considering the motion of two particles in a turbulent flow whose Reynolds and Peclet number are large it is evident that, when the particle are far enough one from the other, molecular diffusion is negligible compared with the turbulent effects and their motion is completely uncorrelated, moreover, since viscosity acts only at the small scales, even the viscous effects can be ignored. Nevertheless if the separation r between the particles is $O(\eta)$ molecular diffusion and viscosity have to be taken into account (if two particles are coincident they can be divided only by molecular effects). For the Lagrangian modeling theory it is necessary that the separation between two particles in a pair is larger than the Kolmogorov microscale η, in other words r/η must not tend to zero. In the previous section it has been noticed that if $r0 \ll \eta$ the time necessary

to the two-particle separation to lie in the inertial subrange is infinite, particles can not separate. If the initial separation is in the dissipative subrange molecular and viscous forces prevent the particles to separate and to be subjected to the inertial forces. On the contrary in the inertial range $\overline{\Delta^2(t)} \propto \epsilon t^3$ and then, even in the limit $\Delta \to 0$ ($\Delta/L \to 0$) e $t \to 0$, the eddies can disperse the particles. In order to be able to use Lagrangian modeling to describe the joint motion of particle pairs it is necessary to find the minimum distance and the shorter time, d and t_d, for which diffusivity and viscosity can be neglected, it is necessary to find a limit in which this is true. This can be achieved by making the Reynolds number tend to infinity while keeping constant the Schmidt number (hypothesis iv) and then ensuring that r is always larger than η ([Durbin (1980)]):

$$\begin{cases} Re \to \infty \\ Sc\, O(1) \end{cases} \tag{2.4.10}$$

or, equivalently,

$$\begin{cases} \nu, \kappa \to 0 \\ Sc\, O(1) \end{cases} \tag{2.4.11}$$

amd

$$\begin{cases} & \Delta \to 0 \\ \dfrac{\Delta}{\eta} \neq 0 & \Delta \gg \eta \end{cases} \tag{2.4.12}$$

If costraints 2.4.11 and 2.4.12 are satisfied the separation between the particles lies in the inertial subrange. It is worth noticing that definition 2.4.6 continues being valid under these assumptions, [Durbin (1980)]. Hence, even dealing with passive scalar with null diffusivity, the results can be extended to real molecules with finite κ. The theory here presented is not valid in the nearby of the source, for ditance less than d or for time shorther than t_d.

Chapter 3

Isotropic turbulence

3.1 Equations for velocity correlations and spectra.

Turbulence is said to be homogeneous if all the fluid dynamic fields form homogeneous random fields. It is referred to be isotropic if all the fluid dynamic fields form isotropic random fields. In this chapter I shall be concerned with isotropic turbulence. No real turbulence can be exactly isotropic, but it is a mathematical idealisation which is convenient only for the approximate descriptiomn of certain types of flow.

Let me now derive the basic dynamic equations for the correlation functions of isoptropic turbulence. The mean value $\overline{\vec{u}(\vec{x},t)}$ should be zero in isotropic turbulence (see [Monin and Yaglom (1975)]), hence the velocity is the same as velocity fluctuations, and the correlation tensor $B_{ij}(\vec{r},t) = \overline{\vec{u_i}(\vec{x},t)\vec{u_j}(\vec{x}+\vec{r},t)}$ should be the form:

$$B_{ij}(\vec{r},t) = [B_{LL}(\vec{r},t) - B_{NN}(\vec{r},t) =]\frac{r_i r_j}{r^2} + B_{NN}(\vec{r},t)\delta_{ij} \tag{3.1.1}$$

where $B_{LL}(\vec{r},t) = \overline{\vec{u_L}(\vec{x},t)\vec{u_L}(\vec{x}+\vec{r},t)}$ and $B_{NN}(\vec{r},t) = \overline{\vec{u_N}(\vec{x},t)\vec{u_N}(\vec{x}+\vec{r},t)}$. In view of the continuity equation the functions B_{LL} and B_{NN} are related by:

$$B_{NN}(r,t) = B_{LL}(r,t) + \frac{r}{2}\frac{\partial B_{LL}(r,t)}{\partial r} \tag{3.1.2}$$

The last formula shows that the tensor $B_{ij}(r,t)$ is completely determined by a singlе scalarr function of the two arguments r and t. Morevoer, [Monin and Yaglom (1975)], it follows from continuity equation that in isotropic turbulence the velocity

fields in uncorrelated with any scalar low variable, e.eg. the pressure field p:

$$B_{pi}(r,t) = B_{pL}(r,t)\frac{r_i}{r} = 0 \tag{3.1.3}$$

This relation is the simplest relation of the theory of isotropic turbulence which can be verified experimentally.
let me now consider the dynamic equation for $B_{ij}(\vec{r},t)$. To find $\frac{\partial}{\partial t}B_{ij}(\vec{r},t$ I must write down the Navier-Stokes equation for the i-th velocity component at the point $\vec{x}$ and the j-th velocity component at the point $\vec{x}+\vec{r}=\vec{x'}$, and multiply the first of them by u'_j and the second for u_i. I then add both equations together and take an average. Finally, the homogeneous turbulence $\frac{\partial}{\partial x_k}$ and $frac\partial\partial x'_k$ can be replaced by $-\frac{\partial}{\partial r_k}$ and $frac\partial\partial r_k$. This procedure leads to the basic dynamic equation realting the second and the third velocity moments in homgeneous turbulence. Now I introduce the assumption of isotropic turbulence. In that case the functions B_{pi} and B_{ip} must be identically vanish and the tensor of second and third order can be expressed in terms of B_{LL} and $B_{LL,L}$ (the significance of $B_{LL,L}$ is clear from the notation). If I substitutethe corresponding expressions in the equation obtained from the Navier-Stokes equation I get the following equation that was first derived by von Karman and Howarth (1938):

$$\frac{\partial B_{LL}(r,t)}{\partial t} = \left(\frac{\partial}{\partial r}+\frac{4}{r}\right)\left[B_{LL,L}(r,t)+2\nu\frac{\partial B_{LL}(r,t)}{\partial r}\right] \tag{3.1.4}$$

The von Karman-Howarth equation plays a basic part in isoptropic turbulence.
In addition to 3.1.4 there is also an equation relating the spectral function $F(k,t)$ (or the spectral energy $E(k,t)=4\pi k^2F(k,t)$) with the third-order spectral function $F(k,t)$ which defines the Fourier transform of the tensor $B_{ij,k}$. Hence the following equation is merely a new form of 3.1.4:

$$\frac{\partial F(k,t)}{\partial t} = 2kF_3(k,t) - 2\nu k^2F(k,t) \tag{3.1.5}$$

This is the required spectral form of the von Karman-Howarth equation and describes the time variation of the wave number k distribution of turbulent energy. It has a simple physical interpretation which is important for understanding the mechanism of turbulent mixing as widely discussed in [Monin and Yaglom (1975)].

3.2 Correlations and spectra containing the temperature.

I consider isotropic turbulence in a temperature inhomogeneous fluid. In this case also the temperature fluctuations form a homogeneous and isotropic random field. Subject to the usual assumption than the velocity $\vec{u}\,(\vec{x},t)$ is small in compariosn with the sound velocity and the temperature changes are small in comparison with the mean absolute temperature, I can assume that the density ρ, the molecular viscosity $\nu = \eta\rho$ and the temperature diffusivity $\chi = \chi_c/c_p\rho$ can be regarded as constants. I shall also adopt that that radiative heat transfer and the heating of the medium due to the kinetic energy dissipation can be neglected. The temperature fluctuations $\vartheta\,(\vec{x},t)$ will then satisfy the usual thermal conduction equation

$$\frac{\partial\vartheta}{\partial t} + u_\alpha\frac{\partial\vartheta}{\partial x_\alpha} = \chi\Delta\vartheta \tag{3.2.1}$$

which is precisely the same as a diffusion equation for a passive admixture with molecular diffusion coefficient χ. I note that, in the termal equation 3.2.1, I can interpret ϑ as the deviation of temperature (or concentration) at given point from the constant mean value $\overline{\vartheta}$. Below I shall start with equation 3.2.1 so that all the subsequent discussion will be valid both for temperature and concentration of a passive admixture. Multiplying equation 3.2.1 for the point $\vec{x}$ by $\vartheta' = \vartheta\left(\vec{x'}\right)$ and the same equation for the point $\vec{x'}$ by $\vartheta = \vartheta\,(\vec{x})$, and adding the two term by term, I find after taking average that in case of homogeneous turbulence

$$\frac{\partial B_{\vartheta\vartheta}(\vec{r},t)}{\partial t} = \frac{\partial}{\partial r_k}\left[B_{k\vartheta,\vartheta}(\vec{r},t) - B_{k\vartheta,\vartheta}(-\vec{r},t)\right] + 2\chi\frac{\partial^2 B_{\vartheta\vartheta}(\vec{r},t)}{\partial r_k\partial r_k} \tag{3.2.2}$$

where I consider $\overline{\vartheta} = 0$, $\vartheta = \vartheta'$ and $B_{\vartheta\vartheta} = B_{\vartheta'\vartheta'} = \overline{\left[\left(\vartheta(\vec{x}) - \overline{\vartheta}\right)\left(\vartheta(\vec{x'}) - \overline{\vartheta}\right)\right]}$. I shall adopt this convention henceforth. If the turbulence is isotropic, then $B_{\vartheta\vartheta}(\vec{r}) = B_{\vartheta\vartheta}(r)$ where $r = |\vec{r}|$ and $B_{k\vartheta,\vartheta}(\vec{r},t) = B_{L\vartheta,\vartheta}(r)\frac{r_k}{r}$. In this case the equation 3.2.2 assumes the form

$$\frac{\partial B_{\vartheta\vartheta}(\vec{r},t)}{\partial t} = 2\left(\frac{\partial}{\partial r} + \frac{2}{r}\right)\left[B_{L\vartheta,\vartheta}(r,t) + \chi\frac{\partial B_{\vartheta\vartheta}(r,t)}{\partial r}\right] \tag{3.2.3}$$

The equation 3.2.3, which plays the role of the von Karman-Howarth equation for the temperaure field, was first established by Corrsin (1951). As in case of the von Karman-Howarth equation, the Corrsin equation 3.2.3 relates two unkown functions $B_{\vartheta\vartheta}(r,t)$ and $B_{L,\vartheta\vartheta}(r,t)$. Equation 3.2.3 can be transformed to a form containing the

temperature spectrum $F_{\vartheta\vartheta}(k,t)$ (or the function $E_{\vartheta\vartheta}(k,t) = E^{(\vartheta)}(k,t) = F_{\vartheta\vartheta}(k,t)$) and the function $F_{L\vartheta,\vartheta}(k,t)$ given by

$$F_{j\vartheta,\vartheta}(\vec{k}) = iF_{L\vartheta,\vartheta}(k)\frac{k_j}{k} \tag{3.2.4}$$

where $F_{j\vartheta,\vartheta}(\vec{k})$ is the Fourier transform of thr vector $B_{j\vartheta,\vartheta}(\vec{r})$. In fact, if I take the 3D Fourier transform of all the terms in 3.2.3 I obtain

$$\frac{\partial F_{j\vartheta,\vartheta}(\vec{k},t)}{\partial t} = iK_j\left[F_{j\vartheta,\vartheta}(\vec{k},t) - F_{j\vartheta,\vartheta}(-\vec{k},t) - 2\chi k^2 F_{\vartheta\vartheta}(\vec{k},t)\right] \tag{3.2.5}$$

By 3.2.4, the last equation can be rewritten as

$$\begin{aligned}\frac{\partial F_{\vartheta\vartheta}(k,t)}{\partial t} &= \Gamma_{\vartheta\vartheta}(k,t) - 2\chi k^2 F_{\vartheta\vartheta}(k,t) \\ \Gamma_{\vartheta\vartheta}(k,t) &= -2kF_{L\vartheta,\vartheta}(k,t)\end{aligned} \tag{3.2.6}$$

or

$$\begin{aligned}\frac{\partial E_{\vartheta\vartheta}(k,t)}{\partial t} &= T_{\vartheta\vartheta}(k,t) - 2\chi k^2 E_{\vartheta\vartheta}(k,t) \\ T_{\vartheta\vartheta}(k,t) &= -8\pi k^3 F_{L\vartheta,\vartheta}(k,t)\end{aligned} \tag{3.2.7}$$

where the terms $\Gamma_{\vartheta\vartheta}(k,t)$ and $T_{\vartheta\vartheta}(k,t)$ represent the turbulent mixing. Equation 3.2.6 (or 3.2.7) is the required spectral form of 3.2.3. Equation 3.2.7 describes the time variation of the wave-number distribution of the temperature fluctuations intensity $\overline{\vartheta'^2} = B_{\vartheta\vartheta}(0)$, which is the natural measure of the inhomogenenity of the temperature field $\vartheta(\vec{x})$. This inhomogenenity measure will vary only under the action of the thermal conduction which leads to an equation for the temperature field. Turbulent mixing of the fluid which is producted by the velocity field $\vec{u}(\vec{x})$ will then play a very important role: it will lead to a random approaches of particles with very different temperature, i.e. it will produce large temperature gradients resulting in a rapid enhancement of heat transfer due to the molecular thermal conduction. If I reformulate these physical ideas in terms of the spectrum language, this will mean that turbulent mixing (described by the term $T_{\vartheta\vartheta}(k,t)$ in 3.2.7) will give rise to a redistribution of the temperature field disturbances over the wave number spectrum; namely, it will lead to a conversion of the intensities $E_{\vartheta\vartheta}(k)$ for small values of k into the values of $E_{\vartheta\vartheta}(k)$ for large k, without any effect of total intensity $\int_0^\infty E_{\vartheta\vartheta}(k)dk = \overline{\vartheta'^2}$. It is clear that the function $T_{\vartheta\vartheta}(k)$ shoud satisty the equation

$$\int_0^\infty T_{\vartheta\vartheta}(k)dk = 0 \tag{3.2.8}$$

In fact, using 3.2.4 I can readily show that the left-hand side of 3.2.8 is equal to $\overline{u_l(\vec{x})\frac{\partial\vartheta^2(\vec{x})}{\partial x_l}} = \overline{\frac{\partial u_l(\vec{x})\vartheta^2(\vec{x})}{\partial u_l}}$, which vanishes beacause the turbulence is homogeneous. Therefore, by integrating 3.2.7 with respect to k I obtain

$$\frac{\partial\overline{\vartheta'^2}}{\partial t} = \frac{\partial}{\partial t}\int_0^\infty E_{\vartheta\vartheta}(k)dk = 2\chi\int_0^\infty k^2 E_{\vartheta\vartheta}(k)dk \tag{3.2.9}$$

as expected.

3.3 The simplest consequences of the correlation and spectral equations.

In this section I analise some simple consequences of the section 3.2. In particular I focus on scalar fields, and especially on the temperaure field. In fact, the knowledge of the beahaviour of the temeprature field is needed in the LSM for buoyant plume rise I shall present in chapter 6. The corresponding dissertation about velocity can be found in [Monin and Yaglom (1975)].

3.3.1 Balance equation for energy and temperature fluctuations intensity.

The equation for the correlation and spectral functions discussed in the section 3.2 involve functions of two variables, r (or k) and t. These equations lead to a number of predictions about the numerical values of parameters describing the turbulence as a whole, i.e. parameters independent of r and k. To obtain these results it is sufficient to expand some equations of section 3.2.1, and then equate the corresponding coefficients on either side of the resulting equation. In particular, if I use the expansion of the correlation function into a Taylor series in power of r, or the spectra into a Taylor series in power of k, I can obtain relations which have a clear physical interpretation and therefore deserve special consideration. I now derive some consequences from the Corrsin equation 3.2.3 for the temperature correlation function. Substituting $r = 0$ into this equation, I obtain

$$\frac{\mathrm{d}\overline{\vartheta^2}}{\mathrm{d}t} = 6\chi B^{II}_{\vartheta\vartheta}(0) = -\frac{12\chi\overline{\vartheta^2}}{\lambda^2_\vartheta} \tag{3.3.1}$$

where $\lambda_\vartheta^2 = -\frac{\overline{\vartheta^2}}{B^{II}_{\vartheta\vartheta}(0)}$ is the temperature microscale introduced by Corrsin (1951). As usual I assumed that $\overline{\vartheta} = 0$ where ϑ is the temperature fluctuation. The length scale λ_ϑ can also ne determined from the formula

$$\frac{1}{\lambda_\vartheta^2} = \frac{2}{\overline{\vartheta^2}}\overline{\left(\frac{\partial\theta}{\partial x}\right)^2} = \frac{2}{\overline{\vartheta^2}U^2}\overline{\left(\frac{\partial\theta}{\partial t}\right)^2} \tag{3.3.2}$$

Equation 3.3.1 describes the rate of decrease of the mean square of temperature fluctuations (the intensity of temperature fluctuations, or ther measure of the temperature inhomogenenity) due to the thermal conductivity. Expanding all the terms in 3.2.3 in series in powers of r^2, and equating the coefficients of r^2 on either side (multiplied by -3) I obtain the following equation for the rate of change of mean square temperature gradient:

$$-\frac{3}{2}\frac{\mathrm{d}}{\mathrm{d}t}B^{II}_{\vartheta\vartheta}(0) = -5B^{III}_{L\vartheta,\vartheta}(0) - 5\chi B^{IV}_{\vartheta\vartheta}(0) \tag{3.3.3}$$

The last term on the right-hand side is always negative. It decribes the decrease in the mean square temperature gradient due to molecular thermal diffusivity. The first term of the right-hand side is always, since it describes the increase in the temperature gradient due to the inertial approach of fluid particles with very different temperature.

3.3.2 Corrsin integrals.

The ordinary differential equation, which is obtained by expanding the partial differential equaion 3.2.3 in power series, describes the time variation of local characteristic of isotropic turbulence at a fixed point in the flow. An equivalent equation can also be obtained by multiplying all teh term of spectral equation 3.2.6 by the corresponding power of k and integrating over all values of k. If, however, I expand all the terms of 3.2.6 in a Taylor series of k, and equate the corresponding coefficients on the right and left-hand sides, I obtain equations which have a completely different character. These new equations relate quantities characterizing the behaviour of spectral densities near the point $k = 0$, i.e. they govern the asymptotic behaviour of the longest wavelength components of the flow variables. Such quantities are the integral characteristics of turbulence, and depend on the values of the correlation function for all the values of r between zero and infinity. The corresponding relations cannot, of course, be verified on the basis of measurements or any other experimental data. The fact that any real turbulence can be regarded as isotropic only

in a finite region plays a decisive role in this context. Nevertheless, the asymptotic relations governing the behaviour of the spectral functions at low wave numbers are interesting from the theoretical viewpoint. Assuming that the functions $F_{\vartheta\vartheta}(k)$ and $F_{L\vartheta,\vartheta}(k)$ can be expanded in Taylor series in the neighborhood of the point $k = 0$, I obtain from equation 3.2.6

$$\begin{aligned} &\frac{\mathrm{d}f_0^{(\vartheta)}}{\mathrm{d}t} = 0 \Rightarrow f_0^{(\vartheta)} = const \\ &\frac{\mathrm{d}f_2}{\mathrm{d}t} = -2g_1^{(\vartheta)} - 2\chi f_0^{(\vartheta)} \\ &\ldots\ldots\ldots\ldots\ldots\ldots\ldots\ldots \end{aligned} \tag{3.3.4}$$

where $f_n^{(\vartheta)}$ and $g_n^{(\vartheta)}$ are the coefficient of k^n in the expansions of $F_{\vartheta\vartheta}(k)$ and $F_{L\vartheta,\vartheta}(k)$. The first of these equations has the form of a conservation law and can be rewritten in the form

$$\int_0^\infty r^2 B_{\vartheta\vartheta}(r)dr = K = const \tag{3.3.5}$$

This result can be simply obtained from 3.2.3. The quantity K is sometimes called *Corrsin integral*. Let me multiply all the term in 3.2.3 by r^2, integrate the resulting equation between $r = 0$ and $r = R$ and then let R tend to infinity. Assuming that the integral 3.3.5 converges, i.e. $B_{\theta\theta}(r)$ tends to 0 more rapidly than r^{-3} as $r \to \infty$, I obtain

$$\int_0^\infty r^2 B_{\vartheta\vartheta}(r)dr = \lim R \to \infty \left[2R^2 B_{L\vartheta,\vartheta}(R)\right] \tag{3.3.6}$$

Hence it is clear that the conservation law 3.3.5 will be valid provided only that the integral on the left-hand side of this equation converges, and the function $B_{L\vartheta,\vartheta}(r)$ tend to zero more rapidly than r^{-2} as $r \to \infty$.

Chapter 4

Locally isotropic turbulence.

4.1 General description of small-scale turbulence at large Reynolds numbers.

4.1.1 Definition of locally isotropic turbulence.

Consider a small space-time region and a given central point $(\vec{x_0}, t_0)$ in this region. I can then define a moving inertial set of coordinates travelling with a constant velocity $\vec{u}(\vec{x_0}, t_0)$ relative to the fixed (or absolute) set such that at time $t = t_0$ its origin lies at the point $\vec{x_0}$. Transition to this set of coordinates means that the usual coordinates x and time t can be replaced by $\vec{r}\vec{x} - \vec{x_0} - \vec{u}(\vec{x_0}, t_0)(t - t_0)$ and $\tau = t - t_0$. The first of these quantities clearly depends on $\vec{u}(\vec{x_0}, t_0)$ and is hence random. $\vec{u}(\vec{x_0}, t_0)$ is now replaced by the relative velocity $\vec{v}(\vec{r}, \tau) = \vec{u}(\vec{x}, t) - \vec{u}(\vec{x_0}, t_0)$. I can now formulate the following basic defintion:
A given turbulence in a space-time region G is called locally isotropic if, for any fixed value $\vec{u}(\vec{x_0}, t_0) = \vec{u}_0$, the multidimensional probability distribution for each finite set of relative velocity $\vec{v}(\vec{r_k}, \tau_k)$, $k = 1, ..., n$, which consists of the values of the velocity $\vec{u}(\vec{x}, t)$ at the $n + 1$ points $(\vec{x_0}, t_0), ..., (\vec{x_n}, t_n)$ of G, is
i) independent of $\vec{u_0}$;
ii) stationary (independent of t_0 in G);
iii)homogeneous (independent of x_0 in G);
iv) isotropic (i.e. invariant under rotations and reflections in the space of vectors $\vec{r}$).
The turbulence with sufficiently large Reynolds number is always locally isotropic

in any region whose linear dimension are less than L and whose time intervals are less than $T_0 = L/U$. In other words, if I restrict the attention to vectors $\vec{r_k}$ and time intervals τ_k such that $r_k \ll L$ and $\tau_k \ll T_0$, then for $Re \gg Re_{cr}$ the probability distribution for any finite set of $\vec{v_k}(\vec{r_k}, \tau_k)$ can be expected to be independet of $\vec{u_0}$ as well as stationary, homgeneous and isotropic.

4.1.2 The Kolmogorov similarity hyphoteses.

I now explicitly define the [Kolmogorov (1941)] hyphoteses. Kolmogorov wrote them for a probability distribution at N space-time points $(\vec{x}, t)$, whereas to my purposes it is sufficient to define them in space region $(\vec{x})$ aat fixed time t. I consider a region G within a turbulent flux and $\vec{x}^{(0)}$, $\vec{x}^{(1)}$,...,$\vec{x}^{(n)}$ are a set of pointsin G. I define now a new set of coordinates and the velocity differences as:

$$\vec{y} = \vec{x} - \vec{x}^{(0)} \tag{4.1.1}$$

$$\vec{v}(\vec{y}) = U(\vec{x}, t) - U(\vec{x}^{(0)}, t) \tag{4.1.2}$$

and f_N is the multidimensional PDF of $\vec{v}$ at the N points $\vec{y}^{(0)}$, $\vec{y}^{(1)}$,...,$\vec{y}^{(n)}$.
Definition of local homogeneity. The turbulence is locally homogeneous in G, if for each fixed N and $\vec{y}^n$ with $n = 1, ..., N$ multidimensional PDF f_N is independent of $\vec{x}^{(0)}$ and of $U(\vec{x}^{(0)}, t)$.
Definition of local isotropy. The turbulence is locally isotropic in G, if it is locally homogeneous and the PDF F_N is invariant under all rotations and translations of the set of points.
Local isotropy hyphotesis Within any turbulent flux with Re sufficiently high, the turbulence is, in good approximation, locally isotropic if G is sufficiently small (i.e. $\forall n |\vec{y}^n| \ll L$) and not in proximity of the bundaries of the flux or of the singularity.
First hypothesis of similarity For locally isoptropic turbulence, the PDF f_N is uniquely determined by the viscosity ν and by the TKE dissipation ϵ.
Second hypothesis of similarity If the modulus of the vectors $\vec{y}^m$ and of their difference $\vec{y}^m - \vec{y}^n$ ($m \neq n$) are large in respect to the η Kolmogorov scale, then the PDF f_N is uniquely determined by the TKE dissipation ϵ and does not depend onthe viscosity ν. I notice that the hyphoteses refer to the velocity differences. The use of the new set of coordinates allows to apply these hyphoteses to any turbulent flux.

4.2 Local structure of the temperature field for high Reynolds and Peclet numbers.

I now consider isotropic turbulence in a velocity and temperature inhomogeneous fluid. In this case also the temperature fluctuations form a homogeneous ans isotropic random field. Subject to the usual assumption than the velocity $\vec{u}\,(\vec{x},t)$ is small in comparison with the sound velocity and the temperature changes are small in comparison with the mean absolute temperature, I can assume that the density ρ, the molecular viscosity $\nu = \eta\rho$ and the temperature diffusivity $\chi = \chi_c/c_p\rho$ can be regarded as constants. I shall also adopt that that radiative heat transfer and the heating of the medium due to the kinetic energy dissipation can be neglected. The temperature fluctuations $\vartheta\,(\vec{x},t)$ will then satisfy the usual thermal conduction equation

$$\frac{\partial\vartheta}{\partial t} + u_\alpha\frac{\partial\vartheta}{\partial x_\alpha} = \chi\Delta\vartheta$$

which is precisely the same as a diffusion equation for a passive admixture with molecular diffusion coefficient χ. Below I shall start with equation 4.2.1 so that all the subsequent discussion will be valid both for temperature and concentration of a passive admixture. I consider the structure of the concentration field $\theta(\vec{x},t)$ for a dinamically passive admixture, mixed by locally isotropic turbulence. I shall suppose that $\theta(\vec{x},t)$ is the temperature transported by the wandering fluid particles and it has not appreciable effect on the turbulence. In other words, I shall consider forced convection in temperature-inhomogeneous fluids in the presence of developed turbulence of dynamic origin. The similarity hypotheses are based on physical ideas indicating that, for sufficiently high Reynolds numbers, the statistical state of velocity fluctuations in each sufficiently small space-time region is isotropic and quasi-stationary, and it is completely defined by the parameters ε and ν. It is natural to expect that the temperature fluctuations due to the mixing of portions of fluid with different initial temperatures will then be isotropic and stationary in small space-time regions. Consequently the scalar field $\theta(\vec{x},t)$ can be regarded as locally isotropic. However there is no reason to suppose that its statistical parameter will depend only on ε and ν. In fact, the evolution of temperature is described by the heat transfer equation containing the molecular temperature diffusivity $\chi = \chi_c/c_p\rho$. Therefore it is clear that the value of χ may affect the local structure of the scalar field $\theta(\vec{x},t)$. This effect cannot be neglected: in the case of intensive turbulent mixing, molecular thermal conductivity plays an important role, since the turbulent motion may lead to

approach of fluid volumes with very different temperatures, i.e. to a rapid increase of temperature gradients. However I must augment ε, ν and χ by one further quantity to obtain the complete set of parameters defining the statisitcal state of small-scale temperature fluctuations. I shall now define this quantity. When I investigate the local structure of the velocity field $\vec{u}(\vec{x},t)$ I assumed that $Re = L\Delta U\nu$ (where ΔU is a tipical velocity difference over a distance L) was sufficiently large, and considered the cascade process of fragmentation of macrostructural inhomogenenities. It was noted that, of all the quantities characterizing large-scale turbulent motions, the only one which affects sufficiently small disturbances is the rate of energy transfer from large-scale to small-scale motions. This finally results in conversion into heat through molecular viscosity. The temperature field can be considered in the same way. I must, however, assume that both the Reynolds number Re and the Peclet number $Pe = L_\vartheta \Delta_\vartheta U/\chi$ are large, where L_ϑ is the length over which there is an appreciable change in the mean temperature $\overline{\vartheta}(\vec{x})$, and $\Delta_\vartheta U$ is a typical change in the mean velocity over the distance L_ϑ (for $L_\vartheta > L$, I can replace L_ϑ and $\Delta_\vartheta U$ with L and ΔU). The cascade quantity fragmentation of velocity-field disturbances will also lead ti the fragmentation of macrostructural temperature inhomogeneities of scale L_ϑ into smaller-scale disturbances of the field $\theta(\vec{x},t)$. the typical temperature fluctuation $\vartheta' = \vartheta - \overline{\vartheta}$ will therefore be a measure of the degree of inhomogeneity of the temperature field in such regions. Following Obukhov it is convenient to take the quantity $H = \frac{1}{2}\rho \int_V \overline{\vartheta'^2} d\vec{x}$ as a measure of the temperature inhomogeneity in a volume V, i.e. to characterize the degree of temperature inhomogeneity of a unit mass by the quantity $\overline{\vartheta'^2}/2$ in analogy with the definition of the kinetic energy $\overline{\vec{u}'^2}/2$. Fragmentation of temperature inhomogeneities will result in the fact that the total measure of temperature inhomogeneity will increasingly concentrate in small-scale disturbances. However the quantity $\overline{\vartheta'^2}/2$ will remain the same for all types of change in temperature. In other words, the quantity $\overline{\vartheta'^2}/2$ satisfies a "conservation law" which is a consequence of the fact that the temperature, like the kinetic energy, does not change during the inertial motion of the fluid particles. A change in the degrre of temperature inhomogeneity can be produced only by molecular thermal conduction, leading to an equalization of temperatures at neighboring points, i.e. to a reduction in $\overline{\vartheta'^2/2}$. Let ε_θ be the mean "dissipation rate of temperature inhomogeneities" i.e. the rate of reduction in the measure of temperature inhomogeneities $\overline{\vartheta'^2}/2$ due to the moleculat thermal conduction. For large value of Re and Pe, the "temperature dissipation rate" will be almost entirely concentrated in the smallest-scale disturbances, and will be equal to the "transport of the temperature-

inhomogeneity measure over the length scale spectrum", i.e. it will be equal to the increase per unit time in the contribution to $\overline{\vartheta'^2}/2$ associated with the small-scale disturbances of scale $l << min(L_\vartheta, L)$ and due to the fragmentation of large-scale temperature field inhomogeneities by the turbulent motions. It is clear that the quantity ε_ϑ may remain consntant in time if the large-scale inhomogeneities of scale L_ϑ are maintained by external heat sources which produce ixed distribution of mean temperature. Unless this is so, ε_ϑ will depend on t. However the time variation of ε_ϑ will be very slow in comparison with the characteristic time scales of sufficiently small-scale turbulent motions. Therefore, when I consider the statistical properties of small-scale temperature distrubance, the quantity ε_ϑ can be regarded as constant. It will, in fact, characterize the macrostructural inhomogeneities and will have an important effect on local isotropic temperature fluctutations. The quantity ε_ϑ is proportional to the coefficient χ and to the mean square of temperature gradient. In fact, I can use the heat transfer equation to show that for sufficiently large volume V, such that I can neglect convective heat transfer through its boundary, the reduction in temperature-inhomogeneity measure will be described by

$$\frac{\mathrm{d}H}{\mathrm{d}t} = -\chi \int_V \rho \overline{[\Delta\vartheta'(\vec{x},t)]^2} \mathrm{d}\vec{x}$$

Consequently, the specific (per unit of mass) rate of reduction is the temperature inhomogeneity measure given by

$$\varepsilon_\vartheta = \chi \overline{(\Delta\vartheta')^2} = \chi \sum_{i=1}^{3} \overline{\left(\frac{\partial\vartheta'}{\partial x_i}\right)^2} \tag{4.2.1}$$

For homogeneous turbulence, the mean convective transport of fluctuations ϑ' is zero not only after averaging over a large volume V but also at each point. In the case of locally isoptropic turbulence, therefore, the contribution of convective transport to the rate of change of $\overline{\vartheta'^2}/2$ will be determined only by the space derivatives of very smooth large-scale components of the flow variables, i.e. it will be negligible throughout. This is associated with the fact that for large Re and Pe I can neglect the effect of molecular thermal conduction on the mean flow, so that the formula 4.2.1 can also written in the form

$$\varepsilon_\vartheta = \chi \overline{(\Delta\vartheta)^2} = \chi \sum_{i=1}^{3} \overline{\left(\frac{\partial\vartheta}{\partial x_i}\right)^2} \tag{4.2.2}$$

This definition of ε_ϑ will be used below. The form of 4.2.2 is very close to the expression for the energy dissipation rate $\varepsilon = \frac{\nu}{2} \sum \overline{\left(\frac{\partial u_i}{\partial x_j} + \frac{\partial u_j}{\partial x_i}\right)^2}$. The quantities ε

and ε_ϑ are also very close to each other in their physical significance. I recall the entropy balance equation in e temperature inhomogeneous fluid

$$\rho T\left(\frac{\partial s}{\partial t}+u_\alpha\frac{\partial s}{\partial x_\alpha}\right)=\sigma_{\alpha\beta}\frac{\partial u_\alpha}{\partial x_\beta}+\frac{\partial}{\partial x_\alpha}\left(\chi_c\frac{\partial T}{\partial x_\alpha}\right) \tag{4.2.3}$$

where $\sigma_{\alpha\beta}$ is the viscous stress tensor. If I use the identity

$$\frac{1}{\vartheta}\frac{\partial^2\vartheta}{\partial x_i^2}=\frac{\partial}{\partial x_i}\left(\frac{1}{\vartheta}\frac{\partial\vartheta}{\partial x_i}\right)+\frac{1}{\vartheta^2}\left(\frac{\partial\vartheta}{\partial x_i}\right)^2 \tag{4.2.4}$$

and the fact that the mean absolute temperature $\overline{\vartheta}=T_0$ can be practically regarded as constant, I may conclude that ε is equal to T_0 multiplied by the mean rate of increase in entropy due to the internal friction (i.e. the molecular viscosity) and ε_ϑ is equal to T_0^2/c_p multiplied by the mean rate of increase in entropy due to the molecular thermal conduction. The quantity H is also found to have a simple physical meaning. Obukhov (1949a) has shown that it is equal to T_0/c_p multiplied by the maximum work which can be extracted from an inhomogeneously heated volume V through a reversible transition of this volume into a stase of thermodynamic equilibrium (i.e. constant temperature). This provides an additional justification for comparing temperature inhomogeneity measure H with the kinetic energy of turbulence, and the temperture dissipation rate ε_ϑ with the energy dissipation rate ε. The quantity ε_ϑ can also be determined from the quantitites characteristic of large-scale mean motion which is independent of the molecular transport coefficients. Since ε_ϑ has the dimension of a square temperature divided by time, the order of magnitude of ε_ϑ can be estimted from the relation

$$\varepsilon_\vartheta\sim\frac{\Delta_\vartheta U\left(\Delta\overline{\vartheta}\right)^2}{L_\vartheta} \tag{4.2.5}$$

where $\Delta_\vartheta U$ and $\Delta\overline{\vartheta}$ are typical changes in the mean velocity and mean temperature over the distances L_ϑ which is an analogous of the relation between L and ε. If I suppose that L and L_ϑ are of the same order of magnitude (this is usually the case), and set $\varepsilon_\vartheta\approx K_{\vartheta\left(\frac{\Delta\overline{\vartheta}}{L}\right)^2}$ where K_ϑ is interpreted as the effective eddy temperature diffusivity, then it will follw that $K_\vartheta\sim\Delta U\sim K$, as expected. I shall use the length scale $L_0=min(L,L_\vartheta)$ which can be identified if L and with L_ϑ if they are of the same order of magnitude. For the statistical turbulence characteristics containing temperature, the quasi-equilibrium range of l will then be defined by the inequality $l<<L_0$. The first similarity hyphotesis will now assume the following

form. *First similarity hyphotesis. In developed turbulence with sufficiently high values of Re and Pe, the multidimensional probability distributuions for velocity and temperature differences at an arbitrary set of points in a spatial region V of diameter $l << L_0$ are invariant under all rotations and translations of this set of points, provided these transformations do not take it beyond the limits of the region V, and are uniquely determined by the parameters ε, ν, ε_ϑ and χ.* Let me to generalize the second similarity hyphotesis to the case of probability distributions containing temperature differences. I note that, for sufficiently high values of Pe, the molecular theraml conducivity which is characterized by χ, may play an appreciable role only for very small-scale disturbances. In fact, the ratio of the typical values of the terms in the heat-transfer equation which describe the convection of heat and molecular thermal conduction is equal to the Peclet number. Therefore, the molecular thermal conduction is important only for disturbances with $Pe << 1$. It is natural to suppose that the Peclet number decreases monotonically with decreasing length scale of the disturbances. Therefore, for a sufficiently large Peclet number of the mean flow, there should exist a subrange of length scales which are small in comparison with L_0 and for which the Peclet number is much greater than unity. In this subrange, all the statistical characteristics should be independent of χ. It can be referred to as the *convective subrange*. If I attempt to determine the order of magnitude for the lower limit of the convective subrange, I encounter a specific difficult connected with the presence of the two quantities ν and χ which have the same dimensions. It follows that the dimensionless parameters of small-scale turbulence which contain temperature will, in general, be functions of the dimensionless parameter $Pr = \nu/\chi$, i.e. the Prandtl number. In particular, the ratio of the length scales of the smallest-scale disturbances which are appreciably effected by molecular thermal conductivity to the Kolomogorov internal length scale $\eta = \left(\nu^3/\varepsilon\right)^{1/4}$ will also be the function of the Prandtl number. therefore, the convective subrange of length scale is determined by inequalities of the form $L_0 >> l >> \lambda(Pr)\eta$ where $\lambda(z)$ is a universal function. Instead of the length scale η I can use the so-called internal temperature length scale

$$\eta_\vartheta = \left(\chi^3/\varepsilon\right)^{1/4} = \eta(Pr)^{-3/4} \tag{4.2.6}$$

However, the conclusion that for $l >> \eta_\vartheta$ I are necessarily within the limits of the convective subrange cannot be regarded as justified, since the possibility of neglecting molecular conductivity in comparison with convection will also depend on the velocity field which is affected by the viscosity ν. However, these considerations are important only in the limiting cases $\nu << \chi$ and $\nu >> \chi$ which appear to be rela-

tively exotic. It will be shown there that when $\nu << \chi$, i.e. $\eta_\vartheta >> \eta$, the convective subrange exteds only to scales $l >> \left(\frac{\nu\chi^2}{\varepsilon}\right)^{1/4} = \left(\eta\eta_\vartheta^2\right)^{1/3}$. In the more usual situation, $Pr \sim 1$, the scales η, η_ε and $\left(\eta\eta_\vartheta^2\right)^{1/3}$ are of the same order of magnitude, and $\lambda(Pr)$ becomes a numerical coefficient of the order of unity. Therefore, for $Pr \sim 1$, the upper limits of the subranges in which the molecular friction or molecular thermal conductivity are still important may be regarded as coincident. Let ,e now consider the *intertial-convective subrange* of length scales $L_0 >> l >> \eta_0 = max(\eta, \eta_\varepsilon)$ which is the intersection of the convective and inertial subrange. For disturbances with length scales lying in this subrange I can neglect both the internal friction and molecular thermal conductivity. In other words I have the following hypothesis. *The second similarity hyphotesis. In developed turbulence with sufficiently high values of Re and Pe, the multidimensional probability distributions for the velocity and temperature differences at a set of points, such that all the distances r_k between the points satisfy the inequalities $L_0 >> r_k >> \eta_0 = max(\eta, \eta_\vartheta)$, are uniquely determined by the values of the parameters ϵ and ϵ_ϑ.* The similarity hyphoteses lead to certain simple consequences with regard to the statistical characteristic of the spatial temperature differences $\Delta_{\vec{r}}\vartheta = \vartheta(\vec{x}+\vec{r}) - \vartheta(\vec{x})$ in turbulent flows with sufficiently large Re and Pe. In particular, it follows from the first similarity hyphotesis that, in the quasi-equilibrium range $r << L_0$, the spatial temperature structure function $D_{\vartheta\vartheta(r)} = \overline{(\Delta_{\vec{r}}\vartheta)^2}$ depends only on $r = |\vec{r}|$, and should be of the form

$$D_{\vartheta\vartheta}(r) = \varepsilon_\vartheta \epsilon^{-1/2} \chi^{1/2} h\left(\frac{r}{\eta_0}; \frac{\nu}{\chi}\right) \tag{4.2.7}$$

where $h(x; z)$ is an universal functions of the two variables. For sufficienlty small r, the difference $\Delta_{\vec{r}}\vartheta$ can be regarded as an aprroximately linear function of $\vec{r}$, so that $D_{\vartheta\vartheta}(r) \sim r^2$ for small r and $h(x; z) \sim x^2$ for small x. I shall assume for simplicity that the number $Pr \sim 1$ and, consequently, the scales η and η_ϑ are of the same order of magnitude. I then have $h(x; Pr) \approx h_0 x^2$ for $x << 1$, and $D_{\vartheta\vartheta}(r) = h_0 \frac{\varepsilon_\theta}{\chi} r^2$ for $r << \eta_\theta$. It is readily shown that the numerical coefficient $h_0 = \frac{1}{2}\frac{\partial^2 h(x;Pr)}{\partial x^2}|_{x=0}$ is independent of Pr. In fact, since according to 4.2.2 $\overline{(\Delta_\vartheta)^2} = \frac{3}{2}D"_{\vartheta\vartheta}(0) = \frac{\varepsilon_\vartheta}{\chi}$ I have

$$D_{\vartheta\vartheta}(r) = \frac{\varepsilon_\vartheta}{3\chi} r^2 \qquad for \quad r << \eta_0 \tag{4.2.8}$$

i.e. $h_0 = 1/3$ and $h(x; Pr) \approx x^2/3$ for $x << 1$. In the other limiting case $r << \eta_\vartheta$ (but $r << L_0$) I can use the second similarity hyphotesis, which leads to the result

that, for such r,

$$D_{\vartheta\vartheta}(r) = C_\vartheta \varepsilon_\vartheta \varepsilon^{-1/3} r^{2/3} \tag{4.2.9}$$

i.e. $h(x; Pr) \approx C_\vartheta x^{2/3}$ for $x >> 1$ where C_ϑ is a universal constant.
In addition to the structure function $D_{\vartheta\vartheta}$ I can also consider the spectrum of local isotropic temperature field, $E_{\vartheta\vartheta}(k) = E^{(\vartheta)}(k)$, or corrispondently one-dimensional spectrum $E_1^{(\vartheta)}(k)$. Similarly to 4.2.7, spectral equations have the form

$$\begin{aligned} E^{(\vartheta)}(k) &= \varepsilon_\vartheta \varepsilon^{-3/4} \chi^{5/4} \varphi^{(\vartheta)}(k\eta_\vartheta; Pr) \\ E_1^{(\vartheta)}(k) &= \varepsilon_\vartheta \varepsilon^{-3/4} \chi^{5/4} \varphi_1^{(\vartheta)}(k\eta_\vartheta; Pr) \end{aligned} \tag{4.2.10}$$

where the function $\varphi^{(\vartheta)}(\zeta; Pr)$ and $\varphi_1^{(\vartheta)}(\zeta; Pr)$ are related to $h(x; Pr)$. The equation 4.2.9 is equivalent to the ther two following equations:

$$\begin{aligned} E^{(\vartheta)}(k) &= B^{(\vartheta)} \varepsilon_\vartheta \varepsilon^{-1/3} k^{-5/3} \\ E_1^{(\vartheta)}(k) &= B_1^{(\vartheta)} \varepsilon_\vartheta \varepsilon^{-1/3} k^{-5/3} \end{aligned} \tag{4.2.11}$$

which are valid for $1/L << k << 1/\eta_\vartheta$. Here $B^{(\vartheta)}$ and ${}_1^{(\vartheta)}$ are universal constants given by

$$\begin{aligned} B^{(\vartheta)} &= \frac{10 C_\vartheta}{9\Gamma(1/3)} \approx 0.4 C_\vartheta \\ B_1^{(\vartheta)} &= \frac{3}{5}{}^{(\vartheta)} \approx 0.25 C_\vartheta \end{aligned} \tag{4.2.12}$$

The formulas 4.2.8 and 4.2.9 (the first of these represents the *temperature two-thirds law*) are due to Obukhov (1949a). The *temperature five-thirds law* 4.2.11, which is equivalent to 4.2.9, was given by Corrsin (1951b). The similarity hypotheses can be also used to obtain various expression for higher-order moments of the differences $\Delta_r \vartheta$, and also the the higher-order joint moments of $\Delta_r \vartheta$ and $\Delta_r \vec{u}$ (the second moment $\overline{\Delta_r \vartheta \Delta_r \vec{u}}$ is zero). Thus, for example, the third-order moment $D_{i\vartheta\vartheta}(\vec{r}) = \overline{\Delta_r u_i (\Delta_r \vartheta)^2}$ is determined (Yaglom 1949b) by the scalar function

$$D_{L\vartheta\vartheta}(r) = \overline{\Delta_r u_L (\Delta_r \vartheta)^2} = \varepsilon_\vartheta \varepsilon^{-1/4} \chi^{3/4} i(r/\eta_\vartheta; Pr) \tag{4.2.13}$$

where $i(r/\eta_\vartheta; Pr)$ is a universal function and

$$D_{L\vartheta\vartheta}(r) = d_1 \varepsilon_\vartheta \varepsilon^{1/2} \chi^{-3/2} r^3 \quad r << min(\eta, \eta_\vartheta) \tag{4.2.14}$$

$$D_{L\vartheta\vartheta}(r) = D_1\varepsilon_\vartheta r \quad L_0 >> r >> max(\eta, \eta_\vartheta) \tag{4.2.15}$$

However the two scalar functions $D_{LL\vartheta} = \overline{(\Delta_r u_L)^2 \Delta_r \vartheta}$ and $D_{NN\vartheta} = \overline{(\Delta_r u_N)^2 \Delta_r \vartheta}$ which define the third-order tensor $D_{ij\vartheta} = \overline{\Delta_r u_i \Delta_r u_j \Delta_r \vartheta}$, are both equal to zero by virtue of the general equation $D_{j\vartheta} = 0$. The situation is more complicated in case of the time differences

$$\Delta_\tau \vartheta = \vartheta(\vec{x}, t+\tau) - \vartheta(\vec{x}, t) \tag{4.2.16}$$

If, however, I are concerned with time intervals τ (or frequencies ω) for which the Taylor frozen turbulence hyphotesis is valid, then the corresponding characteristics can be readily reduced to those of the space differences $\Delta_r \vartheta$, which were discussed above. In particular, for $\eta_\vartheta/\overline{u} << \tau << L_0/\overline{u}$ or $\overline{u}/L_0 << \omega << \overline{u}/\eta_\vartheta$, I have from 4.2.8, 4.2.10, and 4.2.15

$$D_{\vartheta\vartheta}(\tau) = C_\vartheta \varepsilon_\vartheta \varepsilon^{-1/3} \overline{u}^{2/3} \tau^{2/3}, \quad E^\vartheta(\omega) = B_1^{(\vartheta)} \varepsilon_\vartheta \varepsilon^{-1/3} \overline{u}^{2/3} \omega^{-5/3} \tag{4.2.17}$$

$$D_{L\vartheta\vartheta}(\tau) = \overline{\Delta_\tau u_L (\Delta_\tau \vartheta)^2} = D_1 \varepsilon_\vartheta \overline{u} \tau \tag{4.2.18}$$

In conclusion, I emphasize once again that all the above formulas are valid not only for the temperature, but also for the concentration of an arbitrary passive admixture. Therefore, the results given in this subsection will be valid, for example, for the humidity or concentration of carbon dioxide in the atmosphere. The paramters χ and ε_ϑ will, of course, have different values in all these cases.

4.2.1 Local statistical characteristics of turbulence in a thermally stratified fluid.

It was assumed above that temperature behaves as if it were a passive admixture, i.e. it has no appreciable effect on the dynamics of turbulence. However, in the important case of temperature-inhomogeneous fluid in a ravitational field, the temperature cannot be considered as a passive substance. In fact, in this case, temperature fluctuations give rise to density fluctuations which are in turn affectd by buoyancy. Therefore, the temperature distribution generates a field of buoyant acceleration, i.e., it affects the flow dynamics. Consequently, in the case of a thermally stratified fluid, the theory of similarity for small-properties of turbulence must be generalized in some way. I shall assume that the temperature inhomogeneities are small in comparison with the mean temperature of medium $\overline{\vartheta_A} = \vartheta_0$, and that the motion of the

medium is described by the Boussinesq equation of free convection. (Note that I use the letter ϑ for the temperature both when it is regarded to a passive admixture and when it affects the flow dynamics). The equations of free convection differ from the usual fluid dynamics equation for a temperature-inhomogeneous medium only by the presence of an additional term (for the vertical velocity) describing the buoyant acceleration, i.e. $-g\beta\vartheta'$, where $\vartheta' = \vartheta - \overline{\vartheta}$ is the temperature fluctuation, g is the gravitational acceleration and β is the thermal expansion coefficient (equal to $1/\vartheta_0$ for the case of an ideal gas). The presence of this additional term leads two important consequences. First, the vertical direction is a special one, and since the buoyant accelerations appear in motions of all scales, I may suspect that motions of all scales will be anisotropic. Second, to the dimensional parameters characterizing the motion of the fluid, I must now add the buoyancy parameter $g\beta = g/\vartheta_0$ whose dimension is $(ms^{-2}k^{-1})$. The effect of anisotropy, i.e. the dependence of statistical quantities containing the argument $\vec{r}$ or $\vec{k}$ on the angle between $\vec{r}$ or $\vec{k}$ and the vertical, can be eliminated by integrating the corresponding statistical quantities respect to all the possible direction of $\vec{r}$ or $\vec{k}$ (i.e. over the sphere respect to sall the possible direction of r=$|\vec{r}|$). This will result in only the mean data, which will not enable me to establsh unambiguously the corresponding three-dimensional parameters. Instead of integration over a sphere, I can consider the characteristic of two-dimensional fluid dynamical fields in fixed horizontal plane $z = const$, which are isotropic. The conclusions drawn from dimensional considerations, which are applied below to the three-dimensional structure averaged over a sphere, will also be valid for the corresponding two-dimensional characteristics in the $z = const$ plane. In a stratified fluid with large value of Pe and Re, all the turbulence fields can be regarded as locally axially symmetric (i.e. locally homogeneous in all direction and locally isotropic along horizontal directions). Let me now list the dimensional parameters which affect the small-scale structure of the velocity field $\vec{u}(\vec{x}, t)$ and the temperature field $\vartheta(\vec{x}, t)$ in a stratified fluid. The quasi-stationary temperaure fluctuations $\vartheta'(\vec{x}, t)$ in the quasi-equilibrium range are determined, as in a homogeneous fluid, by a constant influx ε_ϑ of the mean fluctuation intensity $\overline{T'^2}/2$ from the large-scale disturbance region, which is balanced by an equal outflow of mean intensity $\overline{T'^2}/2$ as a result of smoothing out of the field $\vartheta(\vec{x}, t)$ by molecular thermal conduction. This process is characterized by the parameters ε_ϑ and χ (together with the parameters which determine the velocity field producing convective mixing). The time evolution of velocity inhomomgeneities is described by the Boussinesq equations, which contain the dimensional parameters ν and g/ϑ_0. However the energy flux transferred from

disturbances of given length scale to disturbances of smaller length scale will now no longer be constant along this length scale spectrum. In fact, for a stable temperature stratification, I have, in addition to energy transfer from one type of disturbance to another, a loss of kinetic energy through work done against buoyancy forces in a broad range of length scales (which leads to conversion of the kinetic energy into potential energy). In the case of unstable stratification, turbulent motion of different scales will draw additional kinetic energy from the potential energy of the medium (the buoyancy forces will accelerate the fluid particles). It is important to note however that the mutual transformation of potential and kinetic energies in a given range of length scales l is determined by the same spectral components of the fluctuations $u'(x,t)$ and $\vartheta'(x,t)$ that are responsible for the transport of temperture inhomogeneity measure along the spectrum in this range. I therefore expect that, if the values of Re and Pe are sufficiently high, for $l << L_0$ the statistical source of the above energy conversions will not depend on the quantitative characteristic of the mean fields $\overline{u}(x,t)$ and $\overline{\vartheta}(x,t)$ having the scale L_0, and will be homogeneous in space e quasi stastionary in time. However, one would still expect that the presence of stratification may have an effect for scales much less than L_0 by producing an anisotropy in the probability distributions, owing to the special role of the dirction of the force of gravity. The sign of the vertical mean-temperature gradient may also be important since it influences the character of the mean mutual conversions of kinetic and potential energies. All this does not prevent the range of sclaes $l << L_0$ from becoming a quasi-equilibrium range in the sense in which this is defined in a nonstratified fluid. The kinetic energy distribution over the length scales in spectrum in this range will now be determined from the balance of inertial transport, the transformation into (postive or negative) potential energy and viscous dissipation. The total energy dissipation ε will then no longer be equal to the energy reaching the upper end of the length range under consideration. Nevertheless, it is reasonable to expect that ε will still influence the energy distribution for scales $l << L_0$, i.e. it will be an important energy parameters. In other word, it is probable that

for the turbulence in a stratified fluid with large Pe and Re there is a quasi-equlibrium range of length scales $l << L_0$ in which the multidimensional probabilty distributions for velocity and temperature differences can be regarded as stationary and homogeneous (but not isotropic, and axially symmetric only relative to the vertical) are uniquely determined by the parameters ε, ε_ϑ, g/ϑ_0, ν and χ.

This is in fact a generalization of the Kolmogorv similarity hypothesis to the case of turbulence in a stratified fluid due to Bolgiano (1959) and Obhukov (1959a). the

presence of additional parameter g/ϑ_0 complicates the use of dimensional reasoning in the study of local statistical properties of turbulence in a stratified medium. I shall use, in fact, the only one combination of ε, ε_ϑ and g/ϑ_0 which has the dimension of length, namely,

$$L_* = \frac{\varepsilon^(5/4)}{\varepsilon_\vartheta^{3/4}(g/\vartheta_0)^{3/2}} \tag{4.2.19}$$

Hence, it follows that, in a stratified medium, the general form of the longitudinal velocity structure function $D_{LL}(\vec{r})$ averaged over all directions of $\vec{r}$ for $|\vec{r}| << L_0$ should be of the form

$$D_{LL}(r) = \frac{1}{4\pi r^2}\int_{\vec{r}=r} D_{LL}(\vec{r})d\vec{r} = \nu^{1/2}\varepsilon^{1/2}\beta_{LL}(\vec{r}/\eta, \eta/L_*, \nu/\eta) \tag{4.2.20}$$

where $\eta = \nu^{3/4}\varepsilon^{-1/4}$ and $\beta_{LL}(x, y, z)$ is a universal function of the three variables. Further specifications of these formulas can be achieved by using the second Kolmogorov hypothesis according to which

the multidimensional distributions for the velocity and temperature differences at arbitrary pairs of points cannot depend on the molecular constants ν and χ provided only that the distances between the points are much greater than a certain fixed length η_0.

This hypothesys will also be valid in the case of thermal stratification, and for the same reasons as in the previous cases. In general, the length η_0 is given by relations of the form $\eta_0 = \eta\lambda(\eta/L_*, \nu/\chi)$ where $\lambda(y, z)$ is a function of the two variables. I shall show belw, however, that η_0 will nearly always be independent of g/ϑ_0. Consequently, $\lambda = \lambda(Pr)$ is independent of η/L_* and the length η_0 in a stratified medium can be choosen in the same way as in the previous subsection. For the sake of simplicity, I shall suppose henceforth that $\nu/\chi = Pr$ is of the order of unity (for air $Pr \approx 0.7$). In that case η_0 can be simply identified with η or with $\eta_\vartheta = \chi^{3/4}\varepsilon^{-1/4}$ which is of the same order of magnitude. Consider the longitudinal and lateral velocity structure functions $D_{LL}(r)$ and $D_{NN}(r)$, and the joint structure function for the temperature and vertical velocity $D_{\vartheta w}(r)$ for $L_0 >> r >> \eta_0$. All these functions are assumed to have been averaged with respect to the direction of the vector $\vec{r}$. In the above range, all these quantities will depend only on $\vec{r}$, ε, ε_ϑ and g/ϑ_0 and

therefore dimensional considerations indicate that

$$\begin{aligned} D_{LL}(r) &= C\varepsilon^{2/3}r^{2/3}f_{LL}(r/L_*) \\ D_{NN}(r) &= C'\varepsilon^{2/3}r^{2/3}f_{NN}(r/L_*) \\ D_{\vartheta\vartheta}(r) &= C_\vartheta\varepsilon_\vartheta\varepsilon^{-1/3}r^{2/3}f_{\vartheta\vartheta}(r/L_*) \\ D_{\vartheta w}(r) &= C"\varepsilon_\vartheta^{1/2}\varepsilon^{1/6}r^{2/3}f_{\vartheta w}(r/L_*) \end{aligned} \tag{4.2.21}$$

where C, C', C_ϑ and $C"$ are dimensionless constants which can be choosen arbitrarly. It will be convenient to assume that the first three of these coincide with corresponding coefficients in the two-thirds law of 4.2.9. I note that for stable and unstable stratification, ie. for different signs of $\mathrm{d}\overline{\vartheta}/\mathrm{d}z$, the functions $f_{LL}(x), ..., f_{\vartheta w}(x)$ may turn out to be different. Since the random fields $\vec{u}(\vec{x},t)$ and $\vartheta(\vec{x},t)$ are locally homogenenous, I can define the densities $F(\vec{k}) = \frac{1}{2}F_{ii}(\vec{k})$, $F_{\vartheta\vartheta}(\vec{k})$ and $F_{\vartheta w}(\vec{k})$ for them when $1/\eta_o >> k = |\vec{k}| >> 1/L_0$. If I write $E(k) = \int_{|\vec{k}|=k} F(\vec{k})d\vec{k}$ and similarly for the function $F_{\vartheta\vartheta}(\vec{k})$ and $F_{\vartheta w}(\vec{k})$, the dimensional considerations show that

$$\begin{aligned} E(k) &= C_1\varepsilon^{2/3}k^{-5/3}\psi(kL_*) \\ E_{\vartheta\vartheta}(k) &= B^{(\vartheta)}\varepsilon_\vartheta\varepsilon^{-1/3}k^{-5/3}\psi_{\vartheta\vartheta}(kL_*) \\ E_{\vartheta w}(k) &= B'\varepsilon_\vartheta^{1/2}\varepsilon^{1/6}k^{-5/3}\psi_\vartheta(r/L_*) \end{aligned} \tag{4.2.22}$$

where $\psi(\zeta)$, $\psi_{\vartheta\vartheta}(\zeta)$ and $\psi_{\vartheta w}(\zeta)$ are universal functions, B' is an arbitrary constant, and the constants C_1 and $B^{(\vartheta)}$ can be conveniently regarded as equal to the coefficients in the five-thirds law given by 4.2.11. When $g/T_0 = 0$, i.e. in the absence of gravitational forces which give rise to startification, the formulas 4.2.21 and 4.2.22 should become identical to the usual formulas for the structure and spectral functions of locally isotropic turbulence $\overline{\Delta_r u \Delta_r \vartheta} = 0$. If, on the other hand, $g/\vartheta_0 \neq 0$ but $r/L_* << 1$, i.e. $r << L_*$ (but $r >> \eta_0$), the the values of the correction function in 4.2.21 can be approximately replaced by their values at zero, i.e. I can use the ordinary two-thirds law which are valid for non-stratified media. Similarly when $k >> 1/L_*$ (but $k << 1/\eta_0$), the correction function in 4.2.22 can be approximately replaced by their values at infinity, i.e. I can use the usual five-thirds law. In other words, *the length scale L_* characterizes the minimum length scale of inhomogeneities beyond which effect of the the stratification is appreciable.* When $L_* >> \eta$ and $L_* >> \eta_\vartheta$ (and this is nearly always the case), I can ignore the stratification for $l >> L_*$ and use the usual form of second Kolmogorov similarity hyphotesis.

the above analysis provides additional support to the ise of the concept of locally isotropic turbulence and the associated similarity hyphoteses for stratified media, but shows that the upper limit of the inertial and inertial-convective length-scales subranges must satisfy the inequalities $l << L$ and $l << L_\vartheta$ as well as $l << L_*$. If $L_* << L_0 = min(L, L_\vartheta)$ then the inertial-convective subrange will be followed by the buoyancy subrange $L_0 >> l \geq L_*$ in which the probability distributions for $\Delta_r \vec{u}$ and $\Delta_r \vartheta$ can be regarded as quasi-stationary and homogeneous but no longer isotropic. the values of dimensionless correction functions in 4.2.21 and 4.2.22 can, in principle, be determined empirically, but the necessary experimental data are not available at present. In the case of stable startification, Bolgiano (1959, 1962) has put foward certain hyphoteses with regard to the asymptotic form of these functions for wave number much less than $1/L_*$, i.e. the length scale much greater than L_*. For a stable stratification, the energy transferred from disturbances of length scale $l \gg L_*$ to smaller-scale disturbances should be much greater than ε, since most of this energy is spent in work against the buoyancy forces, and only a very small fraction of it reaches the small-scale disturbances in which viscous dissipation is concentrated. On this basis, one would expect that even a considerable change in ε will have very little effect on the shape of turbulence spectra in the region of $k \ll 1/L_*$. This has lead Bolgiano to propose that the asymptotic form of the spectra $E(k)$, $E_{\vartheta\vartheta}(k)$, $E_{\vartheta w}(k)$ for $k \ll 1/L_*$ in the case of stable stratification should depend only on the values of parameters ε_ϑ and g/ϑ_0. From this, dimensional considerations yield

$$\begin{aligned} E(k) &= c_1 \varepsilon_\vartheta^{2/5} \left(\frac{g}{\vartheta_0}^{4/5} \right) k^{-11/5} \\ E_{\vartheta\vartheta}(k) &= b^{(\vartheta)} \varepsilon_\vartheta^{4/5} \left(\frac{g}{\vartheta_0}^{-2/5} \right) k^{-7/5} \\ E_{\vartheta w}(k) &= b' \varepsilon_\vartheta^{3/5} \left(\frac{g}{\vartheta_0}^{1/5} \right) k^{-9/5} \end{aligned} \tag{4.2.23}$$

where c_1, $b^{(\vartheta)}$ and b' are universal functions. Consequently one would expect that in case of stable stratification $\psi(\zeta) \approx \zeta^{-8/15}$, $\psi_{\vartheta\vartheta}(\zeta) \approx \zeta^{4/15}$ and $\psi_{\vartheta z}(\zeta) \approx \zeta^{-2/15}$ for $\zeta \ll 1$. Similar considerations lead to the following hypotheses which are equivalent to 4.2.23 about the asymptotic form of the structure functions averaged over all

directions for turbulence in a stratified medium:

$$\begin{aligned} D_{LL}(r) &= c\varepsilon_\vartheta^{2/5}\left(\frac{g}{\vartheta_0}^{4/5}\right) r^{6/5} \\ D_{NN}(r) &= c'\varepsilon_\vartheta^{2/5}\left(\frac{g}{\vartheta_0}^{4/5}\right) r^{6/5} \\ D_{\vartheta\vartheta}(r) &= c_{(\vartheta)}\varepsilon_\vartheta^{4/5}\left(\frac{g}{\vartheta_0}^{-2/5}\right) r^{2/5} \\ D_{\vartheta w}(r) &= c"\varepsilon_\vartheta^{3/5}\left(\frac{g}{\vartheta_0}^{1/5}\right) r^{4/5} \end{aligned} \tag{4.2.24}$$

when $r \gg L_*$, so that $f_{LL}(x) \approx x^{8/15}$, $f_{NN}(x) \approx x^{8/15}$, $f_{\vartheta\vartheta}(x) \approx x^{-4/15}$ and $f_{\vartheta w}(x) \approx x^{2/15}$ for $x \gg 1$. The above formulas are meaningful only if the length scales L_* is much less than the external length turbulence L_0. If, on the other hand, L_* approaches or even exceeds L_0, then not only the Bolgiano hyphoteses about the asymptotic form of the correction functions 4.2.21 and 4.2.22, but the entire similarity theory of this subsection will be invalid. In this last case, the inertial-convective subrange of the spectrum will be followed by a subrange of scales in which quantities characterizing the mean fields $\overline{\vec{u}}(\vec{x},t)$ and $\vartheta(\vec{x},t)$ will play an important role. This refers in particular to the hyphoteses of Shur (1962) and Lumely (1964) about the turbulence spectrum in a free atmosphere according to which the region of validity of five-thirds laws is followed in a stably stratified medium by a region of a smaller wave numbers where the velocity spectrum is proportional to k^{-3} and is determined by the parameters g/ϑ_0 and $\mathrm{d}\overline{\vartheta}(z)/\mathrm{d}z$, in accordance with the formula $E(k) \approx \frac{g}{\vartheta_0}\frac{\mathrm{d}\overline{\vartheta}}{dz}k^{-3}$.

The length scale L_* cannot be precisely defined for most real turbulent flows since the values of ε and ε_ϑ are unknown. A very rough estimate of the order of magnitude of the length scale of turbulence in a stratified medium occupying the half space $z > 0$ can be obtained from the relations $\varepsilon \approx \frac{(\Delta\overline{u})^3}{L}$ and $\varepsilon_\vartheta \approx \frac{\Delta\overline{u}\left(\Delta\overline{\vartheta}\right)^2}{L_\vartheta}$ (see section 4.2.1). Typical legth scales L and L_ϑ of the fields $\overline{u}(z)$ and $\overline{\vartheta}(z)$ in the present case are of the same order of magnitude as the distance z to the wall. Therefore,

$$L_* \approx \frac{(\Delta\overline{u})^3}{\left(\Delta\overline{\vartheta}\right)^{3/2}(g/\vartheta_0)^{3/2}\, z^{1/2}} \tag{4.2.25}$$

Near the wall, the most rapidly varying factor on the right-hand side is $z^{-1/2}$. I thus see that the length scale L_* decreasess with height quite rapidly, whereas the

external scale $L \approx z$ increases rapidly with height. therefore, one would expect that at sufficiently great heights, the length scale L_* will be appreciably less than L, and hence the effect of thermal stratification will begin to appear earlier that the effect of the mean flow parameters. In the case of the atmospheric layer near earth's surface, very approximate solutions due to Obukhov (1959a) show that the ratio z/L_* becomes equal to unity even at heights of the order of 10 m. It is therefore probable that the formulas given above will be valid beginning with heights of the order of 100 m.

Chapter 5

Lagrangian modelling

The Lagrangian stochastic single particle models (SPMs) have been widely tested and applied to many different situations characterised by non-homogenous turbulence and several stability conditions. In thie next section I give a brief summary of the theory of one-particle Lagrangian models ([Thomson (1987), Thomson (1990)]). Then in section 5.2 I will discuss the application of the Lagragian approach for evaluating the parameters of a SDE for temperature fluctuations included in the model for buoyant plume rise presented in chapter 6.

5.1 Lagrangian stochastic single particle model

In the energy spectrum between the Kolmogorov time scale t_η and the velocity correlation Lagrangian time scale T_L the evolution of a particle position and velocity in a turbulent flow can be considered as a bivariate Markov process, i.e. a process were present is correlated to past and future to present, but past and future are statistically independent. In order to avoid the viscous subrange and molecular diffusivity, κ, Lagrangian stochastic models are based on the hypothesis that $t_\eta \to 0$, or, in other words, that $t_\eta \to 0$ (in the atmosphere $Re \sim 10^7$) and that $\kappa \to 0$ ($Pe \to \infty$). Under the Markov assumption, the trajectories of independent fluid particles can be simulated through two stochastic differential equations ([Thomson (1987), Thomson

(1990)]):

$$du_i = a_i\left(\vec{u},\vec{x},t\right)dt + \sqrt{C_0\epsilon}dW_j(t) \tag{5.1.1}$$

and

$$dx_i = u_i dt \tag{5.1.2}$$

where $\vec{x}$ is the particle displacement, $\vec{u}$ is the particle velocity and dW represents the increment of a Wiener process with zero mean and variance:

$$\overline{dW_i(t)dW_j(s)} = \delta_{ij}\delta(t-s)dt \tag{5.1.3}$$

The coefficient $\sqrt{C_0\epsilon}$, where C_0 is an universal constant and ϵ is the dissipation of turbulent kinetic energy, ensures that Kolmogorov scaling in the inertial range is satisfied by the Lagrangian velocity structure function:

$$\overline{du_i(t)du_j(t)} = \delta_{ij}C_0\epsilon dt \tag{5.1.4}$$

As long as C_0 is an universal constant, in principle equation 5.1.4 can be applied to every kind of turbulence. Nevertheless in literature there is no agreement on its values that can show large variations in the different kinds of turbulence considered. To model turbulent absolute dispersion correctly the proper choice for the undetermined term a should be made. It is well known that equations 5.1.1 and 5.1.2 are equivalent to the Fokker-Planck equation:

$$\frac{\partial P_L}{\partial t} + \frac{\partial}{\partial x_i}\left(u_i P_L\right) = -\frac{\partial}{\partial u_i}\left(a_i P_L\right) + C_0\epsilon\frac{\partial^2 P_L}{\partial u_i \partial u_j} \tag{5.1.5}$$

where $P_L = P_L(\vec{u},\vec{x},t;\vec{u_0},\vec{x_0},t_0)$ represents the Lagrangian joint probability density of position and velocity of a single particle, given its position $\vec{x_0}$ and velocity $\vec{u_0}$ at time t_0 and it is generally unknown. Nevertheless it is possible to make an ensamble average of P_L over the Eulerian distribution of initial conditions to obtain the Eulerian PDF of velocities:

$$P_E\left(\vec{u},\vec{x},t\right) = \int P_L\left(\vec{u},\vec{x},t;\vec{u}_0,\vec{x}_0,s\right)P_E\left(\vec{u}_0,\vec{x}_0,s\right)d^3\vec{u}_0 d^3\vec{x}_0 ds \tag{5.1.6}$$

As long as the Fokker-Planck equation 5.1.6 is linear in P_L is satisfied by P_E as well. P_E is known and can be considered as a prescribed property of the flow. Therefore the equation:

$$\frac{\partial P_E}{\partial t} + \frac{\partial}{\partial x_i}\left(u_i P_E\right) = -\frac{\partial}{\partial u_i}\left(a_i P_E\right) + C_0\epsilon\frac{\partial^2 P_E}{\partial u_i \partial u_j} \tag{5.1.7}$$

is a constraint for the term a. In the idealized case of isotropic, homogeneous, stationary turbulence P_E does not depend on $\vec{x}$ and t and is simply function of the velocity. Equation 5.1.7 can be solved to obtain:

$$a_i = \frac{C_0\epsilon}{2P_E}\frac{\partial P_E}{\partial u_i} + \phi_i \tag{5.1.8}$$

that is the so called well-mixed condition and the fundamental constraint that a Lagrangian stochastic model has to satisfy [Thomson (1987)]. This constraint physically implies that if the particles are initially well-mixed they will remain so during the flow evolution, that the solution of the Fokker- Planck equation 5.1.5 are compatible with the Eulerian equations and that direct and inverse diffusion are equivalent. The vector $\overline{\phi}$, where:

$$\frac{\partial \phi_i\left(\mathbf{u},\mathbf{x}\right)}{\partial u_i} = -\frac{\partial P_E}{\partial t} - \frac{\partial u_i P_E}{\partial x_i} \tag{5.1.9}$$

or equivalently

$$\begin{cases} \phi_i\left(\mathbf{u},\mathbf{x}\right) = -\dfrac{\partial}{\partial x_i}\displaystyle\int_{-\infty}^{u_i} u_i P_E\left(\mathbf{u},\mathbf{x}\right) d\mathbf{u} \\ \phi_i \to 0 \qquad per \qquad |u_i| \to 0 \end{cases} \tag{5.1.10}$$

is a divergence free vector that shows that equation has no unique solution.
Only in the case of homogeneous, isotropic turbulence and Gaussian P_E:

$$P_E = \frac{1}{\sqrt{2\pi\sigma^2}} e^{-\frac{u^2}{2\sigma^2}} \tag{5.1.11}$$

the vector $\vec{a}$ can be shown to be unique [Thomson (1987), Borgas and Sawford (1994)]. In this simple situation (adding the hypothesis of stationarity) equation 5.1.1 becomes

$$du_i = -\frac{C_0\epsilon}{2\sigma_2} u_i dt + \sqrt{C_0\epsilon} dW_i(t) \tag{5.1.12}$$

where $\frac{C_0\epsilon}{2\sigma_2}$ is the inverse of the Lagrangian time scale $\frac{1}{T_L}$, hence equation 5.1.12 can also be written as:

$$du_i = -\frac{1}{T_L} u_i dt + \sqrt{C_0\epsilon} dW_i(t) \tag{5.1.13}$$

The linear system formed by equations 5.1.13 and 5.1.2 together with the initial condition that the velocity $\vec{u_0}$ is chosen randomly with distribution $P_E(\vec{u_0})$ can be exactly solved to give the Lagrangian positions PDF [Borgas and Sawford (1994)]:

$$P_L = \frac{1}{(2\pi)^{3/2} D^{1/2}} exp\left[-\frac{1}{2}(x_i - x_i(0)) D_{ij} (x_j - x_j(0))\right] \tag{5.1.14}$$

where

$$D_{ij} = 2\sigma_2 T_L^2 \left[exp\left(-\frac{t}{T_L}\right) \frac{t}{T_L} - 1 \right] \delta_{ij} \tag{5.1.15}$$

Equation 5.1.15 can be easily recognized as the result of [Taylor (1921)] theory of diffusion. It is worth noticing that in this simple case homogenity, isotropy, stationarity (this last request is not necessary for the uniqueness of the solution) and the Gaussian P_E determine the drift term a in the Langevin equation 5.1.1, but this can not be generalized to less idealized condition. In the case of inhomogeneous turbulence or of two-particle models the determination of ϕ is more complex and not unique.

The assumption that in homogeneous turbulence the velocity PDF can be considered Gaussian can be extended to the case of inhomogeneous turbulence, e.g. in the case of neutral boundary layer.

The only difference in equation 5.1 is the dependence of ϵ (and hence of σ_u amd of T_L) on x.

In the inhomogeneous case P_E depends on the spatial coordinates through σ_u (that usually depends only on z) Hence ϕ is not equal to zero as in the homogeneous case, but the equation 5.1.10 has to be solved:

$$\begin{aligned} \phi_i(\mathbf{u}, \mathbf{x}) &= -\frac{\partial}{\partial z} \int_{-\infty}^{u} u P_E(u, z)\, du = -\frac{\partial}{\partial z} \int_{-\infty}^{u} \frac{u}{\sqrt{2\pi}\sigma(z)} e^{-\frac{u^2}{2\sigma^2(z)}} du = \\ &= \frac{\partial}{\partial z}\left[\frac{\sigma(z)}{\sqrt{2\pi}} e^{-\frac{u^2}{2\sigma^2(z)}}\right] = P_E(u,z)\frac{u^2+\sigma^2(z)}{\sigma(z)}\frac{\partial \sigma(z)}{\partial z} \end{aligned} \tag{5.1.16}$$

Therefore, in inhomogeneous turbulence the Langevin equation is written as :

$$du_i = -\frac{u_i}{T_{Li}} dt + \frac{1}{2}\left(1 + \frac{u_i^2}{\sigma_{u_i}^2}\right) \frac{\partial \sigma_{u_i}^2}{\partial x_i} dt + \sqrt{C_0 \epsilon_i} dW_i(t) \tag{5.1.17}$$

Hence the spatial inhomogeneity produce a quadratic term in the velocity of the form:

$$\frac{1}{2} \frac{u_i^2}{\sigma_{u_i}^2} \frac{\partial \sigma_{u_i}^2}{\partial x_i} dt \tag{5.1.18}$$

This term arise from the well-mixed condition and it is needed to balances $\sigma_u \to 0$ at the boundaries of the domain and the resulting explsion of its derivative.

5.2 In the matter of models for buoyant plume rise

The main issue about the model for buoyant plume rise presented in the section 6.2 the evaluation of the temperature dissipation rate, ε_ϑ, defined in 4.2.1 and 4.2.2. A first attempt may be to relate ε_ϑ to σ_ϑ and T_ϑ, as in case of energy dissipation rate ε. In fact, it seems easier to give expressions with simple physical meanings to σ_ϑ and T_ϑ (i.e. $\sigma_\vartheta \propto |\overline{\vartheta} - \vartheta|$ and $T_\vartheta = T_L = b/|\overline{w}|$, see the section 6.2). Hence may be possible to consider $\varepsilon_\vartheta = \frac{2\sigma_\vartheta^2}{C_\vartheta T_\vartheta}$ in analogy with $\varepsilon = \frac{2\sigma_w^2}{C_0 T_L}$. Regarding ε the previous equation can be readily deducted from the temporal Lagrangian structure function $D_{LL}^{(L)}(\tau) = C_0 \varepsilon \tau$. In fact,

$$\begin{aligned} D_{LL}^{(L)}(\tau) &= \overline{[u(t+\tau) - u(t)]^2} \\ &= \overline{u^2(t+\tau)} - 2\overline{u(t+\tau)} + \overline{u^2(t)} \end{aligned} \tag{5.2.1}$$

I have assumed that the turbulence is stationary in small space-time regions (the wide-sense stationarity is enough to our purposes) so that the temporal Lagrangian autocorrelation function $R^{(L)}(t,\tau) = \frac{\overline{u(t)u(t+\tau)}}{\overline{u^2(t)}}$ is only function of τ, i.e. $R^{(L)}(t,\tau) = R^{(L)}(\tau)$, and $\sigma_u^2 = \overline{u^2(t+\tau)} = \overline{u^2(t)}$. Furthermore, for a Markov process the temporal autocorrelation function can be written as $R(\tau) = e^{-\tau/T_L}$ and its first-order Taylor series approximation is $R(\tau) = e^{-\tau/T_L} \approx 1 - \frac{\tau}{T_L} + O(\tau^2)$. Therefore

$$\begin{aligned} D_{LL}^{(L)}(\tau) &= 2\sigma_u^2 - 2\sigma_u^2 R^{(L)}(\tau) \\ &= 2\sigma_u^2 - 2\sigma_u^2 e^{-\tau/T_L} \\ &\approx \frac{2\sigma_u^2 \tau}{T_L} \end{aligned} \tag{5.2.2}$$

and being $D_{LL}^{(L)}(\tau) = C_0 \varepsilon \tau$, I have the expected equation $\varepsilon = \frac{2\sigma_u}{C_0 T_L}$. Is it possible to follow the same way for evaluating ε_ϑ? The first consideration is that, to our knowledge, an expression for the temporal Lagrangian structure function is not prescribed in literature. I found only the Eulerian structure function given by 4.2.17, i.e. $D_{\vartheta\vartheta}(\tau) = C_\vartheta \varepsilon_\vartheta \varepsilon^{-1/3} \overline{u}^{2/3} \tau^{2/3}$. Note that for velocity difference the Lagragian

structure function is different from the Eulerian one:

$$D_{LL}^{(L)}(\tau) = C_0\varepsilon\tau$$
$$D_{LL}(\tau) = C_0\varepsilon^{2/3}U^{2/3}\tau^{2/3} \tag{5.2.3}$$

In the Eulerian expression D_{LL} depends on $U = \overline{u}$, but in the Lagragian form $D_L L$ does not depend on it (the Lagrangian form of the structure function should be always independent of the mean wind). The Eulerian expression 4.2.17 for $D_{\vartheta\vartheta}$ depends on U as well. Is it possible to find a Lagrangian expression for $D_{\vartheta\vartheta^{(L)}}$ independent of U? $D_{\vartheta\vartheta}$ has to have the dimensions of a square temperature (K^2). In the equation 4.2.17, it is a function of ε, ε_ϑ, τ and U. Only the two parameters ε_ϑ and U depends on a length (i.e. in the dimension analysis they contain a (m)). Hence there is no way to make dimensionless $D_{\vartheta\vartheta}$ eliminating only U. A first approximation may be eliminate ε as well to obtain simply $D_{\vartheta\vartheta}^{(L)}(\tau) = C_\vartheta\varepsilon_\vartheta\tau$, but it is not acceptable because of the comments made in section 4.2. The simplest non-dimensional form for $D_{\vartheta\vartheta}^{(L)}(\tau)$ is:

$$D_{\vartheta\vartheta}^{(L)}(\tau) = C_\vartheta\varepsilon_\vartheta\varepsilon\overline{u}^{-2}\tau^2$$

Even assuming that this expression is right (and it is not trivial) and that the temporal autocorrelation function is an exponentially decreasing function for the temperature as well (and it should be right since I have assumed that the temperature admits a Langevin equation as the velocity), the dependence of τ cannot be eliminated (assuming that this dependece has to be eliminated). In fact, following the same method 4.2.20 used to obtain $\varepsilon = \frac{2\sigma_u}{C_0 T_L}$ in the case of velocity, I get $\varepsilon_\vartheta = \frac{2\sigma_\vartheta^2}{C_\vartheta T_\vartheta \frac{U^2}{\tau\varepsilon}}$. Therefore ε_ϑ seems to depends on U and τ. If I reformulate these observations in terms of the spectrum language, I get the same results. A second attempt to obtain a simple form for the temperature dissipation rates may be to derive it from the expression for the third-order structure functions, e.g. $D_{L\vartheta\vartheta}$. Now I focus on the possibility of relating $D_{L\vartheta\vartheta}$ to D_{LL} and $D_{\vartheta\vartheta}$ in order to give an expression to ε_ϑ and on the Lagrangian form of $D_{L\vartheta\vartheta}$ known. The development of the definition of $D_{L\vartheta\vartheta}$, i.e.

$$\begin{aligned} D_{L\vartheta\vartheta} \;=\; & \overline{u(t+\tau)\vartheta^2(t+\tau)} - 2\overline{u(t+\tau)\vartheta(t+\tau)\vartheta(t)} + \overline{u(t+\tau)\vartheta^2(t)} \\ & -\overline{u(t)\vartheta^2(t+\tau)} + 2\overline{u(t)\vartheta(t+\tau)\vartheta(t)} - \overline{u(t)\vartheta^2(t)} \end{aligned} \tag{5.2.4}$$

may lead to some useful relationships. It needs some further investigations. All the considerations given above refer to the case in which the temperature behaves as if it were a passive admixture, i.e. it has no appreciable effect on the dynamics of turbulence. However, in the study of a plume rise, especially for a large fire like the Buncefield one (see 6.4), the temperature cannot be considered as a passive substance. In fact, in this case, temperature fluctuations give rise to density fluctuations which are in turn affected by the buoyancy. Therefore, the temperature distribution generates a field of buoyant accelerations, i.e. it affects the flow dynamics. Consequently, when I study a plume rise, the theory of similarity for small-scale turbulence in a thermally stratified fluid discussed in the subsection 4.2.1 has to be taken in account. Let me summarize the main results showed in subsection 4.2.1 ([Monin and Yaglom (1975), §27.5]). The generalization of Kolmogorov hyphoteses to the case of a stratified fuid is:
For the turbulence in a stratified fluid with large Pe and Re there is a quasi-equlibrium range of length scales $l << L_0$ in which the multidimensional probabilty distributions for velocity and temperature differences can be regarded as stationary and homogeneous (but not isotropic, and axially symmetric only relative to the vertical) are uniquely determined by the parameters ε, ε_ϑ, g/ϑ_0, ν and χ
The multidimensional distributions for the velocity and temperature differences at arbitrary pairs of points cannot depend on the molecular constants ν and χ provided only that the distances between the points are much greater than a certain fixed length η_0
The only combination of ε, ε_ϑ and g/ϑ_0 which has the dimensions of length is

$$L_* = \frac{\varepsilon^(5/4)}{\varepsilon_\vartheta^{3/4}(g/\vartheta_0)^{3/2}}$$

Therefore, *the length scale L_* characterizes the minimum length scale of inhomogeneities beyond which the effect of stratification is appreciable.*
Only if the length scale L_* is much less than the external turbulence length scale L_0 the asymptotic form of the temperature structure function in a stably statified medium is (see [Monin and Yaglom (1975)]):

$$D_{\vartheta\vartheta}(r) = c_{(\vartheta)}\varepsilon_\vartheta^{4/5}\left(\frac{g}{\vartheta_0}^{-2/5}\right) r^{2/5}$$

If I assume that the Taylor frozen turbulence hyphotesis is valid

$$D_{\vartheta\vartheta}(\tau) = c_{(\vartheta)}\varepsilon_\vartheta^{4/5}\left(\frac{g}{\vartheta_0}^{-2/5}\right) U^{2/5}\tau^{2/5}$$

Again, there is no way to make $D_{\vartheta\vartheta}$ dimensionless removing $\overline{u}$, since there is only one other length-depending parameter (i.e. g/ϑ_0) in the above expression. Even assuming that the last equation is the Lagragian form of D_ϑ, as far as I know, it is not possible to find relationships independent of τ. Hence again, the final expression relating ε_ϑ, T_ϑ and σ_ϑ will depend on τ and $\overline{u}$.
I remark that these considerations will be valid only if $L_* \ll L_0$. Hence I need to estimate L_* and L which cannot be precisely defined for most real turbulent flows since ε and ε_ϑ are unknown. This leads [Monin and Yaglom (1975)] to propose a very rough estimate of the order of magnitude of ε and ε_ϑ for turbulence in a stratified medium

$$\varepsilon \approx \frac{\left(\Delta\overline{u}\right)^3}{L}$$

$$\varepsilon_\vartheta \approx \frac{\Delta\overline{u}\left(\Delta\overline{\vartheta}\right)^2}{L_\vartheta}$$

where L_ϑ is the length over which there is an appreciable change in the mean temperature $\overline{\vartheta}(\vec{x})$ and $\Delta_\vartheta U$ and $\Delta\overline{\vartheta}$ are typical changes in the mean velocity and mean temperature over the distances L_ϑ. Typical legth scales L and L_ϑ of the fields $\overline{u}(z)$ and $\overline{\vartheta}(z)$ in the present case are of the same order of magnitude as distance z to the wall. Therefore

$$L_* \approx \frac{\left(\Delta\overline{u}\right)^3}{\left(\Delta\overline{\vartheta}\right)^{3/2}\left(g/\vartheta_0\right)^{3/2} z^{1/2}}$$

Anyway for the purpose of this thesis the most important relation is $\varepsilon_\vartheta \approx \frac{\Delta\overline{u}\left(\Delta\overline{\vartheta}\right)^2}{L_\vartheta}$. Hence the question is if it is possible to estimate L_ϑ, $\Delta_\vartheta U$ and $\Delta\overline{\vartheta}$ only from the ambient temperature and wind profile which are usually available (and e.g. for the Buncefield case). To this purpose I are still looking for some methods in literature to evaluate L_ϑ and the typical changes in the mean velocity and mean temperature over it, just starting from temperature and wind profile and it would allow a simple estimation of ε_ϑ. Through this thesis I specify the forms of ε_θ similarly to [van Dop (1992)] and [Das and Durbin (2005)] in analogy with the case of velocity, so that I consider $\varepsilon_\theta = \frac{2\sigma_\theta^2}{C_\theta T_\theta}$, where $\sigma_\theta = \gamma|\overline{\theta} - \theta_a|$ (in which γ is a tunable parameter) C_θ is the Obukhov-Corrsin constant and T_θ is choosen to be equal to T_L.

Part II

Modelling

Chapter 6

The effect of temperature fluctuations on the spread of a buoyant plume.

6.1 Plume model

The equations governing the rise of a buoyant plume in a uniform crossflow U are given by (e.g. [Briggs (1984)], [Weil (1988)], [Devenish et al. (2010b)])

$$\frac{\mathrm{d}}{\mathrm{d}s}(\pi v b^2) = E \tag{6.1.1a}$$

$$\frac{\mathrm{d}}{\mathrm{d}s}(\pi v w b^2) = \pi b^2 g' \tag{6.1.1b}$$

$$\frac{\mathrm{d}}{\mathrm{d}s}(\pi v g' b^2) = -N^2 \pi b^2 \rho_p w \tag{6.1.1c}$$

where $v = \sqrt{U^2 + w^2}$ is the velocity along the plume axis, s is the distance along the plume axis (centreline), E is the entrainment rate (to be defined below), w is the vertical velocity of the plume, b is the plume radius, N is the (constant) ambient buoyancy frequency and $g' = g(\theta(z) - \theta_a(z))/\theta_0$ is the reduced gravity in which $\theta(z)$ is the potential temperature of the plume at height z, $\theta_a(z)$ is the ambient potential temperature at height z and θ_0 is a reference temperature. Equations (6.1.1a), (6.1.1b) and (6.1.1c) respectively describe the evolution of the volume, momentum (per unit density) and buoyancy fluxes. They are collectively known as the plume equations.

It is commonplace to assume that there are two entrainment mechanisms in a crosswind (e.g. [Hoult et al. (1969)], [Hoult and Weil (1972)], [Webster and Thom-

son (2002)], [Devenish et al. (2010b)]), one due to velocity differences parallel to the plume axis and the other due to velocity differences normal to the plume axis and that the two mechanisms are additive. [Devenish et al. (2010b)] suggested that this additive entrainment assumption be an l^m-norm:

$$E = 2\pi b \left[\left(\alpha |w| \frac{|w|}{v} \right)^m + \left(\beta |w| \frac{U}{v} \right)^m \right]^{1/m}. \tag{6.1.2}$$

Here, I have also assumed that the difference between the horizontal component of the plume velocity and U is small relative to U and that this is valid from the source. Note that entrainment is proportional to the absolute velocity difference in order to avoid spurious detrainment after the plume reaches its maximum rise height. The constant coefficients α and β are associated with the two entrainment mechanisms: α with velocity differences parallel to the plume axis and β with velocity differences normal to the plume axis. Throughout this study I take $\alpha = 0.1$ and $\beta = 0.5$ which are consistent with previous studies (e.g. [Hoult and Weil (1972)], [Briggs (1984)], [Devenish et al. (2010b)], [Devenish et al. (2010a)]). In (6.1.2) $m \geqslant 1$ is a tunable parameter. The effect of a crossflow on a buoyant plume can be characterised by the dimensionless parameter $\tilde{U} = U/(F_0 N)^{1/4}$ where F_0 is the source buoyancy flux. In the weak-wind limit, $\tilde{U} \ll 1$, the first term on the right-hand side of (6.1.2) dominates. When $\tilde{U} \gg 1$ the plume becomes bent-over and the second term on the right-hand side of (6.1.2) dominates. In both asymptotic limits E is independent of m; the dependence on m is at its most sensitive for $\tilde{U} = O(1)$. [Devenish et al. (2010b)] found that $m = 3/2$ gave the best agreement with LES of buoyant plumes in a crosswind and field observations. It is this value that I use throughout this study.

6.2 A hybrid model for buoyant plume rise

In the model proposed by [Webster and Thomson (2002)], the plume equations provide the mean flow and the fluctuations are calculated using an LSM for the velocity components that satisfies the well-mixed condition [Thomson (1987)]. [Webster and Thomson (2002)] only considered fluctuations in the velocity and not the temperature; here I consider both fluctuations of the velocity and temperature. Note that the effect of turbulence generated by the plume is modelled by [Webster and Thomson (2002)] by an additional random increment to the position of a particle. Here I do not include this extra term, instead allowing the interaction of temperature and ve-

locity fluctuations to generate the observed spread. [Webster and Thomson (2002)] also use parameterisations of the ambient turbulent time-scale and dissipation rate rather than basing them on the plume turbulence as I will do here. I use the plume equations, (6.1.1), as a starting point re-expressing them in terms of w, b, θ and time, $t = \int \mathrm{d}s/v$. Let me show how to do it. Expand left-hand sides of 6.1.1:

$$\begin{aligned} b^2\frac{\mathrm{d}v}{\mathrm{d}s} + 2vb\frac{\mathrm{d}b}{\mathrm{d}s} &= E \\ b^2w\frac{\mathrm{d}v}{\mathrm{d}s} + b^2v\frac{\mathrm{d}w}{\mathrm{d}s} + 2vwb\frac{\mathrm{d}b}{\mathrm{d}s} &= b^2g' \\ vb^2\frac{\mathrm{d}g'}{\mathrm{d}s} + g'b^2\frac{\mathrm{d}v}{\mathrm{d}s} + 2g'vb\frac{\mathrm{d}b}{\mathrm{d}s} &= -N^2b^2w. \end{aligned} \tag{6.2.1}$$

Now,

$$\begin{aligned} \frac{\mathrm{d}v}{\mathrm{d}s} &= \frac{1}{2}(U^2+w^2)^{-1/2}\,2w\frac{\mathrm{d}w}{\mathrm{d}s} \\ &= \frac{w}{v}\frac{\mathrm{d}w}{\mathrm{d}s} \end{aligned} \tag{6.2.2}$$

and so 6.2.2 becomes

$$\begin{aligned} \frac{b^2w}{v}\frac{\mathrm{d}w}{\mathrm{d}s} + 2vb\frac{\mathrm{d}b}{\mathrm{d}s} &= E \\ \frac{b^2w^2}{v}\frac{\mathrm{d}w}{\mathrm{d}s} + b^2v\frac{\mathrm{d}w}{\mathrm{d}s} + 2vwb\frac{\mathrm{d}b}{\mathrm{d}s} &= b^2g' \\ vb^2\frac{\mathrm{d}g'}{\mathrm{d}s} + \frac{b^2wg'}{v}\frac{\mathrm{d}w}{\mathrm{d}s} + 2g'vb\frac{\mathrm{d}b}{\mathrm{d}s} &= -N^2b^2w. \end{aligned} \tag{6.2.3}$$

and hence

$$\frac{b^2w}{v}\frac{\mathrm{d}w}{\mathrm{d}s} + 2vb\frac{\mathrm{d}b}{\mathrm{d}s} = E \tag{6.2.4a}$$

$$\left(\frac{b^2w^2}{v} + b^2v\right)\frac{\mathrm{d}w}{\mathrm{d}s} + 2vwb\frac{\mathrm{d}b}{\mathrm{d}s} = b^2g' \tag{6.2.4b}$$

$$vb^2\frac{\mathrm{d}g'}{\mathrm{d}s} + \frac{b^2wg'}{v}\frac{\mathrm{d}w}{\mathrm{d}s} + 2g'vb\frac{\mathrm{d}b}{\mathrm{d}s} = -N^2b^2w \tag{6.2.4c}$$

Combine the first two equations of 6.2.4: (6.2.4b) $-w\times$(6.2.4a) gives

$$b^2v\frac{\mathrm{d}w}{\mathrm{d}s} = b^2g' - Ew$$

and hence

$$\frac{\mathrm{d}w}{\mathrm{d}s} = \frac{g'}{v} - E\frac{w}{b^2 v}. \tag{6.2.5}$$

The equation for b is given by

$$\begin{aligned} 2vb\frac{\mathrm{d}b}{\mathrm{d}s} &= E - \frac{b^2 w}{v}\frac{\mathrm{d}w}{\mathrm{d}s} \\ &= E - \frac{b^2 w}{v}\left(\frac{g'}{v} - E\frac{w}{b^2 v}\right) \\ &= E - \frac{b^2 w g'}{v^2} + E\frac{w^2}{v^2} \end{aligned}$$

and hence

$$\frac{\mathrm{d}b}{\mathrm{d}s} = \frac{E}{2bv} - \frac{bwg'}{2v^3} + E\frac{w^2}{2bv^3} \tag{6.2.6}$$

Substituting 6.2.5 and 6.2.6 in 6.2.4c gives

$$\begin{aligned} vb\frac{\mathrm{d}g'}{\mathrm{d}s} &= -N^2 wb - \frac{bwg'}{v}\frac{\mathrm{d}w}{\mathrm{d}s} - 2g'v\frac{\mathrm{d}b}{\mathrm{d}s} \\ &= -N^2 wb - \frac{bwg'}{v}\left(\frac{g'}{v} - E\frac{w}{b^2 v}\right) - 2g'v\left(\frac{E}{2bv} - \frac{bwg'}{2v^3} + E\frac{w^2}{2bv^3}\right) \\ &= -N^2 wb - \frac{bwg'^2}{v^2} + E\frac{w^2 g'}{bv^2} - \frac{Eg'}{b} + \frac{bwg'^2}{v^2} - E\frac{g'w^2}{bv^2} \\ &= -N^2 wb - \frac{Eg'}{b}. \end{aligned}$$

Thus,

$$\frac{\mathrm{d}g'}{\mathrm{d}s} = -N^2\frac{w}{v} - E\frac{g'}{b^2 v}. \tag{6.2.7}$$

Now, as

$$g' = \frac{g(\theta - \theta_a)}{\theta_0}$$

I can express 6.2.7 in terms of θ. I get

$$\frac{g}{\theta_0}\frac{\mathrm{d}}{\mathrm{d}s}(\theta - \theta_a) = -N^2\frac{w}{v} - E\frac{g'}{b^2 v}$$

and hence

$$\begin{aligned} \frac{\mathrm{d}\theta}{\mathrm{d}s} &= \frac{\mathrm{d}\theta_a}{\mathrm{d}s} - \frac{\theta_0}{g}\left(N^2\frac{w}{v} + E\frac{\overline{g'}}{b^2 v}\right) \\ &= \frac{\mathrm{d}\theta_a}{\mathrm{d}s} - N^2\frac{w\theta_0}{gv} - E\frac{(\theta - \theta_a)}{b^2 v} \end{aligned}$$

To summarise,

$$\begin{aligned}
\frac{\mathrm{d}w}{\mathrm{d}s} &= \frac{g(\theta-\theta_a)}{v\theta_0} - E\frac{w}{b^2v}.\\
\frac{\mathrm{d}b}{\mathrm{d}s} &= \frac{E}{2bv} - \frac{bwg(\theta-\theta_a)}{2v^3\theta_0} + E\frac{w^2}{2bv^3}\\
\frac{\mathrm{d}\theta}{\mathrm{d}s} &= \frac{\mathrm{d}\theta_a}{\mathrm{d}s} - N^2\frac{w\theta_0}{gv} - E\frac{(\theta-\theta_a)}{b^2v}
\end{aligned}$$

or in terms of time, t:

$$\begin{aligned}
\frac{\mathrm{d}w}{\mathrm{d}t} &= \frac{g(\theta-\theta_a)}{\theta_0} - E\frac{w}{b^2}.\\
\frac{\mathrm{d}b}{\mathrm{d}t} &= \frac{E}{2b} - \frac{bw}{2v^2}\frac{g(\theta-\theta_a)}{\theta_0} + E\frac{w^2}{2bv^2}\\
\frac{\mathrm{d}\theta}{\mathrm{d}t} &= \frac{\mathrm{d}\theta_a}{\mathrm{d}t} - N^2\frac{w\theta_0}{g} - E\frac{(\theta-\theta_a)}{b^2}
\end{aligned} \tag{6.2.8}$$

Now,

$$\begin{aligned}
N^2 &= \frac{g}{\theta_0}\frac{\mathrm{d}\theta_a}{\mathrm{d}z}\\
&= \frac{g}{\theta_0 w}\frac{\mathrm{d}\theta_a}{\mathrm{d}t},
\end{aligned} \tag{6.2.9}$$

and hence the governing equations for the flow in terms of b, w and θ are:

$$\frac{\mathrm{d}w}{\mathrm{d}t} = \frac{g(\theta-\theta_a)}{\theta_0} - E\frac{w}{b^2} \tag{6.2.10a}$$

$$\frac{\mathrm{d}b}{\mathrm{d}t} = \frac{E}{2b} - \frac{bw}{2v^2}\frac{g(\theta-\theta_a)}{\theta_0} + E\frac{w^2}{2bv^2} \tag{6.2.10b}$$

$$\frac{\mathrm{d}\theta}{\mathrm{d}t} = -E\frac{(\theta-\theta_a)}{b^2}. \tag{6.2.10c}$$

with $\mathrm{d}\theta_a = \frac{\theta_0 w}{g}N^2\mathrm{d}t$, $\mathrm{d}s = v\,\mathrm{d}t$ and $\mathrm{d}z = w\,\mathrm{d}t$. The equations 6.2.10 reduce to those of a vertically rising plume as $v \to w$ and to a bent-over plume as $w \to 0$. These equations are now used to calculate the mean velocity and temperature (which will be denoted by an overbar). The fluctuating velocity and temperature are denoted by a prime and will be calculated from stochastic differential equations. These are constructed from analogous equations to (6.2.10a) and (6.2.10c) for respectively w' and θ' coupled with LSMs for w' and θ'. I now show the application of a Reynolds

decomposition to the equations for w and θ. Because 6.2.10 are linear in w and θ respectively there are no second-order quantities and there is no feedback on the mean quantities by the fluctuating quantities. Let me assume, first, that $b' = 0$ and hence that is evaluated in terms of the mean quantities alone and, second, that $E = E(\overline{w}; \overline{v}; U)$. Since I assume also that there are no fluctuations in θ_a, the Reynolds decomposition for w is:

$$\begin{aligned} \frac{\mathrm{d}}{\mathrm{d}t}(\overline{w} + w') &= g\frac{\overline{\theta} + \theta' - \theta_a}{\theta_0} - E\frac{\overline{w} + w'}{b^2} \\ &= g\frac{\overline{\theta} - \theta_a}{\theta_0} + g\frac{\theta'}{\theta_0} - E\frac{\overline{w}}{b^2} - E\frac{w'}{b^2} \end{aligned} \tag{6.2.11}$$

from which I get

$$\frac{\mathrm{d}}{\mathrm{d}t}(w') = g\frac{\overline{\theta} - \theta_a}{\theta_0} - E\frac{\overline{w}}{b^2} \tag{6.2.12}$$

and the equation for w' analogous to (6.2.10a):

$$\frac{\mathrm{d}w'}{\mathrm{d}t} = \frac{g\theta'}{\theta_0} - E\frac{w'}{b^2} \tag{6.2.13}$$

where I underline that E is assumed to be a function of the mean quantities only. The Reynolds decomposition for $theta$ is:

$$\frac{\mathrm{d}}{\mathrm{d}t}(\theta) = -E\frac{\overline{\theta} - \theta_a}{b^2} - E\frac{\theta'}{b^2} \tag{6.2.14}$$

from which I get

$$\frac{\mathrm{d}}{\mathrm{d}t}(\overline{\theta}) = -E\frac{\overline{\theta} - \theta_a}{b^2} \tag{6.2.15}$$

and he equation for θ' analogous to (6.2.10c):

$$\frac{\mathrm{d}\theta'}{\mathrm{d}t} = -E\frac{\theta'}{b^2} \tag{6.2.16}$$

The stochastic differential equation for w' is now then given by

$$\mathrm{d}w' = \frac{g\theta'}{\theta_0}\,\mathrm{d}t - E\frac{w'}{b^2}\,\mathrm{d}t - \frac{w'}{T_L}\mathrm{d}t + \frac{1}{2}\left(\frac{1}{w} + \frac{w'}{\sigma_w^2}\right)\mathrm{d}\sigma_w^2 + \sqrt{C_0\varepsilon}\,\mathrm{d}W \tag{6.2.17}$$

where T_L is the time scale on which w' changes, σ_w^2 is the vertical-velocity variance, ε is the mean kinetic energy dissipation rate and C_0 is the constant of proportionality in the second-order Lagrangian velocity structure function which typically has a

value in the range $5-7$ in homogeneous isotropic turbulence (e.g. [Yeung (2002)]); I choose $C_0 = 5$. The last three terms on the right-hand side (RHS) of (6.2.17) are those of [Thomson (1987)] LSM for inhomogeneous turbulence (as would be the case for a Gaussian one-point velocity distribution). The stochastic differential equation for θ' is given by

$$\mathrm{d}\theta' = -E\frac{\theta'}{b^2}\mathrm{d}t - \frac{\theta'}{T_\theta}\mathrm{d}t - \frac{w'}{w}\mathrm{d}\overline{\theta} + \sqrt{C_\theta \varepsilon_\theta}\,\mathrm{d}W_\theta$$

where T_θ is the time scale on which θ decorrelates, ε_θ is the mean scalar dissipation rate and C_θ is the Obukhov-Corrsin constant which typically has a value of 1.6 ([Sreenivasan (1996)]; see also [Monin and Yaglom (1975)], p. 385 and the discussion in §23.5). The form of (6.2.18) is similar to that considered by [van Dop (1992)]. For simplicity I assume that the turbulent temperature statistics are homogeneous. As a particle moves from a region of low to high potential temperature, θ' decreases (since the total potential temperature remains constant in the absence of any thermal diffusivity). The first term on the RHS of (6.2.17), the buoyancy term, and the third term on the RHS of (6.2.18) together ensure that θ is conserved following a particle in the absence of entrainment (e.g. [Pearson et al. (1983)]). The third term of the on the RHS of (6.2.18), i.e. $-\frac{w'}{w}\mathrm{d}\overline{\theta}$ arise from the term $\frac{\mathrm{d}\overline{\theta}}{\mathrm{d}t}$ that implicitly contains fluctuations of velocity. In fact I can write $\frac{\mathrm{d}\overline{\theta}}{\mathrm{d}t}\mathrm{d}t = \mathrm{d}\overline{\theta}\frac{\mathrm{d}t}{\mathrm{d}z}w$. Now I use the Reynolds decomposition for w and I consider the fluctating part w'. Hence I have $\frac{\mathrm{d}\overline{\theta}}{\mathrm{d}t}\mathrm{d}t = \mathrm{d}\overline{\theta}\frac{\mathrm{d}t}{\mathrm{d}z}w' = \mathrm{d}\overline{\theta}\frac{w'}{w}$. In both (6.2.17) and (6.2.18) the terms involving E and the fluctuating quantity represent (in some way) the effect on the turbulence of the entrainment whereas the terms like X'/T_X represent the 'internal' turbulence of the plume. The initial values of w' and θ' are drawn from a joint Gaussian distribution with zero mean and variances σ_w^2 and σ_θ^2 (whose functional form will be specified below). I do not allow for any non-zero initial covariance, $\sigma_{w\theta}$, that may exist in reality.

It remains to specify the forms of σ_w^2, T_L, ε, C_0, ε_θ and T_θ which are all functions of z. I choose $\sigma_w = \alpha|\overline{w}|$ and $T_L = b/|\overline{w}|$. Since

$$T_L = \frac{2\sigma_w^2}{C_0\varepsilon}, \tag{6.2.18}$$

it follows that

$$\varepsilon = \frac{2\alpha^2\overline{w}^3}{C_0 b}. \tag{6.2.19}$$

The mean scalar dissipation rate is given by

$$\varepsilon_\theta = \frac{2\sigma_\theta^2}{C_\theta T_\theta} \tag{6.2.20}$$

where $\sigma_\theta = \gamma|\overline{\theta} - \theta_a|$, in which γ is a tunable constant whose value is choosen in section 6.4 below, and T_θ is choosen to be equal to T_L. The initial values of $\overline{w}$, b and $\overline{g'}$ are also discussed in section 6.4.

The model comprises (6.2.10) for $\overline{w}$, $\overline{\theta}$ and b together with (6.2.17) and (6.2.18) for w' and θ' respectively. The equations are solved numerically using an Euler-Maruyama method. In the numerical implementation of the model it is necessary to limit σ_w^2, T_L and σ_θ as follows. I set

$$\sigma_w = \alpha \max(|\overline{w}|, \overline{w}^*) \tag{6.2.21}$$

and

$$T_L = \frac{b}{\max(|\overline{w}|, \overline{w}^*)} \tag{6.2.22}$$

where $\overline{w}^* = \overline{w}(z_{eq})$ and z_{eq} is the level of neutral buoyancy. The latter is most conveniently obtained from Briggs' (1975) approximate solution of the plume equations in a stably stratified environment in the absence of a crossflow (see also [Devenish et al. (2010a)]). I then obtain

$$z_{eq} = 2^{3/8}\pi^{-1/4}\left(\frac{9\alpha}{10}\right)^{-1/2} F_0^{1/4} N^{-3/4}, \tag{6.2.23}$$

and hence that

$$\overline{w}^* = 2^{-5/8}\pi^{-1/4}\left(\frac{6\alpha}{5}\right)^{-1}\left(\frac{9\alpha}{10}\right)^{1/2} F_0^{1/4} N^{1/4}. \tag{6.2.24}$$

For σ_θ I set

$$\sigma_\theta = \gamma \max(|\overline{\theta} - \theta_a|, \overline{\theta}^*) \tag{6.2.25}$$

where $\overline{\theta}^* = (\theta_0/g)|F_{max}|/V_{max}$ and the subscript max indicates that the quantities are evaluated at the maximum rise height. Following [Briggs (1975)], the maximum rise height is given by

$$z_{max} = 2^{3/4}\pi^{-1/4}\left(\frac{9\alpha}{10}\right)^{-1/2} F_0^{1/4} N^{-3/4}. \tag{6.2.26}$$

and so I get

$$V_{max} = 2^{5/4}\pi^{1/4}\left(\frac{6\alpha}{5}\right)\left(\frac{9\alpha}{10}\right)^{-1/2} F_0^{3/4} N^{-5/4}. \tag{6.2.27}$$

Noting that $F_{max} = -F_0$ (which follows from Briggs' approximate analytical solution) I then get

$$\overline{\theta}^* = \left(\frac{\theta_0}{g}\right)\pi^{-1/4}2^{-5/4}\left(\frac{5}{8\alpha}\right)^{1/2} F_0^{1/4} N^{5/4}. \tag{6.2.28}$$

The model is now applied in a homogeneous stably stratified atmosphere (i.e. constant $\frac{\mathrm{d}\theta_a}{\mathrm{d}t} > 0$) in which the mean wind profile $U(z)$ is also constant. This is done for a first assessment of the qualitative behaviour of the model. I show some plume features in figures 6.1, 6.2, 6.3 6.4 evaluated including (*black solid line*) and not including (*red dashed line*) the temperature fluctuations in order to investigate their effect on the model. I consider a weak-wind limit $\tilde{U} = 0.1$, a bent-over plume $\tilde{U} = 10$ and an intermediate case $\tilde{U} = 1$ so as to examine if the importance of θ' depends on the intensity of the crossflow. In figure 6.5 I show the time evolution of mean square temperature fluctuations. There is no much difference among the three cases that I considered ($\tilde{U} = 0.1$, $\tilde{U} = 10$, $\tilde{U} = 1$) i.e. θ' depends weakly on the intensity of the crossflow. In fact, ϑ' doesn't depend on w or U, only on mean $\overline{w}$, hence I expected ϑ' to have the same order of magnitude for all three cases at the same height. The fluctuations θ' would make a greater (relative) contribution to the SDE for w through the $w - \vartheta$ coupling term $\frac{g\theta'}{\theta_0}$ than to the SDE for ϑ.
In figure 6.3 I plot the evolution of the standard deviation of the particles distibution around the mean height normalised with the wavelength of the plume's oscillations $\lambda = 2\pi U/N$ along the downwind direction x scaled by L_B, where $L_B = F_0/U^3$ is a typical length scale. [Fig.6.1] shows the plume rise height z against the downwind distance x normalised respectively as $\frac{z}{L_B\tilde{U}^{8/3}}$ and $\frac{x}{L_B}$. The plume evaluted with the presented model seems to be slighlty higher than the version in which I don't account for θ'. Figure 6.2 shows the vertical velocity divided by its initial values $\overline{w}_0$ against the height of the centre of mass adimensionalised with initial plume radius b_0. According to [Fig.6.1], $w/\overline{w}_0$ calculated from the model is greater than the version without temperature fluctations near the ground and smaller as the height increases. In figure 6.4 I show the vertical profile of the scalar concentration as a function of the dimensionless height z/b_0. Both the figures 6.3 and 6.4 suggest that the spread of the plume is much larger including temperature fluctuations. Furthermore all of the figures show that the role of the temperature fluctuation become more import as

the intensity of the crossflow increases.
In the previous figures 6.1, 6.2, 6.3 6.4, the tunable parameter γ is choosen to be 0.5. The figures 6.6 and 6.7 provide further information by showing the behaviour of plume height and scalar concentration by varying the value of γ. I choose $\gamma = 0$ (that can be equivalent to the case without temperature fluctuations), $\gamma = 0.1$ and $\gamma = 0.5$. The more evident fact is that there is little difference in the plume height between those simulations with temperature fluctuations and those without. There is more of a difference in the plots of the scalar concentration: they clearly depend on the value of γ stonger that plume height. If I compare the results with $\gamma = 0.1$ and the model with $\gamma = 0$ then the differences are small, perhaps largest for the case when $\tilde{U} = 1$.

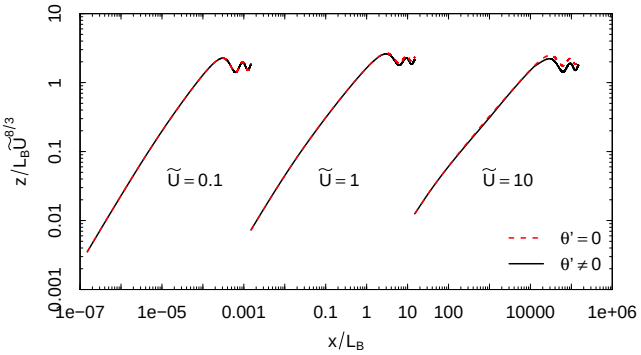

Figure 6.1: The height of the plume centre of mass of the plume against downwind distance.

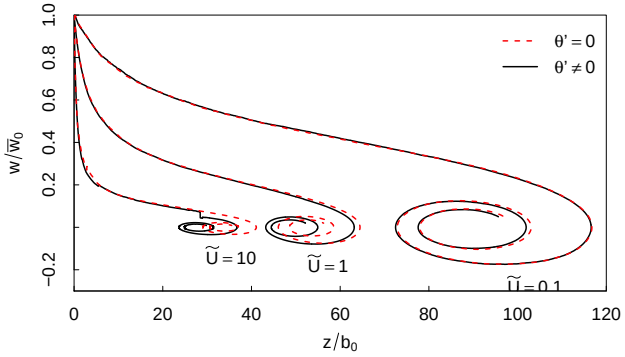

Figure 6.2: The vertical velocity of the plume calculated along the centre of mass.

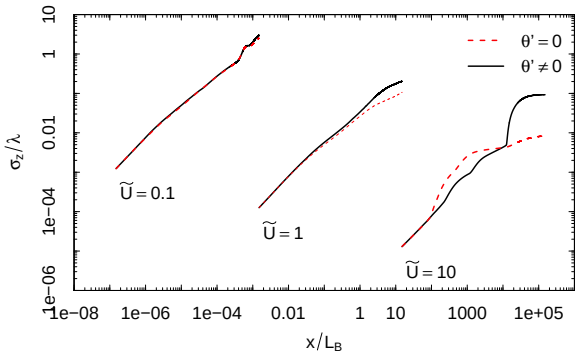

Figure 6.3: Standard deviation of particles position adimensionalised with the wavelength along with the non-dimensional distance from the source.

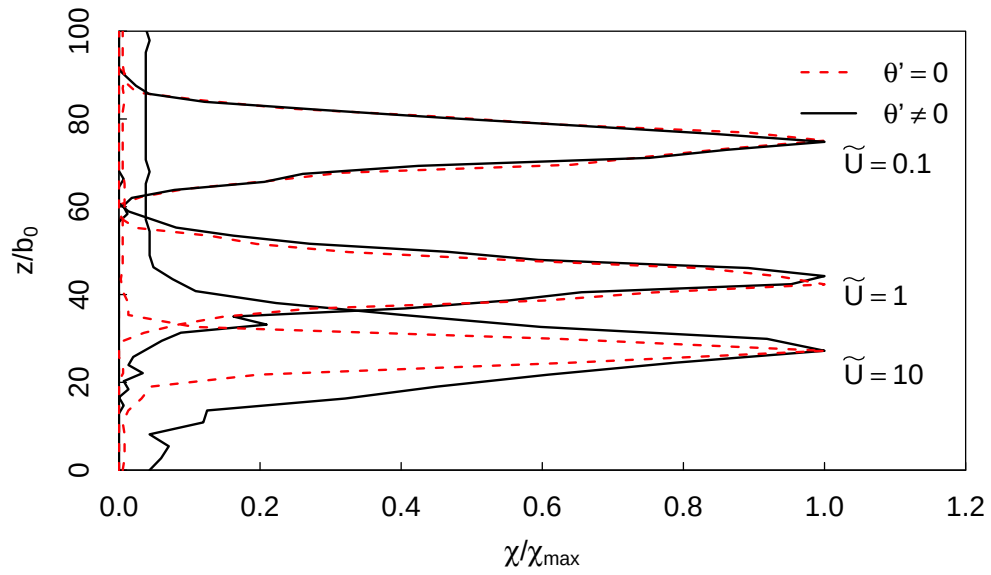

Figure 6.4: The scalar concentration for the plume calculated from the proposed hybrid model (*solid line*). The behaviour not including temperature fluctuations is also shown (*dashed line*).

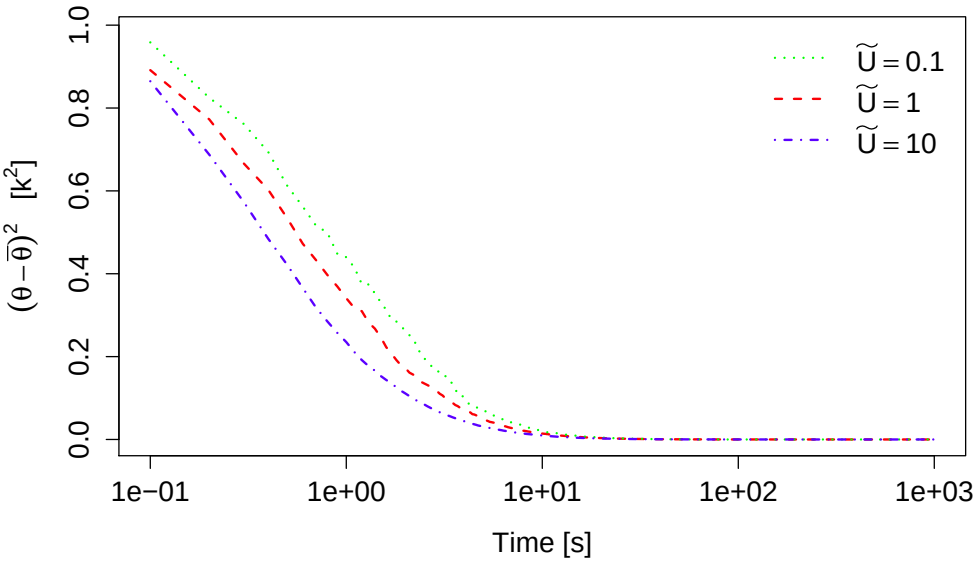

Figure 6.5: The time evolution of mean square temperature fluctuation for three different cases of mean wind: a weak-wind limit $\tilde{U} = 0.1$ (*green dotted line*), a bent-over plume $\tilde{U} = 10$ (*blue dash-dot line*) and an intermediate case $\tilde{U} = 1$ (*red dashed line*).

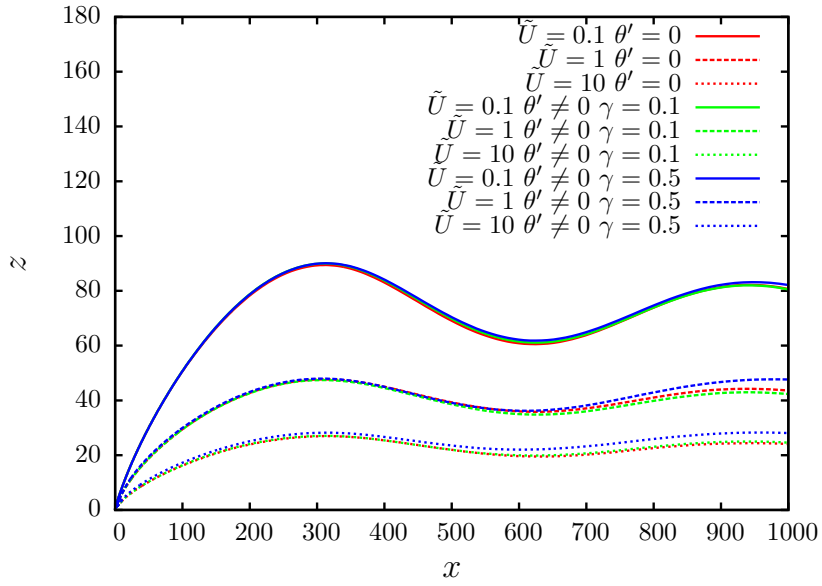

Figure 6.6: Behaviour of the height of the plume centre of mass at the values $\gamma = 0$, $\gamma = 0.1$ and $\gamma = 0.5$ for the three different cases of mean wind: a weak-wind limit $\tilde{U} = 0.1$, a bent-over plume $\tilde{U} = 10$, and an intermediate case $\tilde{U} = 1$

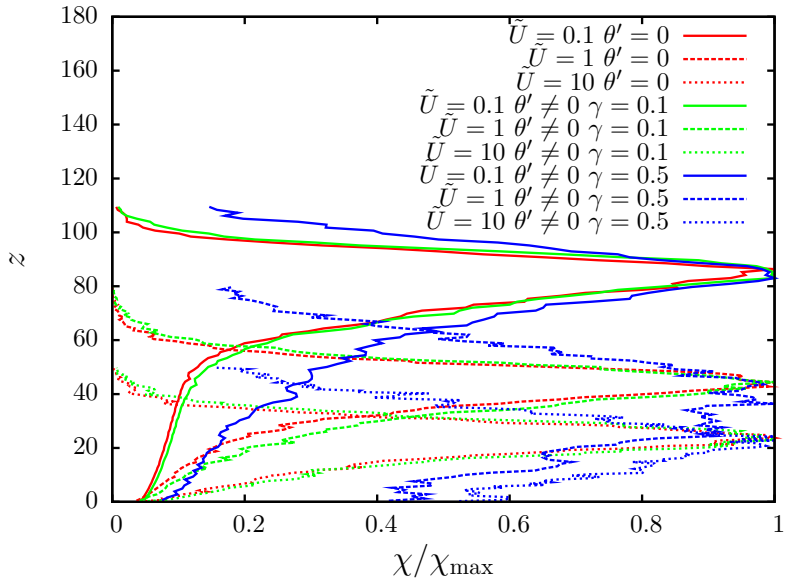

Figure 6.7: Behaviour of the scalar concentration for the plume calculated from the proposed hybrid at the values $\gamma = 0$, $\gamma = 0.1$ and $\gamma = 0.5$ for the three different cases of mean wind: a weak-wind limit $\tilde{U} = 0.1$, a bent-over plume $\tilde{U} = 10$, and an intermediate case $\tilde{U} = 1$

6.3 Comparison with the model of Das and Durbin (2005)

[Das and Durbin (2005), Das and Durbin (2007)] proposed an LSM for temperature fluctuations that is constructed to agree with a known second-order closure. They were interested in dispersion in a stably stratified turbulent flow with a non-buoyant source. When adapted for buoyant plume rise in the same manner as I have done, their model is very similar to the one given above. As a result of consistency of their model with the second-order closure they find that $T_\theta = 9T_L/16$. However, in homogeneous isotropic turbulence, the coefficient C_0 in their model has a value of $8/15$ which is significantly smaller than the value used here and commonly found experimentally and from direct numerical simulations of homogeneous isotropic turbulence. [Pope (2000)] suggested this difference in the value of C_0 may be due to the relatively low-Reynolds-number flows typically used to tune second-order closures. I note in passing that the value of C_θ used by [Das and Durbin (2005), Das and Durbin (2007)] is closer to the value used here.

Let me introduce the simplified form of the model proposed by [Das and Durbin (2005)] whose second-order moments agree with the isotropization of production (IP) model (see e.g. [Pope (2000)], p. 423). This is the same model as was applied to a realistic case with a non-buoyant source by [Das and Durbin (2007)]. In the context of buoyant plume rise, the stochastic differential equation for the vertical velocity takes the form

$$\mathrm{d}w = \left(\frac{g(\overline{\theta}-\theta_a)}{\theta_0} - E\frac{\overline{w}}{b^2}\right)\mathrm{d}t - \frac{9}{10}\frac{\varepsilon}{k}w'\mathrm{d}t - \frac{2}{5}w'\frac{\mathrm{d}\overline{w}}{\mathrm{d}z}\mathrm{d}t - \frac{2}{3}\frac{g\theta'}{\theta_0}\mathrm{d}t + \frac{\mathrm{d}\sigma_w^2}{\mathrm{d}z}\mathrm{d}t + (c_0\varepsilon)^{1/2}\mathrm{d}W \tag{6.3.1}$$

and that for the temperature is given by

$$\mathrm{d}\theta = \left(1-\frac{\overline{w}}{w}\right)\mathrm{d}\theta_a - E\frac{(\overline{\theta}-\theta_a)}{b^2}\,\mathrm{d}t - \frac{8}{5}\frac{\varepsilon}{k}\theta'\mathrm{d}t + c_\theta^{1/2}\mathrm{d}W_\theta \tag{6.3.2}$$

where k is turbulent kinetic energy. Here I have used the same values of the constant coefficients that were used by [Das and Durbin (2007)]. Note that c_0 is not the same as C_0 above but takes the form

$$c_0 = \frac{6}{5} - \frac{2}{5}\frac{\sigma_w^2}{\varepsilon}\frac{\mathrm{d}\overline{w}}{\mathrm{d}z} - \frac{2}{9}\frac{g}{\varepsilon}\frac{\overline{w'\theta'}}{\theta_0} - \frac{2}{3}.$$

The conservation of scalar in stationary turbulence impiles that $\overline{w'\theta'} = 0$. The coefficient c_θ is given by

$$c_\theta = \frac{17}{10}\frac{\varepsilon}{k}\overline{\theta'^2}.$$

It is clear by comparing 6.3.1 with 6.2.17 that $T_L = (10/9)k/\varepsilon$ and, by comparing 6.3.2 with 6.2.18, that $T_\theta = 5k/(8\varepsilon)$. Hence, it follows that $T_\theta = 9T_L/16$ and

$$c_\theta = \frac{17}{16}\frac{\overline{\theta'^2}}{\overline{T_\theta}}.$$

In both the models the term $-\frac{w'}{T_L}\mathrm{d}t$ is considered, see 6.3.1 and 6.2.17. In [Das and Durbin (2005)] this is written as $-\frac{c_1}{2}\frac{\varepsilon}{k}w'\mathrm{d}t$ and $T_L = \frac{2k}{c1\varepsilon} = \frac{10}{9}\frac{k}{\varepsilon}$. In my model $T_L = \frac{2\sigma_w^2}{C_0\varepsilon}$ and by assuming $\sigma_w^2 = \frac{2}{3}k$ I have $T_L = \frac{4}{3C_0}\frac{k}{\varepsilon}$, see [Pope (2000), p 486]. Hence I can obtain $C_0 = 6/5$ by comparison with [Das and Durbin (2005)]. I choose $C_0 = 5$ and hence the two time scales are slightly different $T_L = \frac{10}{9}\frac{k}{\varepsilon}$ and $T_L = \frac{4}{15}\frac{k}{\varepsilon}$, so that T_L in [Das and Durbin (2005)] is $\frac{25}{6}$ times T_L of the model proposed here. Anyway this difference is not necessarily wrong, because the two models differ in the stochastic terms, $c_0\varepsilon^{1/2}\mathrm{d}W$ and $C_0\varepsilon^{1/2}\mathrm{d}W$, with $c_0 \neq C_0$.
In both the models the term $-\frac{\theta'}{T_\theta}\mathrm{d}t$ is considered, see 6.3.2 and 6.2.18 In [Das and Durbin (2005)] this is written as $-\left(c_{1\theta} - \frac{c_1}{2}\right)\frac{\varepsilon}{k}\theta'\mathrm{d}t$ and $T_\theta = \frac{1}{c_{1\theta}-\frac{c_1}{2}}\frac{k}{\varepsilon} = \frac{5}{8}\frac{k}{\varepsilon}$. In my model I consider $T_\theta = \frac{2\sigma_\theta^2}{C_\theta\varepsilon_\theta}$ with $C_\theta = 1.6$ and $T_\theta = T_L = \frac{4}{15}\frac{k}{\varepsilon}$, obtaining by comparison with $T_\theta = \frac{5}{8}\frac{k}{\varepsilon}$ that T_θ in [Das and Durbin (2005)] is $\frac{75}{32}$ times of T_θ in the model proposed here. Choosing $T_\theta = \frac{9}{16}T_L = \frac{3}{20}\varepsilon$, T_L in [Das and Durbin (2005)] is again $\frac{25}{6}$ times T_L of the model proposed here. Again this difference is not necessarily wrong, because the two models differ in the stochastic terms of temperature as well, $c_\theta^{1/2}\mathrm{d}W_\theta$ and $C_0\varepsilon^{1/2}\mathrm{d}W$ and $\sqrt{C_\theta\varepsilon_\theta}\,\mathrm{d}W_\theta$, with $c_\theta \neq C_\theta$.

6.4 Comparison with LES

Here I compare the model with the LES results of [Devenish et al. (2010b)] which were computed using a uniform ambient crosswind and a constant buoyancy frequency. The initialisation of $\overline{w}$, b and $\overline{g'}$ for a pure plume whose initial buoyancy flux is known is not straightforward. For a pure plume rising from a point source $\overline{w} \to \infty$, $\overline{g'} \to \infty$ and $b \to 0$ as $z \to 0$ in such a way that F_0 is finite and non-zero

while the initial momentum and volume fluxes are zero. Even the numerical solution of (6.1.1) for a pure plume requires perturbation of the initial volume and momentum fluxes in order to achieve a non-trivial solution ([Morton et al. (1956)]).

[McCaffrey (1979)] argued that in the lowest region of a fire plume the velocity is independent of the heat release rate and grows like $z^{1/2}$, that is, its behaviour is analogous to a body in free fall. It then follows that in this region $w = \sqrt{2g'z}$. While the physics of this region is not represented in the model presented here, it nevertheless provides a physically based approach of calculating the initial values of $\overline{w}$ and $\overline{g'}$, respectively $\overline{w}_0$ and $\overline{g'}_0$. I estimate w_0 by equating the initial radius $b_0 = 2z$ so that $\overline{w}_0 = \sqrt{b_0\overline{g'}_0}$. Since the initial buoyancy flux $F_0 = \pi b_0^2 \overline{g'}_0 \overline{v}_0$ I obtain a cubic polynomial for either $\overline{w}_0$ or $\overline{g'}_0$ for given b_0:

$$b_0\overline{g'}_0^3 + U^2\overline{g'}_0^2 - \frac{F_0^2}{\pi^2 b_0^4} = 0. \tag{6.4.1}$$

The nature of the roots of this equation can be inferred by analysing the discriminant of (6.4.1):

$$\Delta = \frac{F_0^2}{\pi^2 b_0^4}\left(4U^6 - \frac{27F_0^2}{\pi^2 b_0^2}\right). \tag{6.4.2}$$

Any of the three cases ($\Delta > 0$, $\Delta = 0$, $\Delta < 0$) will produce a physical solution. In the case that there are three real roots ($\Delta > 0$), (6.4.1) shows that two of these roots will be negative (and can thus be discarded). In the problem, the values of F_0 and b_0 are such that Δ is always negative and so the roots consist of one real root and two complex roots.

The focus in this section is on the LES plumes in group A of Table 1 of [Devenish et al. (2010b)]; the same values of F_0, N and U are used in the model. The value of γ is estimated by comparing the LES profiles of σ_θ with $|\overline{\theta} - \theta_a|$ along the centreline of the plume. Figure 6.8 shows these quantities for a representative sample of $\tilde{U}$-values. I find that the best fit is given with γ in the range $0.1 \lesssim \gamma \lesssim 0.5$ and that there is little systematic variation with $\tilde{U}$. I present results with $\gamma = 0.25$, the average value over $\tilde{U}$, and $\gamma = 0.1$ and $\gamma = 0.5$.

In the calculation of the LES results, the plume was allowed to reach a steady state and then sampled over a sufficiently long time period that fluctuations in the plume statistics were small. The LES domain typically allowed for the plume to oscillate for 1–2 wavelengths after the plume reached its maximum rise height (see [Devenish

et al. (2010b), Devenish et al. (2010a)] for more details). The calculation of the LSM results was performed similarly.

Figure 6.9 shows the scalar concentration, χ, beyond the first turning point of the plume computed from the model trajectories and the LES for $0.34 \leqslant \tilde{U} \leqslant 2.73$ (the case with $\tilde{U} = 5.47$ shows very similar behaviour to that of $\tilde{U} = 2.73$ but is not shown for reasons of space). It can be seen that, with the exception of the case with $\tilde{U} = 0.34$, the rise height of the model plume agrees very well with the LES plume. This is true for the model plumes with and without temperature fluctuations. In most cases the spread of the model plume is close to that of the LES with the results for $\gamma = 0.1$ (not shown) closest to the model plume with $\theta' = 0$ and the spread of the model plume (with $\theta' \neq 0$) increasing with increasing γ (as expected).

Figure 6.10 shows the plume width (defined to be the standard deviation of the scalar concentration), $\sigma_{\hat{z}}$ where $\hat{z} = z/F_0^{1/4}N^{-3/4}$, the skewness, $\mathcal{S}_{\hat{z}}$ and the kurtosis, $\mathcal{K}_{\hat{z}}$ for both the model and LES plumes. In order to mitigate the effect of statistical noise in the LES data, three samples of the simulation data are used to calculate mean values and associated error bars (which are taken to be the standard deviation) of $\sigma_{\hat{z}}$ (and the higher order moments to be shown below). As expected, $\sigma_{\hat{z}}$ for the model plume with $\theta' \neq 0$ (for all values of γ) is larger than that of the model plume with $\theta' = 0$ for all values of $\tilde{U}$. It can also be seen that $\sigma_{\hat{z}}$ decreases monotonically with $\tilde{U}$. As the wind speed increases, the plume is more constrained and spreads less in the vertical direction (over a given horizontal distance or travel time). While the LES values do not exhibit the same systematic variation with $\tilde{U}$, the overall trend is also decreasing with increasing $\tilde{U}$. In general, the LES values tend to be higher than the model values. It is possible that lack of resolution in the LES, which may increase the amount of numerical diffusion, coupled with inadequate sampling leads to a greater spread compared with the model plumes. Higher order moments of the scalar concentration show less systematic variation with $\tilde{U}$ due to statistical noise. The skewness, $\mathcal{S}_{\hat{z}}$, tends towards zero as $\tilde{U}$ increases as can be seen in Figure 6.10 for both models with $\theta' \neq 0$ and $\theta' = 0$. The model with $\theta' = 0$ has positive skewness and decreases monotonically with increasing $\tilde{U}$ whereas the model with $\theta' \neq 0$ (for all values of γ), while also generally tending towards zero as $\tilde{U}$ increases, may become negative. The LES values of the skewness are negative and larger in magnitude than the model values; while the results are very noisy, the trend is arguably increasing (towards zero) with increasing $\tilde{U}$. It is possible that greater detrainment in the lower part of the LES plume compared with the model

plume leads to a larger negative skewness in the LES results. Another possibility is that the LES plume tends to meander somewhat and that this is more pronounced in the lower part of the plume; this effect is mitigated (particularly for larger values of $\tilde{U}$) by choosing to calculate the scalar concentration beyond the first turning point. The kurtosis, $\mathcal{K}_{\hat{z}}$, shown in Figure 6.10, increases monotonically for the model with $\theta' = 0$ whereas the model with $\theta' \neq 0$ (for all values of γ) shows an initial increase as $\tilde{U}$ increases, reaching a maximum at $\tilde{U} \approx 1$ and steadily decreasing thereafter. As with the skewness, LES values of the kurtosis suffer from statistical noise but again it is arguable that the overall trend is in keeping with the model that has $\theta' \neq 0$; the values are closer in magnitude to the model values than is the case for the skewness. Both the skewness and the kurtosis show the model tending towards Gaussian values as $\tilde{U}$ increases but it is not clear what the physical reasons are for the departure from Gaussianity as $\tilde{U}$ decreases. However, symmetry considerations suggest that Gaussianity should be recovered as $\tilde{U}$ tends to zero for the model if not for the LES. The values of $\sigma_{\hat{z}}$, $\mathcal{S}_{\hat{z}}$ and $\mathcal{K}_{\hat{z}}$ averaged over $\tilde{U}$ are shown in Table 6.1. It can be seen that the model with $\theta' \neq 0$ and $\gamma = 0.5$ is closest to the LES values for all three quantities.

As may be expected, varying γ in the range 0.1–0.5 produces a greater spread as γ increases. Figure 6.10 shows that this is indeed the case for $\sigma_{\hat{z}}$. Figure 6.10 also shows that the variation of $\mathcal{S}_{\hat{z}}$ with γ is not large but that $\mathcal{S}_{\hat{z}}$ is more likely to become negative as γ increases. The variation of $\mathcal{K}_{\hat{z}}$ with γ is shown in Figure 6.10 with $\mathcal{K}_{\hat{z}}$ decreasing as γ increases. As γ increases, there is possibly a wider variation in the level of neutral buoyancy experienced by each particle and so the scalar distribution becomes less peaked (i.e. the kurtosis decreases). If this is not too large then the greater variation in θ' that occurs close to the ground, and also as γ increases, may explain why there is a tendency for $\mathcal{S}_{\hat{z}}$ to become negative with increasing γ. However, the complexity of the model means that the dependency of $\mathcal{S}_{\hat{z}}$ and $\mathcal{K}_{\hat{z}}$ on γ and $\tilde{U}$ is not straightforward and these explanations should be regarded as speculative.

I also conducted another series of simulations using the relationship between T_θ and T_L derived by [Das and Durbin (2005)] i.e. $T_\theta = 9T_L/16$ (assuming that this may hold more generally than in the context of the second-order closure used by [Das and Durbin (2005)] to derive this result). Figure 6.10 shows that a shorter decorrelation time scale for θ generally reduces the effect of the temperature fluctuations (as expected).

For values of $\tilde{U}$ smaller than those presented here, I found that the disagreement between the model and LES plumes got worse particularly for the rise heights. This may point to deficiencies in the modelling of buoyant plumes in a weak wind though it should also be noted that LES of buoyant plumes with small $\tilde{U}$ were more sensitive to resolution than large $\tilde{U}$ (see the discussion in [Devenish et al. (2010b)]).

	$\sigma_{\hat{z}}$	$\mathcal{S}_{\hat{z}}$	$\mathcal{K}_{\hat{z}}$
LES plume	0.448	-0.640	4.817
Model plume $\theta' = 0$	0.192	0.106	2.578
Model plume $\theta' \neq 0$: $\gamma = 0.25$	0.271	0.029	5.908
Model plume $\theta' \neq 0$: $\gamma = 0.1$	0.216	0.079	6.164
Model plume $\theta' \neq 0$: $\gamma = 0.5$	0.321	-0.013	4.578

Table 6.1: The standard deviation, skewness and kurtosis of the scalar concentration averaged over all $\tilde{U}$-values for the model plumes (both $\theta' \neq 0$ and $\theta' = 0$) and the LES plume. The LES values are averages over three samples of the simulation data.

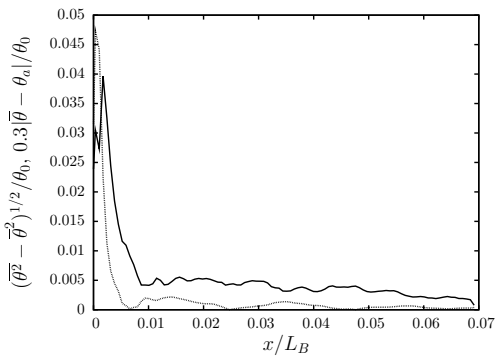

(a) $\tilde{U} = 0.34, \quad \gamma = 0.3$

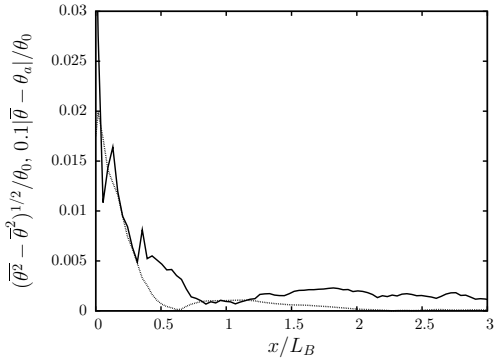

(b) $\tilde{U} = 1.03, \quad \gamma = 0.1$

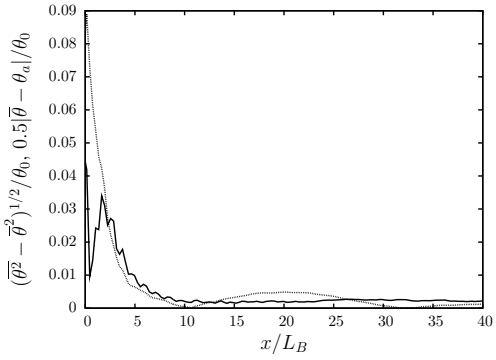

(c) $\tilde{U} = 2.06, \quad \gamma = 0.5$

Figure 6.8: LES profiles of $(\overline{\theta^2} - \overline{\theta}^2)^{1/2}/\theta_0$ (solid) and $\gamma|\overline{\theta} - \theta_a|/\theta_0$ (dotted) as a function of downwind distance, x, scaled by $L_B = F_0/U^3$ (with the source at the origin) for three representative values of $\tilde{U}$.

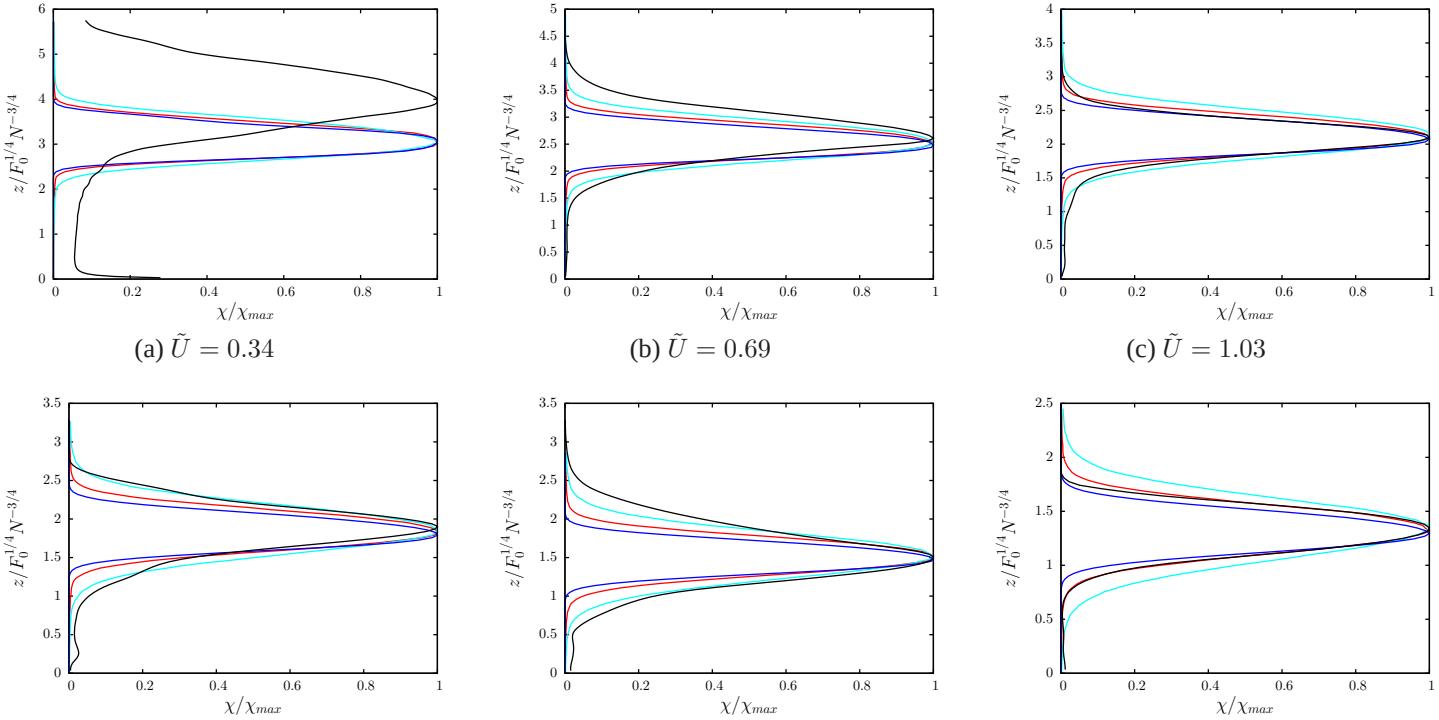

(a) $\tilde{U} = 0.34$ (b) $\tilde{U} = 0.69$ (c) $\tilde{U} = 1.03$

(d) $\tilde{U} = 1.37$ (e) $\tilde{U} = 2.06$ (f) $\tilde{U} = 2.73$

Figure 6.9: The scalar concentration normalised by its maximum value as a function of height for $\tilde{U}$ in the range $0.34 \leqslant \tilde{U} \leqslant 2.73$. The black line is the LES plume, the blue line the model plume with $\theta' = 0$ and the red and cyan lines the model plumes with $\theta' \neq 0$ for respectively $\gamma = 0.25$ and $\gamma = 0.5$.

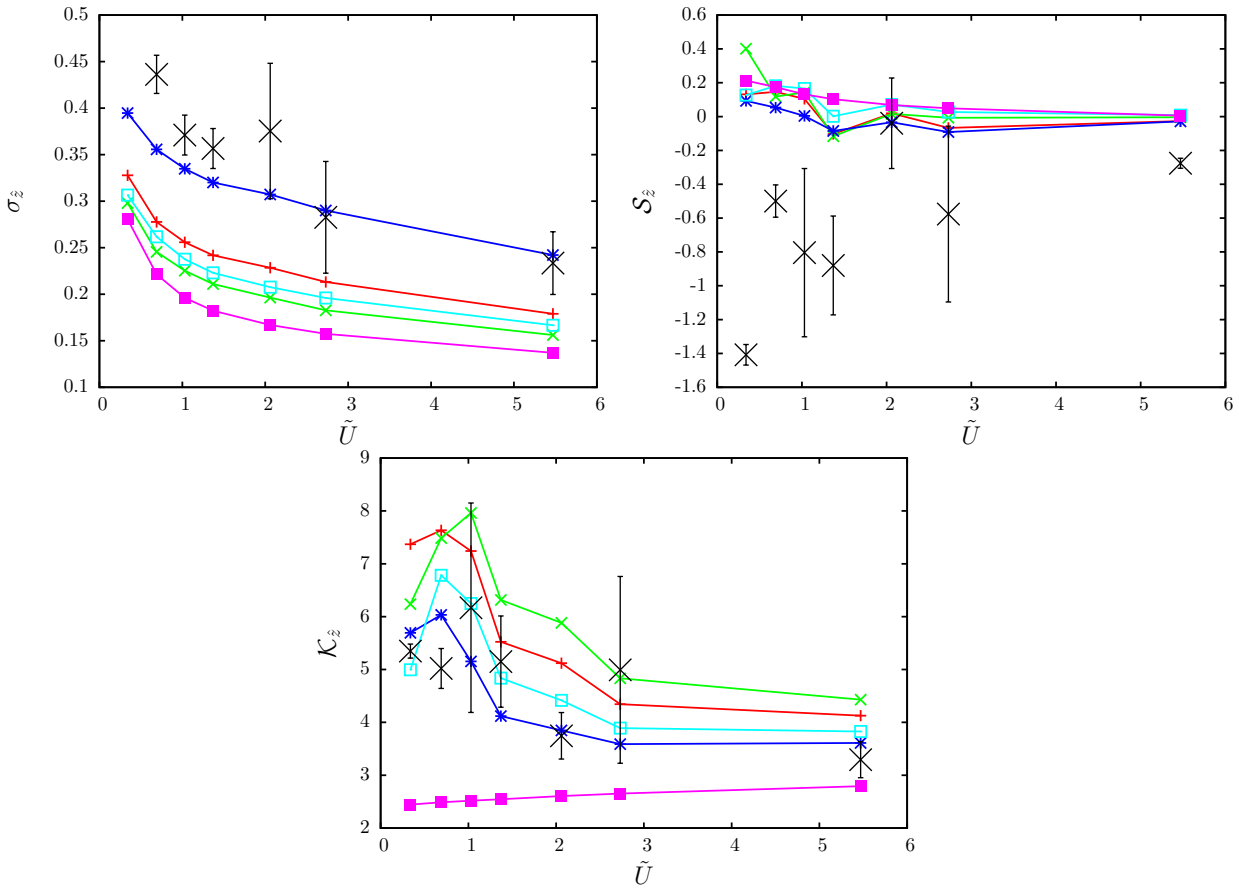

Figure 6.10: The standard deviation, the skewness and the kurtosis of χ as a function of $\tilde{U}$. The solid lines represent the model with $\theta' = 0$ (purple); $\theta \neq 0$, $\gamma = 0.1$ (green), $\gamma = 0.25$ (red), $\gamma = 0.5$ (blue); and the case with $T_\theta = 9T_L/16$ for which $\gamma = 0.25$ (cyan). The points indicate the LES results; the point corresponding to $\tilde{U} = 0.34$ is not shown but has a value of 1.08.

6.5 Real case

The explosion and fire at the Buncefield oil depot in December 2005 produced the largest plume of black carbon in Europe since the end of the second world war.
A major explosion at the Buncefield oil depot in Hemel Hempstead, Hertfordshire, UK just after 0600 UTC on Sunday, 11th December 2005 resulted in the largest peacetime fire in Europe to date (figure 6.11 from the website
`http://www.metoffice.gov.uk/`).
The blast was heard as far away as the Netherlands, a distance of some 200 miles. The Buncefield Major Investigation Board reported that the main explosion was caused by the ignition of a flammable vapour cloud resulting from an overfilled petrol storage tank (Buncefield Major Investigation Board, 2006). Forty-three people were injured in the incident, but fortunately there were no fatalities. Significant damage was caused to local homes and offices and around 2000 people were evacuated. At the height of the blaze, 20 large fuel storage tanks were alight. Each tank was reported to hold up to 3 million gallons of fuel (unleaded petrol, super-unleaded petrol, motor spirit, gas oil, ultra-low sulphur diesel, and jet fuel). No efforts were made to bring the main fire under control during Sunday, as fire crews assessed the situation, determined the best strategy to tackle the blaze and assembled fire-fighting equipment. On Monday, serious efforts to cool and then extinguish the fire with foam and water were undertaken by the fire brigade. The main fire was systematically extinguished during Tuesday and Wednesday.
Comparisons of LES of this plume with observations showed that the LES plume captured many aspects of the observed plume, in particular, the rise height and the detrainment of the plume in different directions at different heights [Devenish and Edwards (2009)]. Comparison of the LES plume with an LSM of the form proposed by [Webster and Thomson (2002)], i.e. with no temperature fluctuations, showed that the LES results had a greater vertical spread than the LSM results (see Fig. 18 of [Devenish et al. (2010b)]). This observation has, in part, motivated the present study. In this section, I return to the original problem and apply the model introduced in section 6.2 to the Buncefield plume.
The nearest hourly meteorological observations from the UK surface synoptic network are from Heathrow and Northolt. In addition, high temporal resolution surface observations from the Met Offices Meteorological Research Unit (MRU) at Cardington are available as 30, 10 and 1 minute mean values. Throughout the incident, routine upper air radiosonde profiles were available twice daily from ascents

at Herstmonceux and Nottingham at 0000 UTC and 1200 UTC. The same wind and temperature profiles as used by [Devenish and Edwards (2009)] or [Devenish et al. (2010b)] are used here (see figure 6.12 and 6.13). In this section, the assumption of constant buoyancy frequency and uniform crosswind used in sections 6.2 and 6.4 are relaxed to allow for realistic profiles of temperature and ambient wind. In addition, the model presented in section 6.2 is extended to include two equations for the horizontal momentum flux, one for each horizontal component of the ambient wind (e.g. [Weil (1988)]). The equation for each horizontal component of the mean velocity of the plume, $\overline{u}_i$, then takes the form

$$\frac{\mathrm{d}\overline{u}_i}{\mathrm{d}t} = -\frac{E(\overline{u}_i - U_i)}{b^2} \tag{6.5.1}$$

where U_i is the ith horizontal component of the ambient wind and i ranges over the zonal and meridional components of the wind. Fluctuations in both of these components are not treated here.

Let me show how to obtain the term 6.5.1. I consider the ambient wind $\vec{U} = (u_{1A}, u_{2A})$ of [Fig.6.12] and I introduce the components of the plume velocity u_1 and u_2 (the zonal and meridional components respectively). I remark that I do not consider any fluctuations in u_1 and u_2 so that $u_1 = \overline{u_1}$ and $u_2 = \overline{u_2}$, $v = \sqrt{u_1^2 + u_2^2 + w^2}$ and of the plume position x and y so that $s = \sqrt{x^2 + y^2 + z^2}$, the plume equations 6.1.1 become:

$$\begin{aligned}
\frac{\mathrm{d}}{\mathrm{d}s}(vb^2) &= E \\
\frac{\mathrm{d}}{\mathrm{d}s}(vwb^2) &= b^2\overline{g'} \\
\frac{\mathrm{d}}{\mathrm{d}s}\left(vb^2(u_1 - u_{1A})\right) &= -vb^2\frac{\mathrm{d}u_{1A}}{\mathrm{d}s} \\
\frac{\mathrm{d}}{\mathrm{d}s}\left(vb^2(u_2 - u_{2A})\right) &= -vb^2\frac{\mathrm{d}u_{2A}}{\mathrm{d}s} \\
\frac{\mathrm{d}}{\mathrm{d}s}(vwb^2) &= b^2 g' \\
\frac{\mathrm{d}}{\mathrm{d}s}(vg'b^2) &= -N^2b^2w
\end{aligned} \tag{6.5.2}$$

Once again, a set of SDEs can be deduced from equation 6.5.2. Expand left-hand sides:

$$\begin{aligned}
b^2\frac{\mathrm{d}v}{\mathrm{d}s} + 2vb\frac{\mathrm{d}b}{\mathrm{d}s} &= E \\
b^2 w\frac{\mathrm{d}v}{\mathrm{d}s} + b^2 v\frac{\mathrm{d}w}{\mathrm{d}s} + 2vwb\frac{\mathrm{d}b}{\mathrm{d}s} &= b^2 g' \\
b^2(u_1-u_{1A})\frac{\mathrm{d}v}{\mathrm{d}s} + 2v(u_1-u_{1A})b\frac{\mathrm{d}b}{\mathrm{d}s} + b^2 v\frac{\mathrm{d}u_1}{\mathrm{d}s} - vb^2\frac{\mathrm{d}u_{1A}}{\mathrm{d}s} &= -vb^2\frac{\mathrm{d}u_{1A}}{\mathrm{d}s} \\
b^2(u_2-u_{2A})\frac{\mathrm{d}v}{\mathrm{d}s} + 2v(u_2-u_{2A})b\frac{\mathrm{d}b}{\mathrm{d}s} + b^2 v\frac{\mathrm{d}u_2}{\mathrm{d}s} - vb^2\frac{\mathrm{d}u_{2A}}{\mathrm{d}s} &= -vb^2\frac{\mathrm{d}u_{2A}}{\mathrm{d}s} \\
vb^2\frac{\mathrm{d}g'}{\mathrm{d}s} + g'b^2\frac{\mathrm{d}v}{\mathrm{d}s} + 2g'vb\frac{\mathrm{d}b}{\mathrm{d}s} &= -N^2b^2w.
\end{aligned} \tag{6.5.3}$$

Now,

$$\frac{\mathrm{d}v}{\mathrm{d}s} = \frac{1}{2}(u_1^2+u_2^2+w^2)^{-1/2}\left(2w\frac{\mathrm{d}w}{\mathrm{d}s}+2u_1\frac{\mathrm{d}u_1}{\mathrm{d}s}+2u_2\frac{\mathrm{d}u_2}{\mathrm{d}s}\right) = \frac{1}{v}\left(w\frac{\mathrm{d}w}{\mathrm{d}s}+u_2\frac{\mathrm{d}u_1}{\mathrm{d}s}+u_2\frac{\mathrm{d}u_2}{\mathrm{d}s}\right) \tag{6.5.4}$$

and so (6.5.3) becomes

$$\frac{b^2w}{v}\frac{\mathrm{d}w}{\mathrm{d}s} + 2\frac{u_1b^2}{v}\frac{\mathrm{d}u_1}{\mathrm{d}s} + 2\frac{u_2b^2}{v}\frac{\mathrm{d}u_2}{\mathrm{d}s} + 2vb\frac{\mathrm{d}b}{\mathrm{d}s} = E \tag{6.5.5a}$$

$$\frac{b^2w^2}{v}\frac{\mathrm{d}w}{\mathrm{d}s} + 2\frac{u_1b^2w}{v}\frac{\mathrm{d}u_1}{\mathrm{d}s} + 2\frac{u_2b^2w}{v}\frac{\mathrm{d}u_2}{\mathrm{d}s} + b^2v\frac{\mathrm{d}w}{\mathrm{d}s} + 2vwb\frac{\mathrm{d}b}{\mathrm{d}s} = b^2g' \tag{6.5.5b}$$

$$\frac{b^2w(u_1-u_{1A})}{v}\frac{\mathrm{d}w}{\mathrm{d}s} + \frac{b^2u(u_1-u_{1A})}{v}\frac{\mathrm{d}u_1}{\mathrm{d}s} + \frac{b^2u_2(u_1-u_{1A})}{v}\frac{\mathrm{d}u_2}{\mathrm{d}s} + 2v(u_1-u_{1A})b\frac{\mathrm{d}b}{\mathrm{d}s} + vb^2\frac{\mathrm{d}u_1}{\mathrm{d}s} = 0 \tag{6.5.5c}$$

$$\frac{b^2w(u_2-u_{2A})}{v}\frac{\mathrm{d}w}{\mathrm{d}s} + \frac{b^2u(u_2-u_{2A})}{v}\frac{\mathrm{d}u_1}{\mathrm{d}s} + \frac{b^2u_2(u_2-u_{2A})}{v}\frac{\mathrm{d}u_2}{\mathrm{d}s} + 2v(u_2-u_{2A})b\frac{\mathrm{d}b}{\mathrm{d}s} + vb^2\frac{\mathrm{d}u_2}{\mathrm{d}s} = 0 \tag{6.5.5d}$$

$$vb^2\frac{\mathrm{d}g'}{\mathrm{d}s} + \frac{b^2wg'}{v}\frac{\mathrm{d}w}{\mathrm{d}s} + \frac{b^2u_1g'}{v}\frac{\mathrm{d}u_1}{\mathrm{d}s} + + \frac{b^2u_2g'}{v}\frac{\mathrm{d}u_2}{\mathrm{d}s} + 2g'vb\frac{\mathrm{d}b}{\mathrm{d}s} = -N^2b^2w \tag{6.5.5e}$$

Combine the first two equations of (6.5.5): (6.5.5b) $-w\times$(6.5.5a)

$$b^2v\frac{\mathrm{d}w}{\mathrm{d}s} = b^2g' - Ew$$

and hence

$$\frac{\mathrm{d}w}{\mathrm{d}s} = \frac{g'}{v} - E\frac{w}{b^2v}. \tag{6.5.6}$$

Combine the first and the third equation of (6.5.5): (6.5.5c) $-(u_1 - u_{1A})\times$(6.5.5a):

$$b^2 v \frac{\mathrm{d}u_1}{\mathrm{d}s} = -E(u_1 - u_{1A})$$

and hence

$$\frac{\mathrm{d}u_1}{\mathrm{d}s} = E\frac{-E(u_1 - u_{1A})}{b^2 v}. \tag{6.5.7}$$

Combine the first and the fourth equation of (6.5.5): (6.5.5d) $-(u_2 - u_{2A})\times$(6.5.5a):

$$b^2 v \frac{\mathrm{d}u_2}{\mathrm{d}s} = -E(u_2 - u_{2A})$$

and hence

$$\frac{\mathrm{d}u_2}{\mathrm{d}s} = E\frac{-E(u_2 - u_{2A})}{b^2 v}. \tag{6.5.8}$$

Consider the equation (6.5.5a) for b and substitute (6.5.6), (6.5.7) and (6.5.8):

$$\begin{aligned}
2vb\frac{\mathrm{d}b}{\mathrm{d}s} &= E - \frac{b^2 w}{v}\frac{\mathrm{d}w}{\mathrm{d}s} - \frac{b^2 u_1}{v}\frac{\mathrm{d}u_1}{\mathrm{d}s} - \frac{b^2 u_2}{v}\frac{\mathrm{d}u_2}{\mathrm{d}s} \\
&= E - \frac{b^2 w}{v}\left(\frac{g'}{v} - E\frac{w}{b^2 v}\right) + \frac{b^2 u_1 E(u_1 - u_{1A})}{v^2 b^2} + \frac{b^2 u_2 E(u_2 - u_{2A})}{v^2 b^2} \\
&= E - \frac{b^2 w g'}{v^2} + E\frac{w^2}{v^2} + \frac{u_1 E(u_1 - u_{1A})}{v^2} + \frac{u_2 E(u_2 - u_2 a)}{v^2}
\end{aligned}$$

and hence

$$\frac{\mathrm{d}b}{\mathrm{d}s} = \frac{E}{2bv} - \frac{bwg'}{2v^3} + E\frac{w^2}{2bv^3} + \frac{Eu_1(u_1 - u_{1A})}{2bv^3} + \frac{Eu_2(u_2 - u_2 a)}{2bv^3}$$

Substituting (6.5.6), (6.5.7), (6.5.8) and (6.5.9) in (6.5.5e)

$$\begin{aligned}
vb\frac{\mathrm{d}g'}{\mathrm{d}s} &= -N^2 wb - \frac{bwg'}{v}\frac{\mathrm{d}w}{\mathrm{d}s} + \frac{bu_1 g'}{v}\frac{\mathrm{d}u_1}{\mathrm{d}s} + \frac{bu_2 g'}{v}\frac{\mathrm{d}u_2}{\mathrm{d}s} - 2g'v\frac{\mathrm{d}b}{\mathrm{d}s} \\
vb\frac{\mathrm{d}g'}{\mathrm{d}s} &= -N^2 wb - \frac{bwg'}{v}\left(\frac{g'}{v} - E\frac{w}{b^2 v}\right) - \frac{bu_1 g'}{v}\left(-E\frac{u_1 - u_{1A}}{b^2 v}\right) - \frac{bu_2 g'}{v}\left(-E\frac{u_2 - u_{2A}}{b^2 v}\right) \\
&\quad -2\ g'v\left(\frac{E}{2bv} - \frac{bwg'}{2v^3} + E\frac{w^2}{2bv^3}\right) \\
vb\frac{\mathrm{d}g'}{\mathrm{d}s} &= -N^2 wb - \frac{bwg'^2}{v^2} + E\frac{w^2 g'}{bv^2} + E\frac{u_1(u_1 - u_{1A})g'}{bv^2} + E\frac{u_2(u_2 - u_{2A})g'}{bv^2} - \frac{Eg'}{b} + \frac{bwg'^2}{v^2} \\
&\quad -E\ \frac{g'w^2}{bv^2} - E\frac{g'u_1(u_1 - u_{1A})}{bv^2} - E\frac{g'u_2(u_2 - u_{2A})}{bv^2} \\
vb\frac{\mathrm{d}g'}{\mathrm{d}s} &= -N^2 wb - \frac{Eg'}{b}.
\end{aligned}$$

Thus,

$$\frac{\mathrm{d}g'}{\mathrm{d}s} = -N^2\frac{w}{v} - E\frac{g'}{b^2 v}$$

Now, as

$$g' = \frac{g(\theta - \theta_a)}{\theta_0}$$

I can express (6.5.9) in terms of θ. I get

$$\frac{g}{\theta_0}\frac{\mathrm{d}}{\mathrm{d}s}(\theta - \theta_a) = -N^2\frac{w}{v} - E\frac{g'}{b^2 v}$$

and hence

$$\begin{aligned}\frac{\mathrm{d}\theta}{\mathrm{d}s} &= \frac{\mathrm{d}\theta_a}{\mathrm{d}s} - \frac{\theta_0}{g}\left(N^2\frac{w}{v} + E\frac{g'}{b^2 v}\right)\\ &= \frac{\mathrm{d}\theta_a}{\mathrm{d}s} - N^2\frac{w\theta_0}{gv} - E\frac{(\theta - \theta_a)}{b^2 v}\end{aligned} \tag{6.5.9}$$

To summarise:

$$\begin{aligned}\frac{\mathrm{d}w}{\mathrm{d}s} &= \frac{g(\theta - \theta_a)}{v\theta_0} - E\frac{w}{b^2 v}.\\ \frac{\mathrm{d}u_1}{\mathrm{d}s} &= E\frac{-(u_1 - u_{1A})}{b^2 v}\\ \frac{\mathrm{d}u_2}{\mathrm{d}s} &= E\frac{-(u_2 - u_{2A})}{b^2 v}\\ \frac{\mathrm{d}b}{\mathrm{d}s} &= \frac{E}{2bv} - \frac{bwg(\theta - \theta_a)}{2v^3\theta_0} + E\frac{w^2}{2bv^3}\\ \frac{\mathrm{d}\theta}{\mathrm{d}s} &= \frac{\mathrm{d}\theta_a}{\mathrm{d}s} - N^2\frac{w\theta_0}{gv} - E\frac{(\theta - \theta_a)}{b^2 v}\end{aligned}$$

or in terms of time t, adding the equations for the ambient temperature and velocity

profiles:

$$\begin{aligned}
\frac{\mathrm{d}w}{\mathrm{d}t} &= \frac{g(\theta-\theta_a)}{\theta_0} - E\frac{w}{b^2}. \\
\frac{\mathrm{d}\theta}{\mathrm{d}t} &= \frac{\mathrm{d}\theta_a}{\mathrm{d}t} - N^2\frac{w\theta_0}{g} - E\frac{(\theta-\theta_a)}{b^2} \\
\frac{\mathrm{d}b}{\mathrm{d}t} &= \frac{E}{2b} - \frac{bw}{2v^2}\frac{g(\theta-\theta_a)}{\theta_0} + E\frac{w^2}{2bv^2} \\
\frac{\mathrm{d}u_1}{\mathrm{d}t} &= E\frac{-(u_1-u_{1A})}{b^2} \\
\frac{\mathrm{d}u_2}{\mathrm{d}t} &= E\frac{-(u_2-u_{2A})}{b^2} \\
\frac{\mathrm{d}u_{1A}}{\mathrm{d}t} &= w\frac{\mathrm{d}u_{1A}}{\mathrm{d}z} \\
\frac{\mathrm{d}u_{2A}}{\mathrm{d}t} &= w\frac{\mathrm{d}u_{2A}}{\mathrm{d}z} \\
\frac{\mathrm{d}\theta_a}{\mathrm{d}t} &= w\frac{\mathrm{d}\theta_a}{\mathrm{d}z}
\end{aligned} \tag{6.5.10}$$

where $N^2 = \frac{g}{\theta_0}\frac{\mathrm{d}\theta_a}{\mathrm{d}z} = \frac{g}{\theta_0 w}\frac{\mathrm{d}\theta_a}{\mathrm{d}t}$.
By comparing the two equations 6.5.10 and 6.2.9 the equation 6.5.1 is proved. Note that N (and hence $\mathrm{d}\theta_a$) is not constant. The expression for E is the same used in the previous cases, justifiable statement assuming that the difference between ambient and plume velocities is small relative to the ambient one.
Figures 6.14 and 6.15 show respectively the plume height the standard deviation of the particles distibution around the plume height as function of the downwind direction $X = \sqrt{x^2+y^2}$ on the plane (x, y). In [Fig.6.14] I plot as well some trajectories of the fictitious particles released from the source for the LSM. Comparing output from the Met Offices atmospheric dispersion model, NAME, with satellite imagery suggested that the plume was reaching a height of about 3000 m. This estimation was supported by a report from a commercial airline pilot. This was supported by a call received from Southampton Air Traffic Control shortly after 10am with a report from a commercial airline which indicated that the smoke plume was rising to a height of 9000 ft (2743 m) within the Atmosphere. A high pressure system dominated the weather over the south of the UK during Sunday 11th December 2005. A stable Atmosphere existed, which suppressed vertical mixing.A shallow strongly stable layer with temperature increasing with height (a temperature inversion) ex-

isted at the ground up to a height of about 100 m. Above this layer up to a height of about 400 m above ground, the Atmosphere was approximately neutral in stability. Above this neutral layer the Atmosphere was stable throughout with a strongly stable layer up to about 1200 m. Above, a shallow neutral layer existed at the ground (100 m in depth). The Atmosphere was stable above and was strongly stable up to height of about 1900 m with a number of small temperature inversions. Furthermore the plume was detected at a height of approximately 2000 m above Bournemouth by the Metoffice FAAM (Facility for Airborne Atmospheric Measurements) aircraft on Monday 12th December and was reported to be roughly 11 miles wide with a maximum height of 5000 ft (1524 m) on Tuesday 13th December. [Fig.6.14] shows that the particles of proposed LSM reach a maximum height just lower than 3000 m and the main plume height (i.e the equilibrium height for the plume) is included between 1500 m and 2000 m. This is roughly in line with observations from satellite imagery and the FAAM aircraft especially considering the range of the standard deviation of particles positions around the mean height (see [Fig.6.15]).
Figure 6.16 shows the scalar concentration computed from the LSM with and without temperature fluctuations. Results are presented with $\gamma = 0.25$ and $\gamma = 0.5$. The initial buoyancy flux was comparable with that estimated from the explosion at the oil depot and used in the original LES study [Devenish and Edwards (2009)]. The LES results are also shown in the same figure. In contrast with the previous section (see Fig. 6.9), the scalar concentration shown in Fig. 6.16 includes the rising part of the plume as that was how the LES results were calculated. It can be seen that while the model plumes do not rise quite as high as the LES plume, there is a small increase in height as the value of γ increases. Similarly, and not unexpectedly, the spread of the model plumes increases with increasing γ. The values of $\sigma_{\hat{z}}$ for all four cases are: 396 m (LES); 324 m (model plume with $\theta' \neq 0$ and $\gamma = 0.5$); 272 m (model plume with $\theta' \neq 0$ and $\gamma = 0.25$); 258 m (model plume with $\theta' = 0$).

Figure 6.11: The blaze at the Buncefield oil depot.

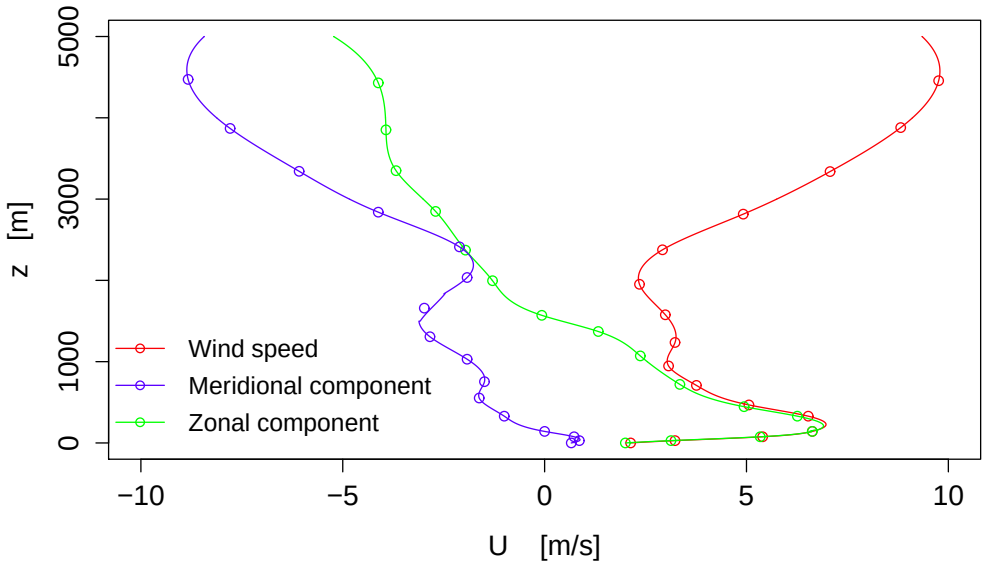

Figure 6.12: The ambient initial wind profile at time of Buncefield explosion.

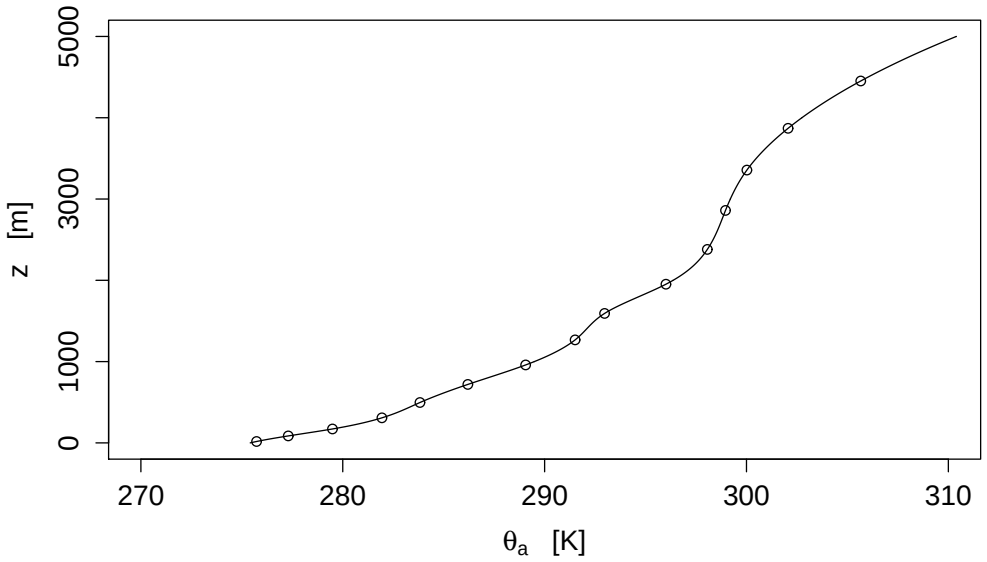

Figure 6.13: The ambient initial potential temperature profile at time of Buncefield explosion.

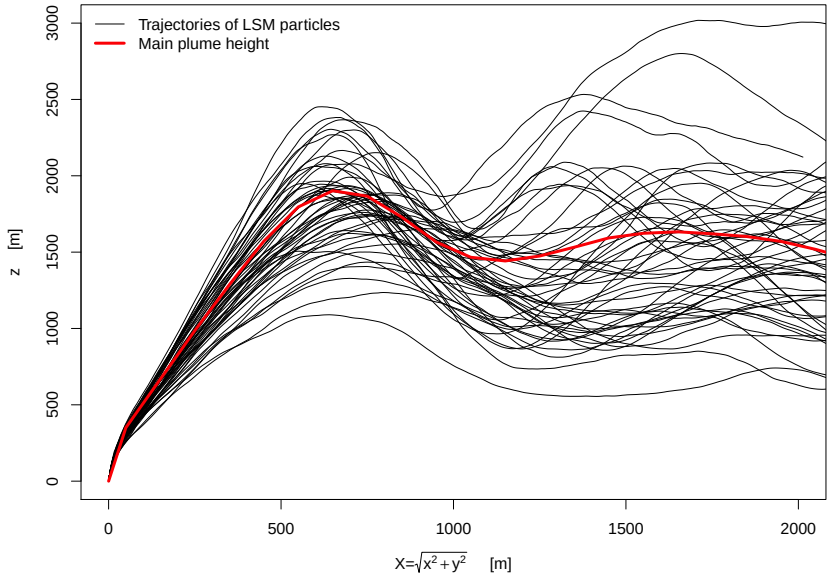

Figure 6.14: Main plume height (red) and particles trajectories (black) generated by the LSMo as function of the downwind direction $X = \sqrt{(x^2 + y^2)}$ on the plane (x, y)

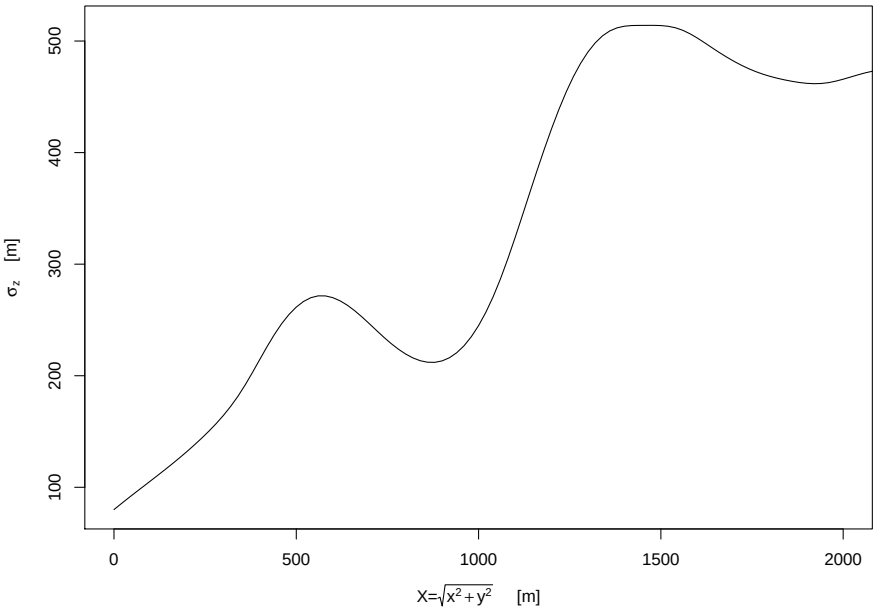

Figure 6.15: Standard deviation of the particles distibution around the mean height as function of the downwind direction $X = \sqrt{(x^2 + y^2)}$ on the plane (x, y)

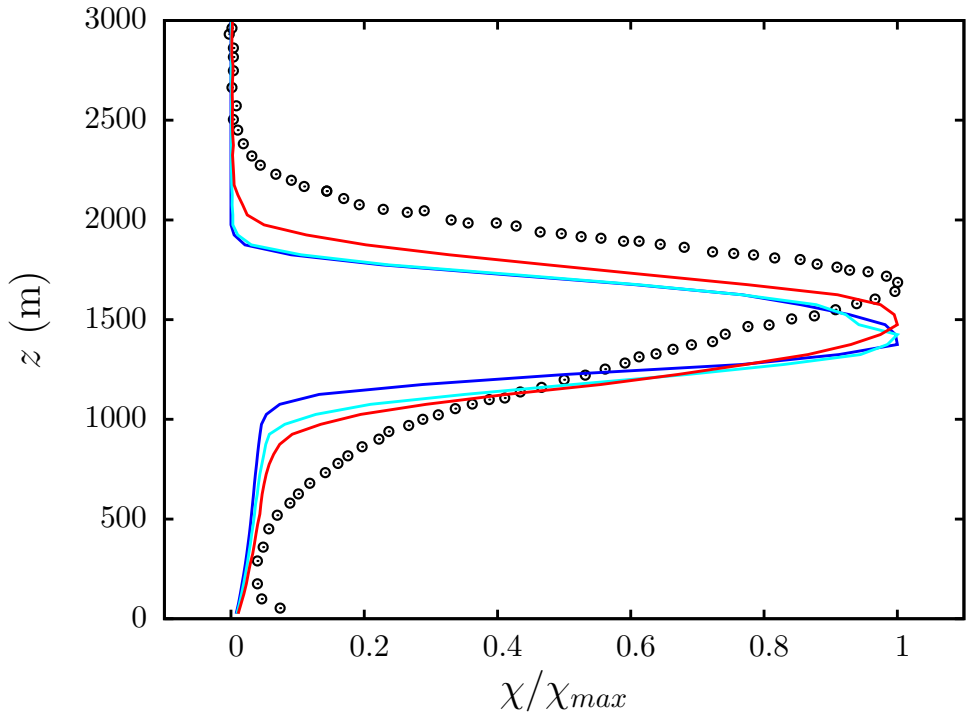

Figure 6.16: The scalar concentration normalised by its maximum value for the Buncefield case described in the text: the black circles are the LES results; the model plumes with $\theta' \neq 0$ are shown by the red and cyan lines for $\gamma = 0.5$ and $\gamma = 0.25$ respectively; the blue line is the model plume with $\theta' = 0$.

Chapter 7

Analytical offline approach for concentration fluctuations and higher order concentration moments.

7.1 Model formulation.

In a fixed reference frame with respect to the source location, the moments of concentration of a passive tracer emitted from a continuous source are defined as:

$$\overline{c^n}(x,y,z) = \int_0^\infty c^n p_c(c;x,y,z)dc \tag{7.1.1}$$

where c is the instantaneous concentration, $p_c(c;x,y,z)$ is the concentration PDF in the fixed system, x is the downwind distance, y the crosswind direction and z is the vertical coordinate. In the FPM approach, the ensemble dispersion of a plume is viewed as the sum of a number of instantaneous plumes. The motion of the centroid of each instantaneous plume is considered in a fixed coordinate system relative to the source, whereas the concentration distribution within the instantaneous plume is calculated relatively to the plume centroid. Following [Gifford (1959)], I assume the contributions due to meandering and to relative diffusion are statistically independent; the concentration PDF can be written as:

$$p_c(c;x,y,z) = \int_0^\infty \int_{-\infty}^\infty p_{cr}(c;x,y,z,y_m,z_m)p_m(x,y_m,z_m)dy_m dz_m \tag{7.1.2}$$

where $p_m(x,y_m,z_m)$ is the PDF of centroid position, $p_{cr}(c;x,y,z,y_m,z_m)$ is the relative concentration PDF in a reference frame relative to (y_m,z_m). Further I assume

that the plume meander in the crosswind direction is independent from the one in the vertical direction; the turbulence field is stationary and horizontally homogeneous; the wind shear can be neglected. Moreover I use of Taylor frozen turbulence hypothesis, i.e. $x = Ut$, , where $U = \overline{u}$ is the mean wind and t is the plume travel time. Substituting equation 7.1.2 in equation 7.1.1 I have:

$$\overline{c^n}(x,y,z) = \int_0^\infty \int_{-\infty}^\infty \left[\int_0^\infty c^n p_{cr}(c;x,y,z,y_m,z_m)dc \right] p_m(x,y_m,z_m)dy_m dz_m \tag{7.1.3}$$

and using the definition of nth-order relative concentration moments $\overline{c_r^n}(x,y,z)$:

$$\overline{c_r^n}(x,y,z,y_m,z_m) = \int_0^\infty c^n p_{cr}(c;x,y,z,y_m,z_m)dc \tag{7.1.4}$$

it is possible to obtain:

$$\overline{c^n}(x,y,z) = \int_0^\infty \int_{-\infty}^\infty \overline{c_r^n}(x,y,z,y_m,z_m) p_m(x,y_m,z_m)dy_m dz_m \tag{7.1.5}$$

Equation 7.1.5 summarizes the idea of the FPMs stating that the concentration field can be evaluated through two different contributions: the meandering of the plume centroid $p_m(x,y_m,z_m)$ that has to be simulated, and the relative concentration statistics $\overline{c_r^n}(x,y,z,y_m,z_m)$ that has to be parameterized.

7.2 Relative concentration moments parameterization.

Following [Yee and Wilson (2000)] and [Luhar et al. (2000)], p_{cr} can be represented by the gamma distribution:

$$p_{cr}(c;x,z,z_m) = \frac{\lambda^\lambda}{\overline{c_r}\Gamma(\lambda)} \left(\frac{c}{\overline{c_r}}\right)^{\lambda-1} exp\left(-\frac{\lambda c}{\overline{c_r}}\right) \tag{7.2.1}$$

where $\lambda = 1/i_{cr}^2$ and $i_{cr} = \frac{\sigma_{cr}(x,y,z)}{\overline{c_r}(x,y,z)}$ is the relative concentration fluctuation intensity, $\Gamma(\lambda)$ is the gamma function, and $\overline{c_r}$ is the mean concentration relative to the instantaneous plume centroid. Substituting 7.2.1 in the term within the square brackets of equation 7.1.3, it is possible to show the following property of p_{cr} :

$$\overline{c_r^n} = \int_0^\infty c^n p_{cr}(c;x,y,z,y_m,z_m)dc = \int_0^\infty c^n \frac{\lambda^\lambda}{\overline{c_r}\Gamma(\lambda)} \left(\frac{c}{\overline{c_r}}\right)^{\lambda-1} exp\left(-\frac{\lambda c}{\overline{c_r}}\right) dc = \frac{1}{\lambda^n}\frac{\Gamma(n+\lambda)}{\Gamma(\lambda)}\overline{c_r}^n \tag{7.2.2}$$

Hence the nth-order moment of relative concentration is proportional to the the first moment of relative concentration raised to the nth power. Using this statement in 7.1.5 I have:

$$\overline{c^n}(x,y,z) = \frac{1}{\lambda^n}\frac{\Gamma(n+\lambda)}{\Gamma(\lambda)}\int_0^\infty\int_{-\infty}^\infty \overline{c_r}^n(x,y,z,y_m,z_m)p_m(x,y_m,z_m)dy_m dz_m \tag{7.2.3}$$

Using the independence assumption between vertical and lateral diffusion, it is possible to factorize both the meander PDF and the relative mean concentration, and hence the absolute concentration, as:

$$p_m(x,y_m,z_m) = p_{ym}(x,y_m)p_{zm}(x,z_m) \tag{7.2.4}$$

$$\overline{c_r}(x,y,z,y_m,z_m) = \overline{c_{zr}}(x,z,z_m)p_{yr}(x,y,y_m) = \frac{Q}{U}p_{zr}(x,z,z_m)p_{yr}(x,y,y_m) \tag{7.2.5}$$

Where Q is the emission rate and the term $\frac{Q}{U}$ give to pdf the dimension of a concentration. Introducing this factorization in 7.2.3 I have:

$$\overline{c^n}(x,y,z) = \frac{1}{\lambda^n}\frac{\Gamma(n+\lambda)}{\Gamma(\lambda)}\frac{Q}{U}\int_0^\infty\left(\int_{-\infty}^\infty p_{ym}(x,y_m)p_{yr}(x,y,y_m)dy_m\right)p_{zm}(x,z_m)p_{zr}(x,z,z_m)dz_m \tag{7.2.6}$$

Since I have supposed the total crosswind expansion to be a Gaussian without boundary, the contribution to concentration moments from the lateral meander can be carried out analytically as in [Luhar et al. (2000)] to yield:

$$\begin{aligned}\overline{c^n}(x,y,z) &= \frac{1}{\lambda^n}\frac{\Gamma(n+\lambda)}{\Gamma(\lambda)}\frac{Q}{U}\frac{\sigma_{yr}}{\left(\sqrt{2\pi}\sigma_{yr}\sqrt{n\sigma_{ym}^2+\sigma_{yr}^2}\right)^n}exp\left[-\frac{ny^2}{2\sqrt{n\sigma_{ym}^2+\sigma_{yr}^2}}\right] \\ &\int_0^H p_{zm}(x,z_m)p_{zr}(x,z,z_m)dz_m\end{aligned} \tag{7.2.7}$$

where H is the vertical domain size, σ_{yr} and σ_{ym} are respectively the relative and barycentre standard deviation for the y direction. The expression used for σ_{yr} is (see [Franzese (2003)]):

$$\sigma_{yr}^2 = \frac{g_y\epsilon(t+t_s)^3}{\left[1+\left(\frac{g_y\epsilon t^2}{2\sigma_v^2 T_{Lv}}\right)^{\frac{2}{3}}\right]^{\frac{3}{2}}} \tag{7.2.8}$$

where g_y is the one dimensional Richardson constant, ϵ is the dissipation rate of turbulent kinetic energy, T_{Lv} is the transverse Lagrangian time scale, σ_v^2 the turbulence transverse velocity variance and $t_s = (\sigma_0^2/(g_y\epsilon))^{\frac{1}{3}}$ accounts for a finite initial source size . Equation 7.2.8 corresponds to the inertial range relative dispersion formulation at small time, and tends to [Taylor (1921)]s limit at large time. The independence between meander and relative contribution allows to write $\sigma_y^2 = \sigma_{ym}^2 + \sigma_{yr}^2$ and obtain σ_{ym}^2 from this equation, with the crosswind spread σ_y^2 given by [Taylor (1921)]s formula or deduced by the mean filed input required in the meandering component evaluation. Being $\overline{c_{zr}}^n = \left(\frac{Q}{U}p_{zr}\right)^n$, an expression for p_{zr} is needed.
Both for the case of homogeneous turbulence and for the case of the wind tunnel boundary layers I considered, I choose the relation of [Franzese (2003)] assuming that the particle mean distribution around the centre of mass is Gaussian and includes multiple reflections at the boundaries:

$$p_{zr}(x,z,z_m) = \frac{1}{\sqrt{2\pi}\sigma_{zr}} \sum_{n=-N}^{N} \left[exp\left(-\frac{(z - z_m + 2nH)^2}{2\sigma_{zr}^2}\right) + exp\left(-\frac{(z + z_m + 2nH)^2}{2\sigma_{zr}^2}\right)\right] \tag{7.2.9}$$

where N is the number of reflection and it is taken equal to 10. Although the equation 7.2.9 represent a simple reflected Gaussian form (Franzese, 2003), it was found to provide good overall agreement with the experiments. A skewed PDF obtained as the sum of two reflected Gaussian PDFs ([Luhar et al. (2000)]; [Dosio and de Arellano (2006)]) and especially suited for skewed turbulence can be also used here, e.g. in the case of convective boundary layer (CBL) or highly asymmetrical canopies (see appendix A). Anyway throughout this thesis I used the 7.2.9 for p_{zr} given that it provides good results in the comparison with various data, although it si very simple.
An expression for the standard deviation of vertical relative position is needed. The vertical dispersion coefficient corresponds to the inertial range behaviour for small times, as equation 7.2.8 for crosswind direction, whereas accounts for the boundaries effect that reduces the vertical spreading at large times, see [Mortarini et al. (2009)].

$$\sigma_{zr}^2 = \frac{\alpha_N g_z \epsilon (t + t_s)^3}{\left[1 + \alpha_D \left(g_z \epsilon t^3\right)^{\frac{2}{3}}\right]^{\frac{3}{2}}} \tag{7.2.10}$$

where g_z is the one dimensional Richardson constant for vertical direction and the parameters α_N and α_D are introduced to set the contribution of two different behaviours for small and large time.
Equation 7.2.7 shows that, in order to give a complete closure for relative concentration moments, an expression for λ, and thus for i_{cr}, is required. The concentration fluctuations are primarily caused by the variation in the external intermittency produced exclusively by the meandering motion near the source, but in the far field the

in-plume fluctuations became predominantly; inside the instantaneous plume boundaries, the fluctuations arise solely from an internal intermittency due to internal concentration fluctuations produced by the turbulent mixing processes (e.g., strain and rotation of concentration gradients by velocity gradients, dissipation due to molecular diffusive processes). Without taking into account i_{cr}, the absolute concentration fluctuations $i_c = \frac{\sigma_c(x,y,z)}{\overline{c}(x,y,z)}$ became zero as soon as the meander contribution is negligible. Measurements of lateral cross-sections of the fluctuation intensity i_c of a point source plume in the absolute frame ([Yee et al. (1994)]) show that i_c has a minimum at the mean plume centreline and increases markedly towards the plume edges. I note that the U-shaped profile for i_c predicted by the experimental data ([Gailis et al. (2007)]) is due entirely to the external fluctuations resulting from the bulk meandering of the plume. It is expected that the internal plume intermittency reflecting the internal fine-scale fluctuations should result also in a U-shaped profile for i_{cr}, similar to the U-shaped profile for i_c due to the external plume intermittency reflecting the plume meander. In view of this, [Gailis et al. (2007)] propose the following functional form for i_{cr} derived from [Gifford (1959)] 2-D FPM:

$$i_{cr}^2 = \left(1 + i_{cr0}^2\right)\left(\frac{\overline{c_r}}{\overline{c_{r0}}}\right)^{-\zeta} - 1 \tag{7.2.11}$$

where i_{cr0} is the i_{cr} minimum, c_{r0} is the c_r maximum and ζ is a shape parameter with values in the interval $[0, 1]$. The values of i_{cr0} and ζ are choosen, for any x, to have the best agreement with experimental data. [Gailis et al. (2007)] obtain the values $\zeta = \frac{1}{5}$ for crosswind direction, $\zeta = \frac{3}{4}$ for vertical one and i_{cr0} are less than unity, applying their model to a water channel simulation that reproduce at small scale the Mock Urban Setting Test (MUST) conducted at the U.S. Army Dugway Proving Ground, Dugway, Utah in September 2001. This choice is made because it is the only for height-dependent parameterization and takes into account the conservation of TKE dissipation in the vortex scale reduction close to the boundaries.

7.3 Evaluation of centroid vertical location PDF.

Most of the recent versions of fluctuating plume model are coupled with a Lagrangian Stochastic Model for the particle trajectories in order to calculate the mean concentration field. In the presented version of FPM I use the [Cassiani and Giostra (2002)] approach to evaluate the vertical location PDF p_{zm}. This approach has the

advantage of independence from the method use to evaluate the mean concentration field $\overline{c}(x, y, z)$, thus relaxing the need for Lagrangian modelling. Hence $\overline{c}(x, y, z)$ can be derived both from measurements and numerical evaluation. Once the mean field $\overline{c}(x, y, z)$ is known, the evaluation of p_{zm} only requires the mean height $\overline{z}$ and the vertical location variance σ_z.
The definition of crosswind-integrate concentration is:

$$\overline{c_y}(x, z) = \int_{-\infty}^{\infty} \overline{c}(x, y, z) dy \tag{7.3.1}$$

It corresponds to marginal PDF definition. In this context the concentration can be seen as the density of probability that mass of a pollutant is at a given point and given instant. Hence, reminding that the downwind dispersion in negligible, $\overline{c_y}$ corresponds with $p_z(x, z)$. In particular, in order to satisfy the normalisation condition $\int_{-\infty}^{\infty} \overline{c_y}(x, z) dz = 1$, I can write:

$$p_z(x, z) = \frac{\overline{c_y}(x, z)}{\int_0^H \overline{c_y}(x, z) dz} \tag{7.3.2}$$

Where the indefinite integral is replaced with the integral over the vertical domain $[0, H]$. Substituting the definition 7.3.1 in the equation 7.3.2 it follows that:

$$p_z(x, z) = \frac{\overline{c_y}(x, z)}{\int_0^H \int_{-\infty}^{\infty} \overline{c}(x, y, z) dy dz} \tag{7.3.3}$$

The double integral in the denominator represent the source term $\frac{Q}{U}$. From dimensional analysis, it is obvious that the source emission term Q has the dimension of a particles flux. Discrete values of $p_z \triangle z$ can be specified directly by sampling the crosswind-integrated concentration normalised according to 7.3.3 in N points, where $\triangle z = 1/N$ is the the spatial scale of the grid. Thus it is possible to write:

$$\overline{z}(x) = \sum_{i=1}^{N} p_{zi}(x, z) \triangle z_i \tag{7.3.4}$$

where the subscript i selects the ith point of the grid. Analogously relationships can be obtained for the high order moments, e.g.:

$$\sigma_z^2(x) = \sum_{i=1}^{N} (z_i - \overline{z})^2 p_{zi}(x, z) \triangle z_i \tag{7.3.5}$$

Now the [Cassiani and Giostra (2002)] linear transformation is used to evaluate the meandering barycentre PDF p_{zm}; it is equal to [Luhar et al. (2000)] linear transformation, but it is apply on the points of the calculation grid instead of trajectories given by a Lagrangian single particle model. This method allows to remove the need for SPM though maintaining the same phisycal meaning of [Luhar et al. (2000)] linear transformation and to reduce the computational time also considering that the grid points are less than the number of particle released in a SPM. [Luhar et al. (2000)] derive the trajectory of the instantaneous plume centre of mass $z_m(x)$ from the particle trajectory $z(x)$ (or equivalently $z(t)$ assuming frozen turbulence) generated by a SPM using the following linear transformation (see appendix B for the details):

$$z_m(x) = \frac{\sigma_z^2 - \sigma_{zr}^2}{\sigma_z^2}(z(x) - \overline{z}(x)) + \overline{z}(x) \tag{7.3.6}$$

where σ_z^2 and σ_{zr}^2 are respectively the absolute and relative vertical positions variances. As in [Cassiani and Giostra (2002)] I use the same linear transformation but applied to grid spacing instead of Lagrangian trajectories:

$$z_{mi}(x) = \frac{\sigma_z^2 - \sigma_{zr}^2}{\sigma_z^2}(z_i(x) - \overline{z}(x)) + \overline{z}(x) \tag{7.3.7}$$

Introducing the definition of grid spacing for the total dispersion and the barycentre dispersion as $\Delta z = z_i(x) - \overline{z}(x)$ and $\Delta z_m = z_{mi}(x) - \overline{z}(x)$ respectively, (note that $\overline{z_m} = \overline{z}$) it follows:

$$\Delta z_{mi}(x) = \frac{\sigma_z^2 - \sigma_{zr}^2}{\sigma_z^2}\Delta z(x) \tag{7.3.8}$$

A relation between the PDFs of two stochastic processes linearly related such as $z_m(x)$ and $z(x)$ is given by $p_z\Delta_z = p_{zm}\Delta_{zm}$, see appendix . In this way, the previous value of $p_{zi}\Delta_{zi}$ is exactly the value of $p_{zmi}\Delta_{zmi}$ for an instantaneous plume centroid located at z_{mi}. I note that Δ_{zm} is smaller than Δ_z by the factor $\frac{\sigma_z^2-\sigma_{zr}^2}{\sigma_z^2}$, so that the value of p_{zm} is greater than p_z. This is a compression of the grid spacing of the barycentre PDF that reduces the variance conserving at the same time the skewness, the kurtosis and all the scaled moments. The resulting form of PDF is:

$$p_{zm} = \begin{cases} 0 & \text{out of the compressed concentration field} \\ p_z\frac{\Delta z}{\Delta z_m} & \text{in the compressed concentration field} \end{cases} \tag{7.3.9}$$

Once p_{zm} is known, it is possible obtain:

$$\sigma_{zm}^2(x) = \sum_{i=1}^{N}(z_{mi} - \overline{z})^2 p_{zmi}(x,z) \triangle z_{mi} \tag{7.3.10}$$

$$\overline{z'^3_m(x)} = \overline{(z_m - \overline{z})^3(x)} = \sum_{i=1}^{N} (z_{mi} - \overline{z})^3 p_{zmi}(x, z) \triangle z_{mi} \tag{7.3.11}$$

and equivalently all the higher moments. Hence, the final form of FP I propose is obtained by rewriting the integral in 7.2.7 as:

$$\int_0^H p_{zm}(x, z_m) p_{zr}(x, z, z_m) dz_m = \sum_{i=1}^{N} p_{zm}(x, z_{mi}) p_{zr}(x, z, z_{mi}) \Delta z_{mi} \tag{7.3.12}$$

In such a sense, the method is a simplification of the [Luhar et al. (2000)] approach. Although being simpler and faster, from a mathematical point of view the method is equivalent to the [Luhar et al. (2000)] one.

7.4 Test Case

In this section three test cases are simulated to check the model behaviour. First, the model is applied to homogeneous turbulence and it is used to verify the well-mixed condition. Special attention to the second moment of concentration is given by comparing the results with analytical expressions found by [Thomson (1990)] and [Ferrero and Mortarini (2005)]. The other two test cases verify the behaviour of the model for inhomogeneous turbulence in water and wind tunnel simulations of the neutral boundary layer. First, I consider the water tunnel measurements of scalar concentration for three idealized urban canopies with different aspect ratios of [Huq and Franzese (2013)]. I compare the results obtained from the model both to the [Huq and Franzese (2013)] data, who encompass plume spread and concentration of a passive scalar continuously released from a near-ground point source, and to the [Huq and Franzese (2013)] Gaussian Model. Then the model is compared to the data-set of [Nironi (2013)] and [Nironi et al. (2013)] describing the evolution of a fluctuating pollutant plume within a wind tunnel simulation of a neutral boundary layer. The [Nironi (2013)] data set extends the popular study of [Fackrell and Robins (1982a)], about concentration fluctuations from point sources by including measurements of concentration skewness and kurtosis and investigations about the influence of source conditions on higher order concentration m oments.The data set is also completed by a detailed description of the velocity statistics.
I underline that the FPM introduced here, has the capability for evaluating the concentration PDF without a coupled LSM, given only a mean concentration field. The

flexibility of the models is validated using three different evaluations of the mean field: a simple SPM in homogenoeus turbulence, a Gaussian model in the water boundary layer and an experimental data in the wind tunnerl bounday layer.

7.4.1 Homogeneous turbulence

In this section I present the results of the numerical simulation given by model in homogeneous turbulence. This is a first validation and represents a good approximation for the crosswind direction even in more realistic kinds of turbulence. The mean and mean square concentration fields in the inertial range are investigated and compared with the theoretical predictions found by [Thomson (1990)] and [Ferrero and Mortarini (2005)] and [Luhar et al. (2000)]. [Thomson (1990)] develops an analytical solution obatined from two Langevin equations for the particles separation and barycentre. His approach is based on the stochastic processes theory, it prescribes a complete three dimensional model for two-particles dispersion in homogeneous turbulence and it is based on a Gaussian PDF for the particles separation. Following Thomson [Thomson (1990)], [Ferrero and Mortarini (2005)] prescribe an analytical formula for the fluctuation concentrations based on the Richardson form for the PDF separation. Morevoer [Ferrero and Mortarini (2005)] develop a single particle model with a gaussian PDF for the position. In particular [Ferrero and Mortarini (2005)] evaluated the mean concentration and the concentration fluctuations by using the single particle P_1 and on the two-particle separation P_2 PDFs, respectively as (see section 2.4):

$$\overline{c(x,t)} = \int P_1(y,s|x,t)S(y)dy$$

$$\overline{c^2(x,t)} = \int P_2(y_1,y_2,s,s|x_1,x_2,t,t)S(y)dy$$

being $S(y)$ the amount of tracer released per unit of volume that is consider, for sake of simplicity, a discrete Gaussian source distribution. Then [Ferrero and Mortarini (2005)] calculate $\overline{c(x,t)}$ using a Gaussian form for P_1 (note that the $\overline{c(x,t)}$ obtained by [Ferrero and Mortarini (2005)] has itself a Gaussian form.), and $\overline{c^2(x,t)}$ using the Richardson PDF for P_2.
Concerning the separation PDF they found that for $t < t_0$ and $t > T_L$ (where t is the time, t_0 is the cross-over time and T_L is the velocity correlation Lagrangian time scale) it is Gaussian, confirming the [Batchelor (1952)] and [Monin and Yaglom

(1971)] results, while in the intermediate subrange it departs from the Gaussian PDF and agrees with the Richardson PDF (as also found [Thomson (1990)] and [Boffetta and Sokolov (2002)]). From equation 7.2.7 it is clear that an analytical solution for concentration moments can also be carried out from fluctuating plume model (see e.g. [Luhar et al. (2000)]) only if the total and meander expansions are Gaussian and only for the case of free (i.e. not bound) variables. I consider the one-dimensional case and I refer to the position variable as y and to velocity variable as v given that the homogeneous turbulence is a good approximation for the lateral direction.; the generalization to two and three dimensions is trivial if only free variables are considered. The mean field required to develop the model is obtained by the simplest SPM. In homogeneous turbulence the velocity PDF can be considered as Gaussian yielding a simple expression for the Langevin equation:

$$\mathrm{d}v = -\frac{1}{T_L} v \cdot dt + \sqrt{C_0 \epsilon} \cdot dW(t) \tag{7.4.1}$$

where $-\frac{1}{T_L} v$ is the drift term, $dW(t)$ is incremental Wiener processes with zero mean and variance , ϵ is the TKE dissipation and is C_0 the Kolmogorov universal constant that ensures the model consistency with the Lagrangian velocity structure function as introducted in chapter 5. The homogeneity assumption allows to use the Gaussian relative PDF 7.2.9 of [Franzese (2003)] instead of the skewed one of [Dosio and de Arellano (2006)]. Furthermore with the hypothesis of free variable, hence without boundary reflections, equation 7.2.9 turns into a simple Gaussian distribution. Figure 7.1 show the mean concentration field computed with the FPM (black lines) presented in this chapter plotted over filled contours representing respectively the results obtained from the simple SPM of equation 7.4.1 used as data input for the FPM on the top-right and the analytical form obtained by [Ferrero and Mortarini (2005)] from their single particle model with gaussian PDF on the top-left. Both the figures above evidenced a very good agreement with the FPM. The figure 7.1 below show the absolute standard deviation σ_z, the baricentre standard deviation σ_z, and the relative standard deviation σ_{zr}. σ_z is compared to [Taylor (1921)] analytical form (equivalent to the [Thomson (1990)] σ_z) and the agreement results very good. The figure shows also the typical behaviour of a FP: near the source the total dispersion is dominated by the barycentre part so that $\sigma_z \sim \sigma_{zm}$ and $\sigma_{zr} \sim 0$, whereas far from the source the plume becomes well-mixed by spreading on the entire vertical domain and the relative part is therefore predominantly $\sigma_z \sim \sigma_{zr}$ and $\sigma_{zm} \sim 0$.
Figure 7.2 shows the mean concentration field $\overline{c(t, y)}$ evaluated from the simple SPM founded on Langevin equation written in equation 7.4.1 compared with analytical

formulae of [Ferrero and Mortarini (2005)] single particle model, of [Luhar et al. (2000)] FPM for crosswind direction. In particular I show the time evolution of the mean field divided by its intial value $\frac{\overline{c(t,y)}}{\overline{c(0,y)}}$ at $y = 0$, $y = 0.04$, $y = 0.08$ and $y = 0.12$. In $y = 0$ I show as well the comparison with the [Luhar et al. (2000)] FPM. In figure 7.3 I present the same results, but for normalised mean concentration field, i.e. for the PDF $p_y(t, y)$, focusing the attention on the spatial evolution at the fixed time $t = 0.01T_L$, $t = 0.1T_L$, $t = T_L$ and $t = 10T_L$. The model accurately reproduces the expected behaviour of the evolution time of mean concentration at given points and of the spatial evolution of y-PDF at fixed times. In homogenoeus turbulence my FPM coincides with the analytical version of [Luhar et al. (2000)] for crosswind direction because the expression for the drift term of equation 17.1 coupled with the [Luhar et al. (2000)] (or [Cassiani and Giostra (2002)]) linear transformation for crosswind direction (i.e $y_m = \frac{\sigma_y^2 - \sigma_{yr}^2}{\sigma_y^2}$ being $\overline{y} = \overline{y_m} = 0$) ensures that the meandering PDF is Gaussian and hence the equivalence between the two methods.
The second moment, i.e. the mean square concentration field, is now investigated. [Ferrero and Mortarini (2005)] found that the Richardson PDF give bette results at small times, while at larger times the model results agree with the formula based on a Gaussian PDF. This result demonstrates that the Gaussian PDF is able to satisfactorily predict concentration fluctuation only for times greater than the Lagrangian time scales, but when we are interested in the behaviour at very short times the Richardson separation PDF should be accounted for. This result is particularly interesting because in many practical applications the concentration fluctuations occur at very short times near the source. Hence in the figures about the second moment of concentration, the form prescribed by [Ferrero and Mortarini (2005)] has to be considered only at very short time. Moreover, the model of [Ferrero and Mortarini (2005)] is a one-dimensional model, hence the comparison with the y-direction of a two-dimensional FPM might be not proper. Nevertheless, as I show in the following figures, the agreement is very good and it is not trivial.
As shown in 7.4, the FPM results agree with the expected behaviour of $\overline{c^2}$ evaluated with the two analytical predictions of [Thomson (1990)] and [Ferrero and Mortarini (2005)] respectively. The two analytical models are also compared themselves in figure 7.4, although the figures evidence that the shape of $\overline{c^2}$ obtained from SPM fit slightly better the first one. In order to make this statement more noticeable, figure 7.5 shows the comparison among the FPM analytical version and the considered check-up analytical models, i.e. the two above-mentioned analytical prediction and the analytical version FPM of [Luhar et al. (2000)] for crosswind direction, for the

time evolution of the second-order moment of concentration normalised by its intial vlaue $\frac{\overline{c^2}(t,y)}{\overline{c^2}(0,y)}$ at given points $y = 0$, $y = 0.04$, $y = 0.08$ and $y = 0.12$. My FPM coupled with the simple SPM of equation 7.4.1 coincides with the analytical one of [Luhar et al. (2000)], as in the case of mean field, and the equivalence between two methods is checked out again. It is evident that the FPM values is more similar to [Thomson (1990)] solution model than [Ferrero and Mortarini (2005)] one. In spite of the choice of a Gaussian distribution both for the centroid and the relative PDFs in homogeneous turbulence, the FPM produces a slope of mean square concentration larger than the [Thomson (1990)] one in the intermediate range. In fact, the slope of $\overline{c^2}$ approach [Ferrero and Mortarini (2005)] form between $t = T_L$ and $T = 5T_L$ conferming the statement that in the intermediate subrange the separation PDF departs from the Gaussian distribution and agrees with the Richardson one.
Figure 7.6 shows a long-time simulation from FPM for testing the predicted asymptotic behaviour of the mean and of the mean square concentration at large times. Above I show that $\bar{c} \propto \sqrt{t}$ considering a Gaussian PDF, below that $\overline{c^2} \propto t^{-1}$ by using a Gaussian form for the separation PDF [Thomson (1990)].
In figure 7.7 the concentration fluctuation intensity are presented, by showing the behaviour of i_c in time and space (above and below respectively). Once the mean and mean square concentration fields are evaluated, the concentration fluctuation intensity is trivial calculate from equation $i_c = \frac{\sigma(t,y)}{\bar{c}(t,y)}$ for any model. The figure shows a good agree between FPM and [Thomson (1990)] both in time and in space. For the time evolution the model results are in good agreement with the previsions, including the prediction of a peak followed by a monotonic decay with distance. The decrease of i_c until zero for large time is a validation test for well-mixed condition. As a matter of fact, $i_c \to 0$ when the barycentre contribution is negligible. At large distances from the source the plume is spread over the whole vertical extension of the domain. Hence the relative part became predominantly, i.e. $\sigma_z \sim \sigma_{zr}$ and $\sigma_{zm} \sim 0$, validating the well-mixed condition. The anomalous behaviour of i_c immediately near the source is a characteristic of FPM and it is shared with several FPM versions present in literature. In the figure on the right it is possible to visualise the expected U shaped behaviour in space and the decrease and the flattening for the large time display the validity of well mixed condition again.

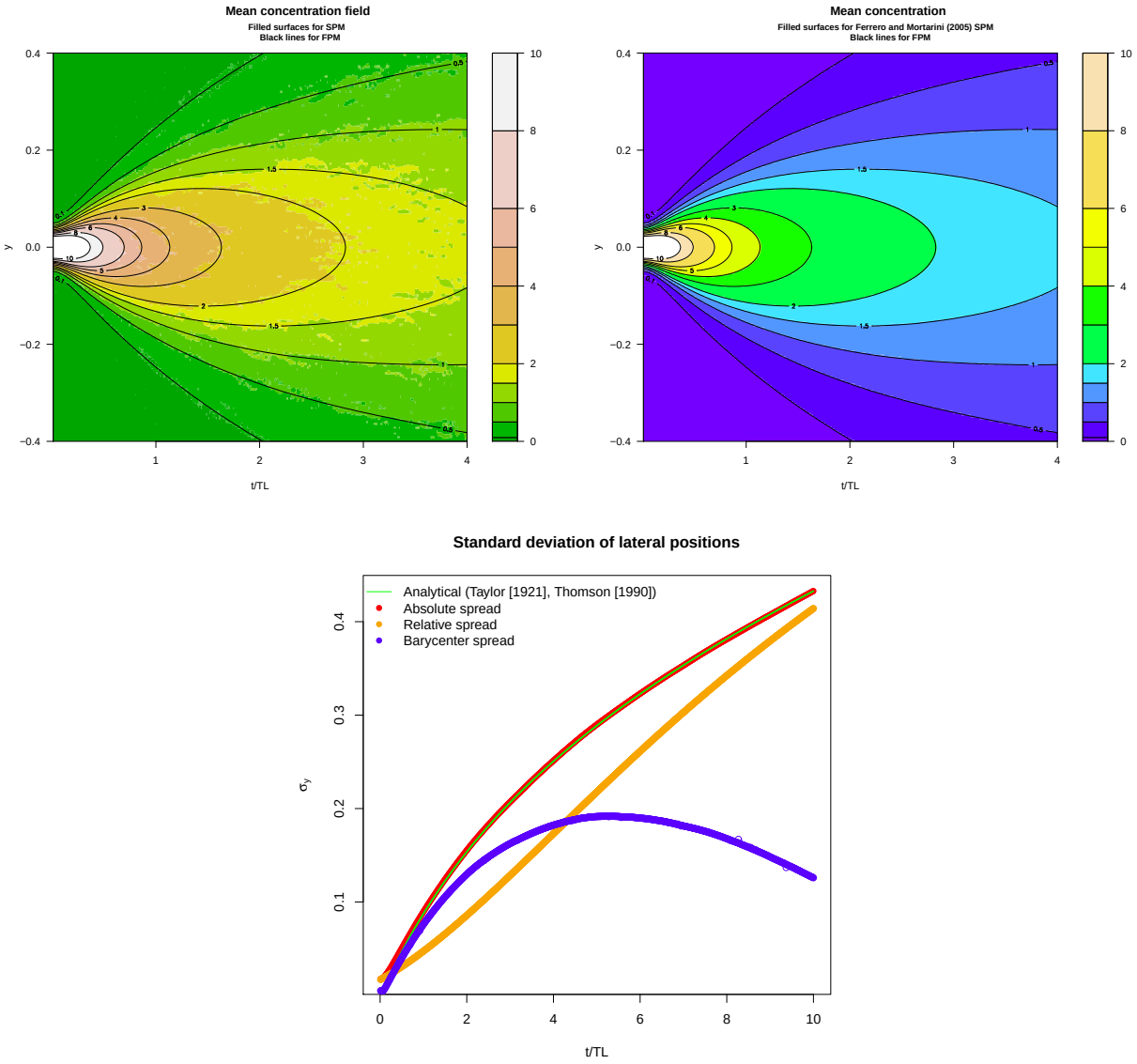

Figure 7.1: Mean concentration field in homogenous isotropic turbulence (above): the filled contours on the left represent the single particle model (see section 5.1 and subsection 7.4.1) used as input, the filled contours on the right represent mean field obtained by the single particle model of [Ferrero and Mortarini (2005)], the black contours correspond to the fluctuating plume model presented in sections 7.1, 7.2 and 7.3.
Standard deviation of particle positions (below): comparison between FPM and analytical expression of [Taylor (1921)].

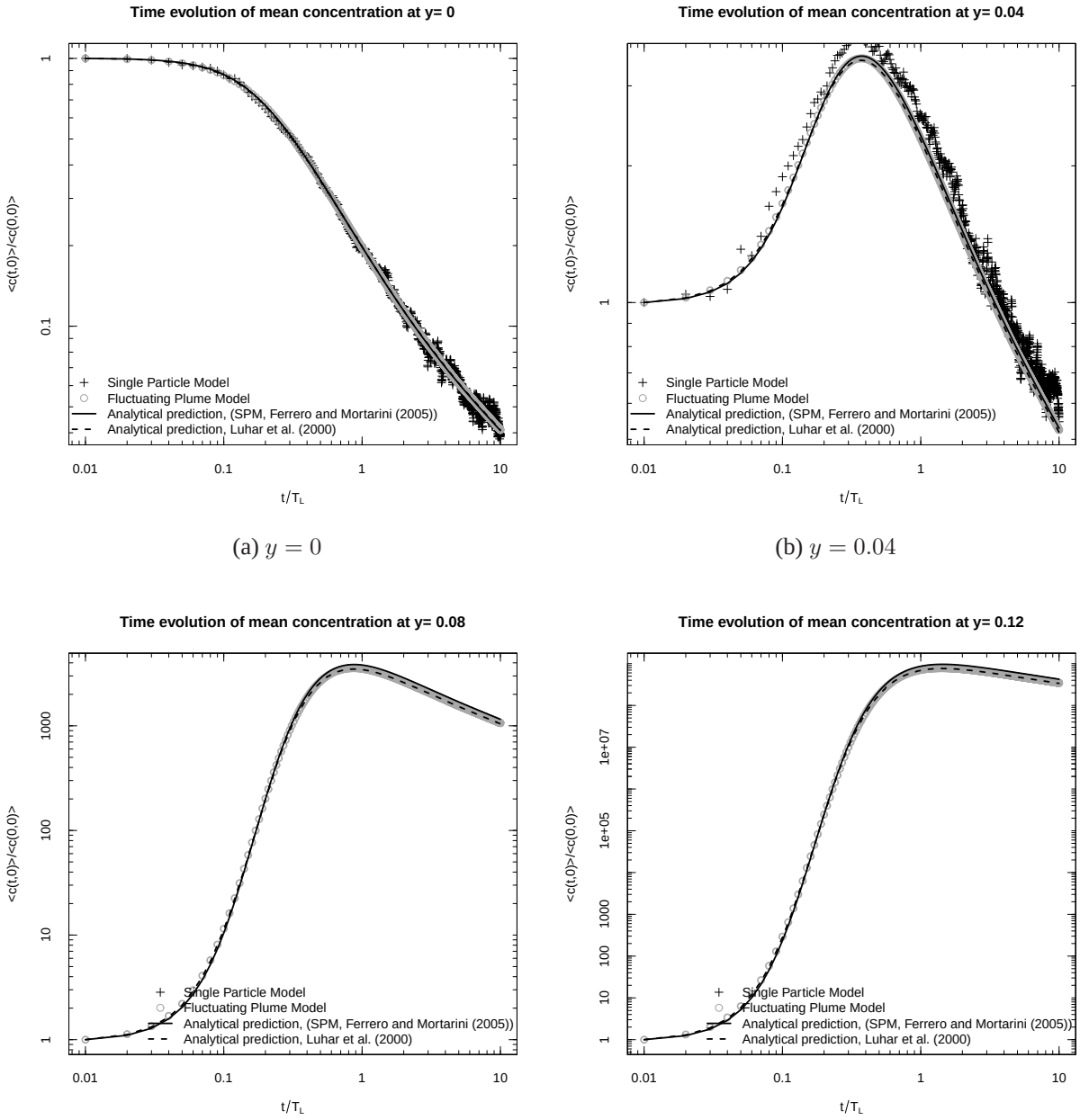

(a) $y = 0$

(b) $y = 0.04$

(c) $y = 0.08$

(d) $y = 0.12$

Figure 7.2: Time evolution of mean concentration field $\overline{c(t,y)}$ in homogeneous and isotropic turbulence at centreline $y = 0$ and at the locations $y = 0.04$, $y = 0.08$ and $y = 0.12$. Comparison among the fluctuating plume model, the analytical previsions present in literature ([Ferrero and Mortarini (2005)] SPM and [Luhar et al. (2000)] FPM) and the single particle model of section 5.1.

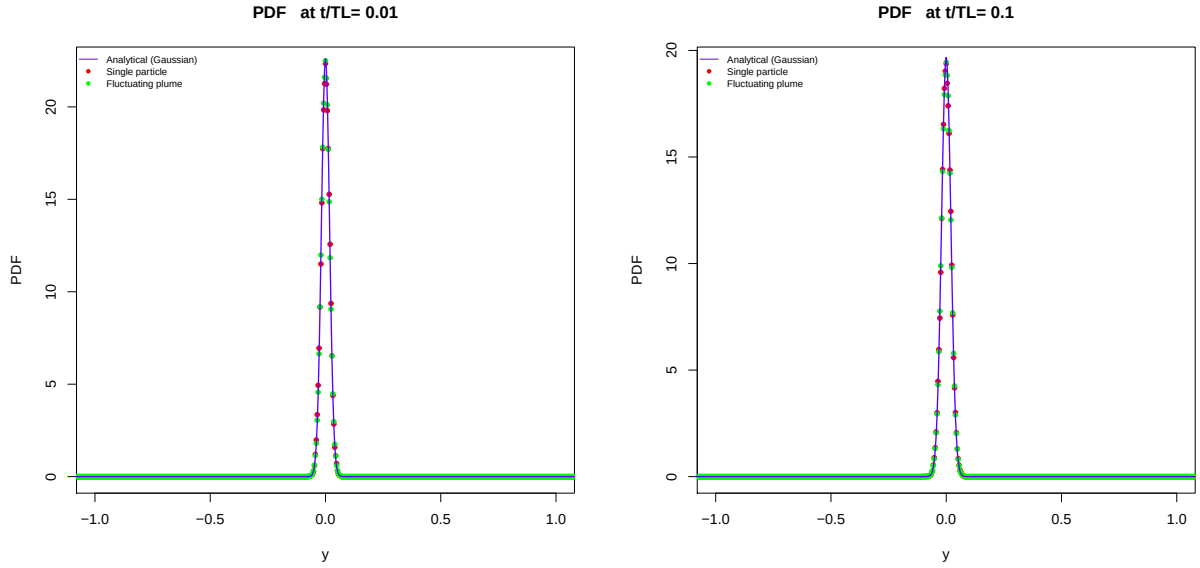

(a) $t = 0.01T_L$

(b) $t = 0.1T_L$

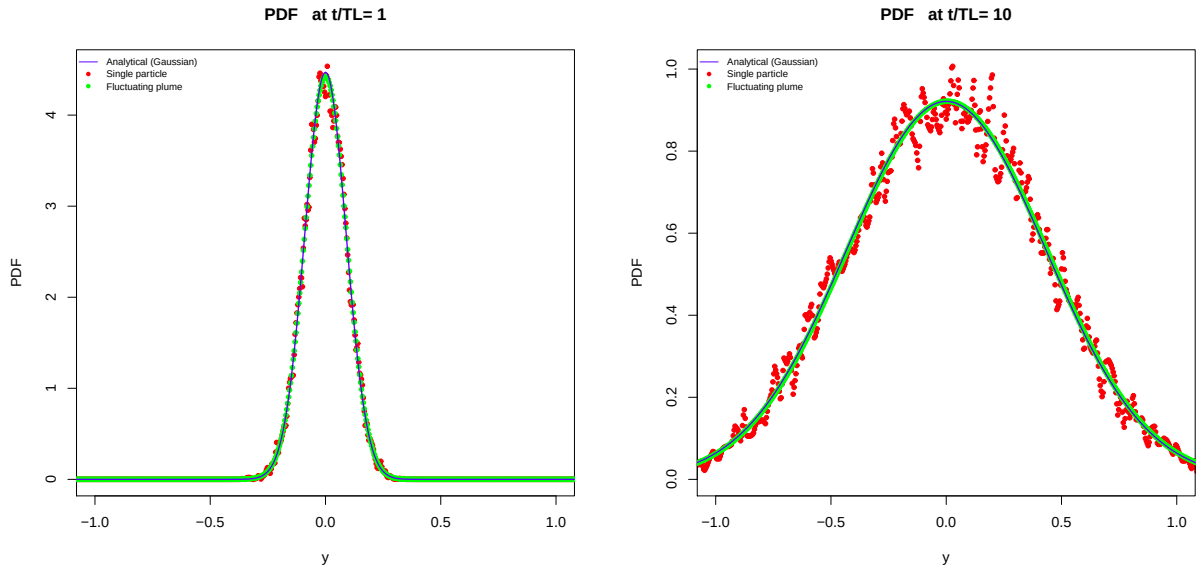

(c) $t = T_L$

(d) $t = 10T_L$

Figure 7.3: Spatial evolution of probability density function $p_y(t, y)$ in homogeneous and isotropic turbulence at the fixed time $t = 0.01T_L$, $t = 0.1T_L$, $t = T_L$ and $t = 10T_L$. Comparison among the fluctuating plume model, the analytical previsions present in literature and the single particle model of section 5.1 .

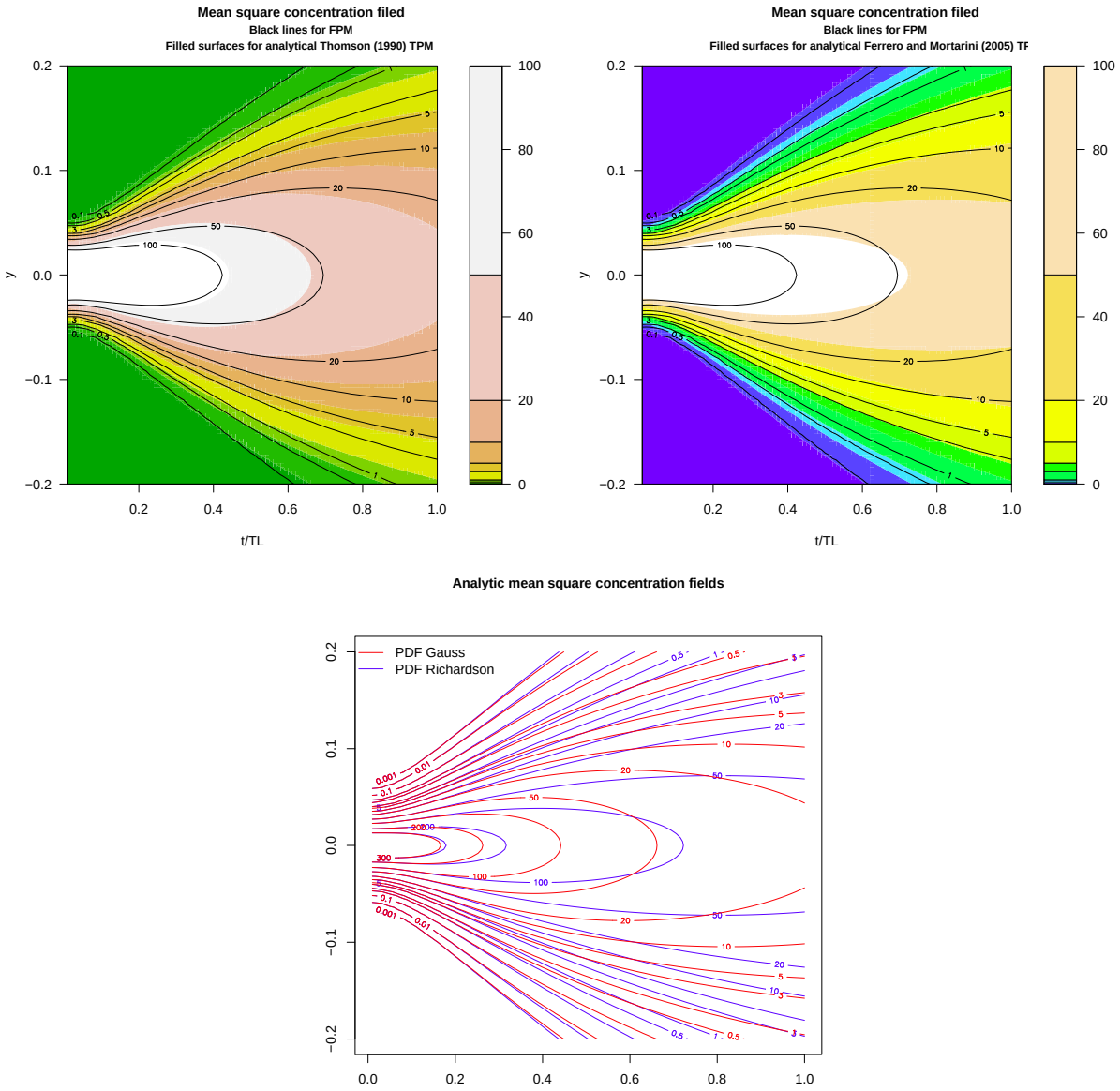

Figure 7.4: Mean square concentration field: in the the two figures above, the filled contours on the left represent the [Thomson (1990)] analytical TPM, the filled contours on the right represent the [Ferrero and Mortarini (2005)] analytical TPM, the black contours correspond to the FPM; in the figure above the red ann blue contour-lines show the [Thomson (1990)] and the [Ferrero and Mortarini (2005)] concentration second moments contour-lines respectively.

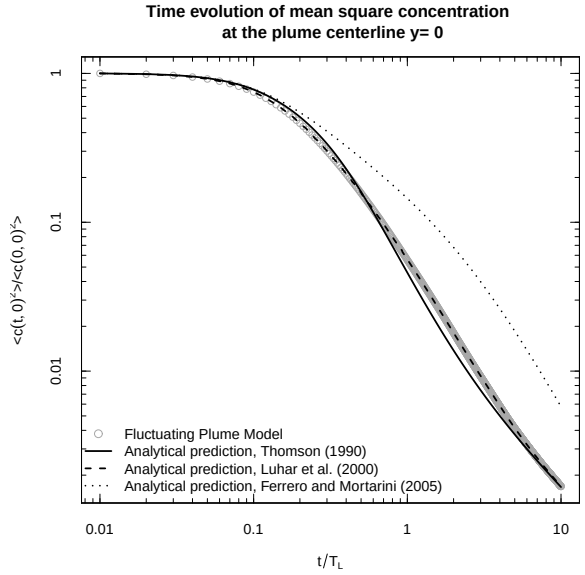

(a) $y = 0$

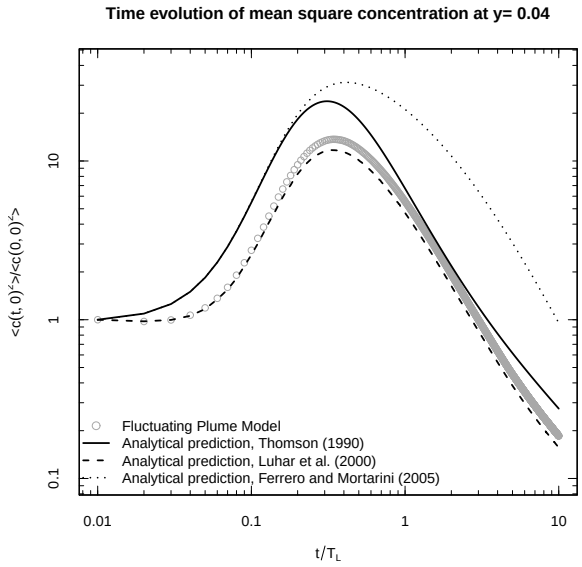

(b) $y = 0.04$

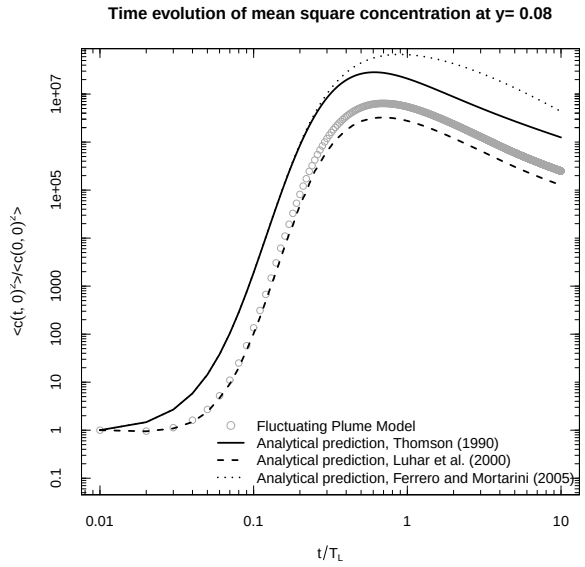

(c) $y = 0.08$

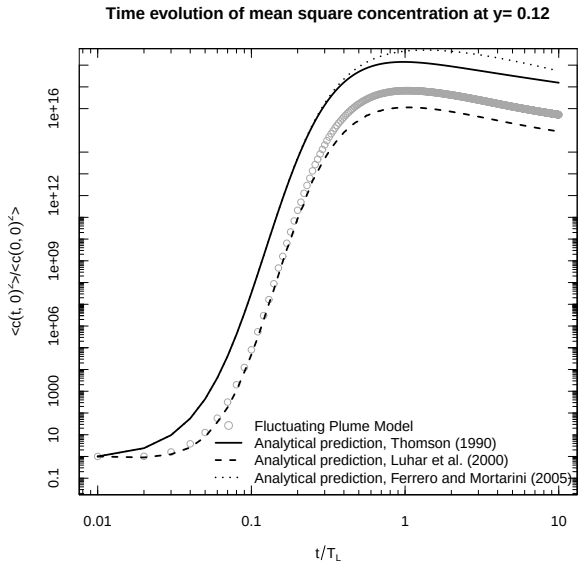

(d) $y = 0.12$

Figure 7.5: Time evolution of mean square concentration field $\overline{c^2}(t, y)$ in homogeneous and isotropic turbulence at centreline $y = 0$ and at the locations $y = 0.04$, $y = 0.08$ and $y = 0.12$. Comparison among the fluctuating plume model, the analytical previsions from two particles models present in literature i.e [Thomson (1990)] and [Ferrero and Mortarini (2005)].

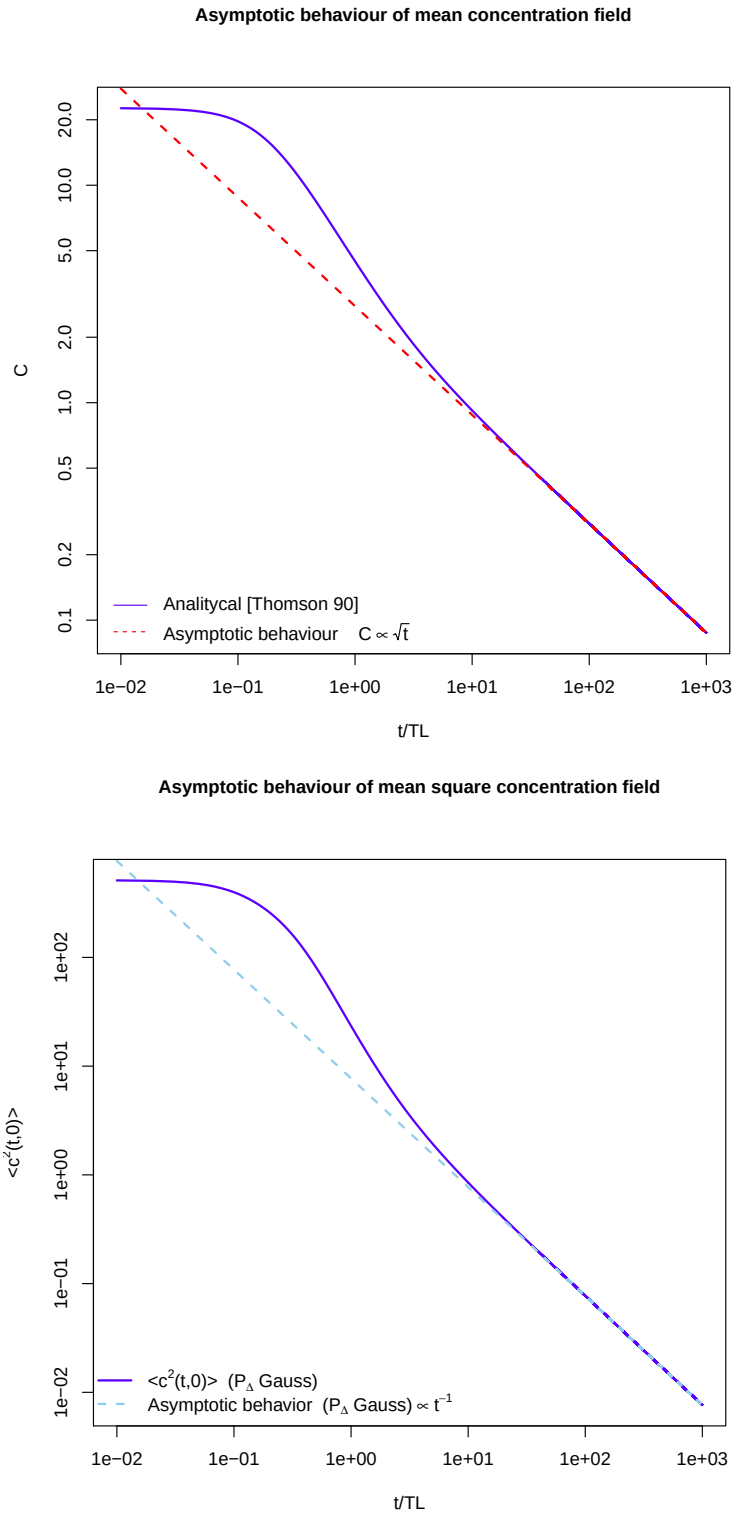

Figure 7.6: Asymptotic behaviour at large times ($t >> T_L$) of mean and mean square concentration field. The black contours correspond to the fluctuating plume model presented in sections 7.1, 7.2 and 7.3 and it is compared to the forms prescribed in literature considering Gaussian PDFs (i.in particular $\overline{c} \propto \sqrt{t}$ by using a SPM with Gaussian PDF, $\overline{c^2} \propto t^{-1}$ by using a Gaussian form for the separation PDF).

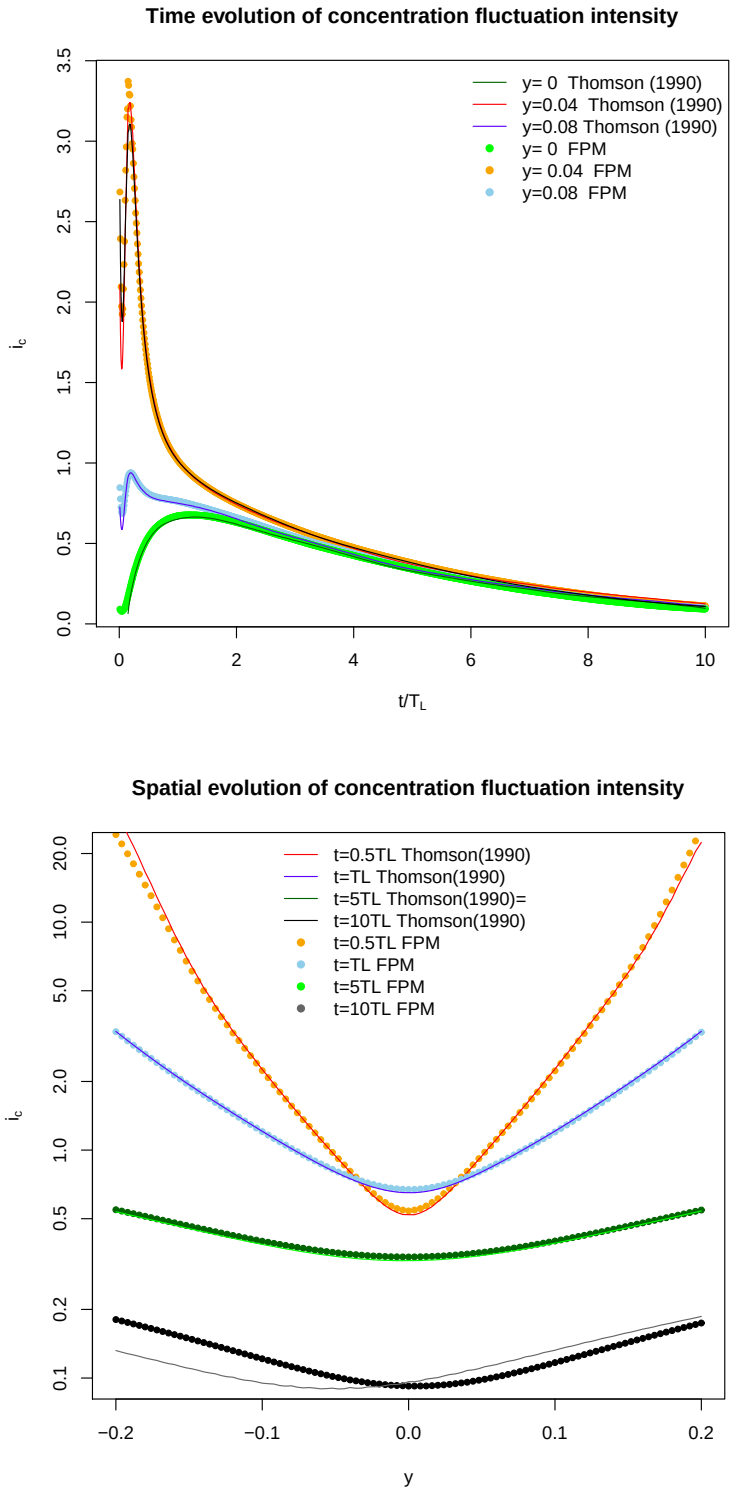

Figure 7.7: Concentration fluctuation intensity as a function of non-dimensional time at three different y-locations ($y = 0$, $y = 0.04$ and $y = 0.08$) above, and as a function of space at different times (i.e. distances to the source $t = 0.5T_L$, $t = 0T_L$, $t = 5T_L$ and $t = 10T_L$) below: comparison between FPM and [Thomson (1990)].

7.4.2 Water tunnel boundary layer

The interaction of atmospheric flow with the buildings of an urban area generates a boundary layer with specific characteristics. The vertical structure of urban boundary layers comprises a roughness sub-layer near the ground and an inertial sublayer above. In the lowest part of the roughness sub-layer, the buildings form a canopy layer. Difficulties arise in developing guidelines for predictive analysis as turbulence characteristics depend upon unique building arrangements and geometry. The Mock Urban Setting Test (MUST) field experiment (see [Biltoft (2001)]) has been undertaken using a large scale model of an urban canopy, where the roughness elements were formed by arrays of shipping containers. Anyway, meteorological data in the urban boundary layer are not as available as from rural sites. The application of the presented FPM to a real case scenario, like MUST, represents a further investigation about the behaviour of the model, and it is one of the development lines I will consider in my research.
Throughout this thesis the model in a canopy layer is applied to HF laboratory experiment.In particular I apply the fluctuating plume model to the [Huq and Franzese (2013)] laboratory experiment undertaken in a water tunnel at the Environmental Fluids Laboratory at the University of Delaware. They present measurements of turbulence, velocity and mean concentration of a passive scalar released from a continuous point source for three model urban canopies with different aspect ratios $A_r = \frac{H}{w_b} = 0.25$, $A_r = \frac{H}{w_b} = 1$ and $A_r = \frac{H}{w_b} = 3$ where H and w_b are the building height and width. The measurements for the canopy with $A_r = 0.25$, which consists of a regular series of prisms, were taken by [Macdonald and Ejim (2002)], while the measurements with $A_r = 1$ (arrays of cubes) and $A_r = 3$ (arrays of tall prisms) are new. The building length in the along-wind direction B is constant. [Huq and Franzese (2013)] took velocity and scalar measurements in the xz plane along the centreline $y = 0$ of the canpoy layer, where x, y and z indicate the alongwind, the crosswind and the vertical directions, respectively. The scalar source is a pipe at ground level $z = 0$, at the centreline of the canopy $y = 0$, at the center of the row $x = 0$. All experiments simulate in-canopy dispersion in the near field and the plume vertical dimension is smaller or comparable to the mean building height.
[Huq and Franzese (2013)] use the simple simple vertically-reflected Gaussian plume model presented by [Franzese and Huq (2001)], which was applied to study dispersion above the canopies of four cities. The mean concentration field $\bar{c}$ of a passive tracer emitted from a ground-level continuous source ($y = z = 0$) is approximated

by the vertically reflected Gaussian formula:

$$\overline{c}(t,x,z) = \frac{Q}{U\pi\sigma_y(t)\sigma_z(t)} exp\left(-\frac{y^2}{2\sigma_y^2} - \frac{z^2}{2\sigma_z^2}\right) \tag{7.4.2}$$

The transverse dispersion coefficient σ_y is calculated using [Taylor (1921)] theory, assuming horizontally homogeneous turbulence. The turbulence diffusion analysis of [Taylor (1921)] gives linear plume growth for $t < T_L$ (e.g., in the near field) and parabolic growth for $t > T_L$ (e.g., in the far field). The far field parabolic formulation corresponds to the configuration of a plume larger than the turbulence length scale. Inside the canopy the turbulence length scales are comparable to the lateral spacing of the building and to their height. Since in their study they focus on the near field below canopy dispersion, the plume does not grow larger than the turbulence length scales, and only the near field approximation of [Taylor (1921)] formula is needed:

$$\sigma_y^2 = \sigma_{y0}^2 + \sigma_v^2 t^2 \tag{7.4.3}$$

where σ_{y0} is the plume standard deviation at the source and σ_v^2 the variance of the Lagrangian transverse velocity.
The vertical dispersion coefficient σ_z is defined for ground level source in neutral atmosphere as:

$$\sigma_z^2 = \sigma_{z0}^2 + b^2\sigma_w^2 t^2 \tag{7.4.4}$$

where σ_{z0} is the plume vertical standard deviation at the source and b (set to $b = 1$) in an empirical constant. The values of U, σ_v and σ_w in the [Huq and Franzese (2013)] model are calculated as:

- Equation 7.4.3 is written as $\sigma_y^2 = \sigma_{y0}^2 + \frac{\sigma_v}{U}^2 x^2$ and the ratio $frac\sigma_v U$ is obtained by best fit to experimental data of σ_y which are measured at different distances x.
- The relationship $\sigma_w = \frac{2}{3}\sigma_v$ is assumed in accord with field measurements and equation 7.4.4 become $\sigma_z^2 = \sigma_{z0}^2 + \frac{4}{9}\frac{\sigma_v}{U}^2 x^2$.
- U is estimated by best fit of equation 7.4.2 to the measured concentrations.

Values of quantities used in the Gaussian model and for scaling the data are summarized in the table 7.1.

In the application of the [Cassiani and Giostra (2002)] method for evaluating the barycentre PDF I choose as mean field input the Gaussian model of equation 7.4.2. This assumption removes the need for SPM and makes the FPM simple and very fast to compute. Further, I use [Franzese (2003)] expression 7.3.9 for $p_z r$. Figure 7.8 shows the growth rate of $\frac{\sigma_z}{L_z}$ as a function on a non-dimensional distance $\frac{x}{UT_w}$ evaluated from FPM along with the Gaussian model and experimental data by [Huq and Franzese (2013)]. The FPM compares well with the [Huq and Franzese (2013)] results. The figure shows the linear plume growth according with equation 7.4.4 and the curves approach the source size as x tends to zero as expected. The difference between FPM and the Gaussian model in the far field is justified by 7.4.4 that contains only the near field (but not the far field) approximation of [Taylor (1921)] theory. The evolution of mean concentration, non-dimensionalized as $\frac{\bar{c}UL_zL_y}{Q}$ with the scaled distance from the source $\frac{x}{UT}$ with $T = \sqrt{T_w T_y}$, is plotted in figure 7.9. Again, the FPM agrees well with both the Guassian mdoel and data of [Huq and Franzese (2013)]. The figure shows that two models curves follow the -2 power law decay of concentration with distance from the source. I remark that the use of the Guassian model as input of the FPM allows to evaluate the evolution of the of the concentration standard deviation without using SPM. The normalised standard deviation $\frac{\sigma_c}{\bar{c}(0)}$ along with the scaled distance $\frac{x}{B}$ from the source of the normalised standard deviation (plotted in figure 7.10). Again, the fluctuating plume fits well with the water tunnel data ([Huq (2012)]). The use of the constant values of 7.1 for the turbulence parameter instead of the measured profiles of U, σ_w, σ_u and $\overline{uw}$ provided by [Huq and Franzese (2013)] is a simplification for both the first and the second moment. In order to include them, I may use a single particle model for inhomoneneous turbulence as mean field input. It would allow to take in account for the turbulence inhomogeneity. Nevertheless the purpose for this case is achieved. In fact, I can show good results in 7.10 for the second moment of concentration using only the mean field of 7.9 and evaluated in few seconds. The evaluation of third and fourth order moments concentration is not presented because of the lack of experimental data available.

$\frac{H}{w_b}$	Q	σ_0	H	U_∞	σ_w	σ_v	T_w	T_v	L_z	L_y	U_b	U
0.25	2.18	0.50	5.00	7.80	0.47	0.70	1.07	0.71	5.00	5.00	5.20	5.20
1	1.40	0.20	3.20	9.40	0.21	0.31	1.55	0.56	3.20	1.75	5.20	2.70
3	1.40	0.20	9.60	11.00	0.15	0.22	6.43	0.78	9.60	1.75	7.70	2.80

Table 7.1: Aspect ratios A_r, release rate $Q(cm^3s^{-1})$, source size $\sigma_{y0} = \sigma_{z0} = \sigma_0(cm)$, building height $H(cm)$, free-stream velocity $U_\infty(cms^{-1})$, vertical and transverse velocity variances $\sigma_w^2(cm^2)$ and $\sigma_v^2(cm^2)$, vertical and transverse time scale $T_w(s)$ and $T_v(s)$, length scales $L_z(cm)$ and $L_y(cm)$, rooftop level wind speed $U_b(cms^{-1})$, mean wind $U(cms^{-1})$

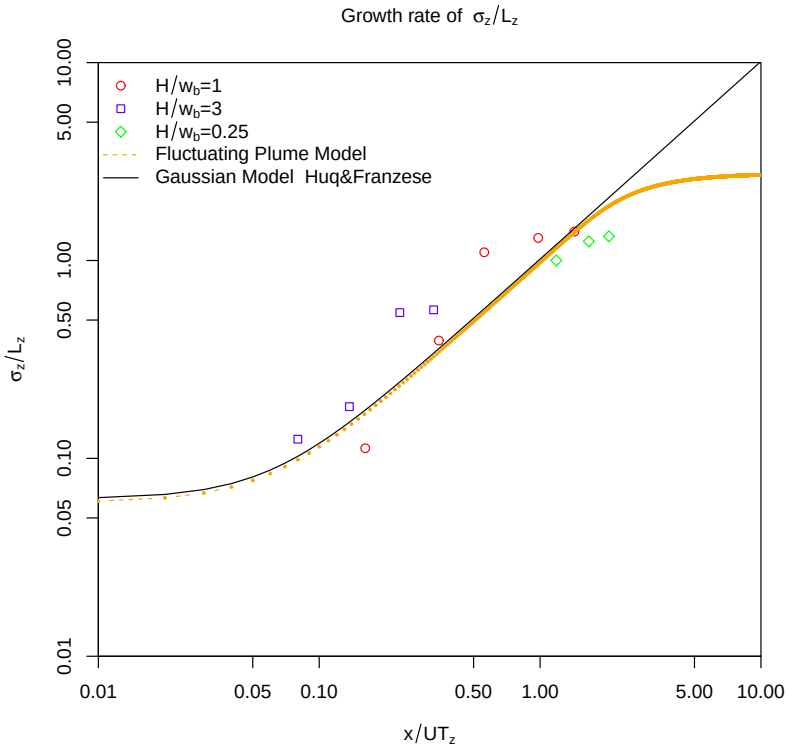

Figure 7.8: Growth rate of non-dimensional vertical standard deviation at $y = 0$ function of the non-dimensional distance from the source: comparison among the proposed FPM, the Gaussian model and the experimental data of [Huq and Franzese (2013)].

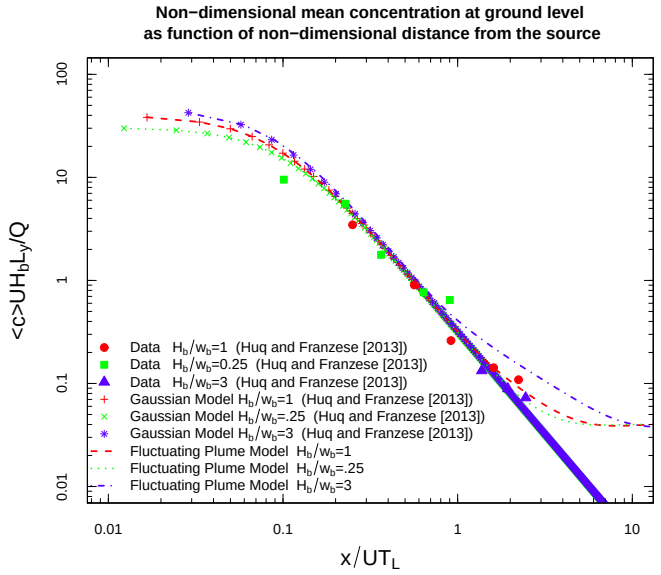

Figure 7.9: Non-dimensional mean concentration at the ground, at centreline of the canopy as function of non-dimensional distances from the source in comparison with the Gaussian model and the water tunnel data of [Huq and Franzese (2013)]

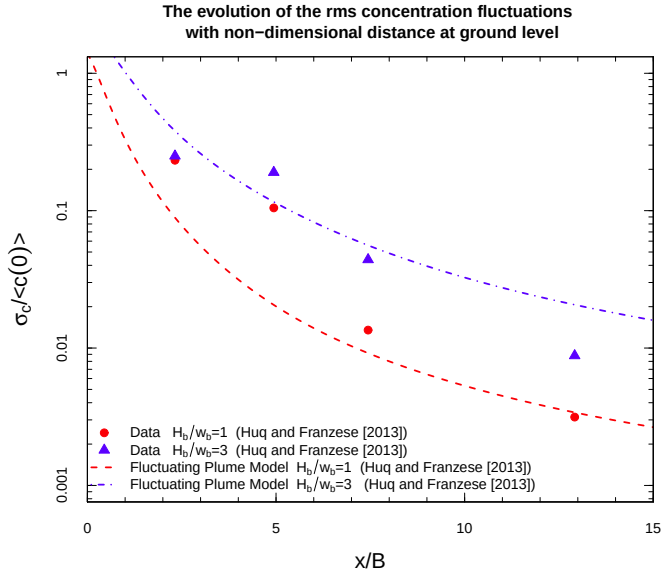

Figure 7.10: Non-dimensional root mean square concentration at the ground, at centreline of the canopy as function of non-dimensional distance from the source in comparison with the water tunnel data of [Huq (2012)]

7.4.3 Wind tunnel boundary layer

I take advantage of recent wind tunnel experiments of [Nironi et al. (2013)] and [Nironi (2013)]. I test again the reliability of the FPM in estimating the concentration moments of a passive tracer in neutral boundary layer. [Nironi (2013)] experimental data providing a detailed description of the concentration and of the velocity statistics and hence of the evolution of a fluctuating passive pollutant within the turbulent boundary layer. [Nironi (2013)] experimental data extend the popular study of [Fackrell and Robins (1982a)] about concentration fluctuations and fluxes from point sources by including measurements of concentration skewness and kurtosis. The data set is completed by an exhaustive information on both the temporal and spatial structure of the flow which is not common. Therefore I choose [Nironi (2013)] experimental mean concentration field as input for the [Cassiani and Giostra (2002)] calculation for the barycentre PDF in my FPM. I aim to evaluate the first moments of concentration given only the experiemntal field. Until now, I considered two simple models: a SPM in homogeneous turbulence in subsection 7.4.1 and a Gaussian model in subsection 7.4.2. Here the information on both the temporal and spatial structure of the flow would me to carry out a detailed SPM for inhomogenoeus turbulence. In particular [Nironi (2013)] data include one-point velocity statistics, two-points spatial correlations, integral length scales, spectra, turbulent kinetic energy budget, turbulent diffusivities, vertical and transversal profiles of first four moments of concentration PDF at several distances downwind. The full experimental data set is available on the website `http://www.ec-lyon.fr/`.
In order to apply the offline version of the FPM I started by applying equation 7.3.3 to the mean concentration field of [Nironi (2013)] to get the vertical position PDF p_z. Then I get the barycentre PDF p_{zm} from equation 7.3.9 by using [Cassiani and Giostra (2002)] liner transformation 7.3.7. Equation 7.3.9 contains the relative variance σ_{zr} that has to be parameterised as in equation 7.2.10 along with the relative part of the motion described by the PDF p_{zr} of equation 7.2.10. All the parameters I need for calculating σ_{zr} and p_{zr} is provided by [Nironi (2013)] data or can be evaluated from it. In figure 7.11 I plotted the non-dimensional vertical profiles of mean longitudinal velocity U, of TKE dissipation rate ϵ and of root mean square of the velocity components σ_u, σ_v and σ_w from which I evualated the parameters in the FPM. Figure 7.11 provide as well the vertical plume spread σ_z from experimental data that I use in applying equation 7.3.9. In figure 7.11, δ is the boundary layer depth and u_f is the friction velocity. The source is located at $z_s/\delta = 0.19$ and the source diameter is

$d_s/\delta = 0.00375$.
The reliability of the FPM is tested against the experimental measurements of mean concentration in Figure 7.12 (the two plot above) at various distances from the source. I underline the experimental data of mean field is the input of the FPM. Then I evaluate both the first and the higher moments of concentration by using equations 7.2.7 and 7.3.12. The two plots below in figure 7.12 show the comparasion between the model and the data for the standard deviation of concentration at the same downwind distance. Figure 7.13 show the vertical profiles of non-dimensional third (above) and fourth (below) moments of concentration at various distances downwind. Central concentration moments up to the fourth order are related to the moments $\overline{c^n}$ about 0 by means of the following relations:

$$\begin{aligned} m_1 &= C = \overline{c^1} \\ m_2 &= \sigma_c^2 = \overline{c^2} - C^2 \\ m_3 &= \overline{c^3} - 3\overline{c^2}C + 2C^3 \\ m_4 &= \overline{c^4} - 4\overline{c^3}C + 6\overline{c^2}C^2 - 3C^4 \end{aligned} \tag{7.4.5}$$

and then I considered the ith root of the moments, i.e. $M_i = \sqrt[i]{m_i}$, so that all the statistics plotted in the figures have the dimension of a concentration. The first comment about the figures of concentration statistics is that, for all the four moments, the FPM works better at the distance $x/\delta = 1.25$ from the source i.e. for the lines plotted in black in the figures. This is not casual. In effect I choose all the values in the parameterisation for the relative part, and so for $\sigma_z r$, p_{zr} and i_{cr}, giving the better agreement with the data at the downwind distance $x/\delta = 1.25$. The choice of $x/\delta = 1.25$ as reference distance from the source is not arbitrary. In fact by choosing larger downwind distance, the comparsion near the source get worse and, vice versa, if I choose smaller distance, the comparison deteriorate in the far field. Hence I can hypothesise the x-dependence of the relative part in a FPM. This may be primarily due to the parameters i_{cr0} and ζ in the [Gailis et al. (2007)] equation 7.2.11 for i_{cr}. In particular i_{cr} may be depend on spatial coordinates not only in the vertical direction but also in the downwind distance x, and so on the time.
Furthermore the comparison deteriorates with the rise of the order of the concentration moments. This is expected as the higher order statistics become very sensitive to the initial condition and a small change in the values of the parameterisation of FPM relative part can lead to great difference in statistics, especially in third and fourth moments.

Furthermore I highlight that all the information I used for parameterising p_{zr}, σ_{zr} and i_{cr} derive from a mean field that obviously can't exhaustively describe the concentration fluctuations. However the figures 7.12 shows that the FPM is able to reproduce well the first two moments of concentration. In figure 7.13 the FPM fits quite wellhe third and the fourth moments of [Nironi (2013)], although the comparison is not good as in case of the first two momets. In figure 7.13 is noticeable as well that the worst agreement is for the smallest distance from the source $x/\delta = 0.003125$, i.e. for the blue lines. First, it may due to the choiche of values for the relative part parameters that better fit the distance $x/\delta = 1.25$. Secondly, it may due to the effect of source size. In fact, in a FPM the effect of source size enters only in the equation for σ_{zr} and $p_z r$ whereas, for instance in a SPM, the source size effects can be included in the release of the particles.
I finally remark that all the statistics evaluated by the FPM derive exclusively from an experimental data and the need for a simultaneous Lagragian model is relaxed. Nevertheless this offline FPM give results comparable to the other FPM version without any coupling with Lagragian modelling.

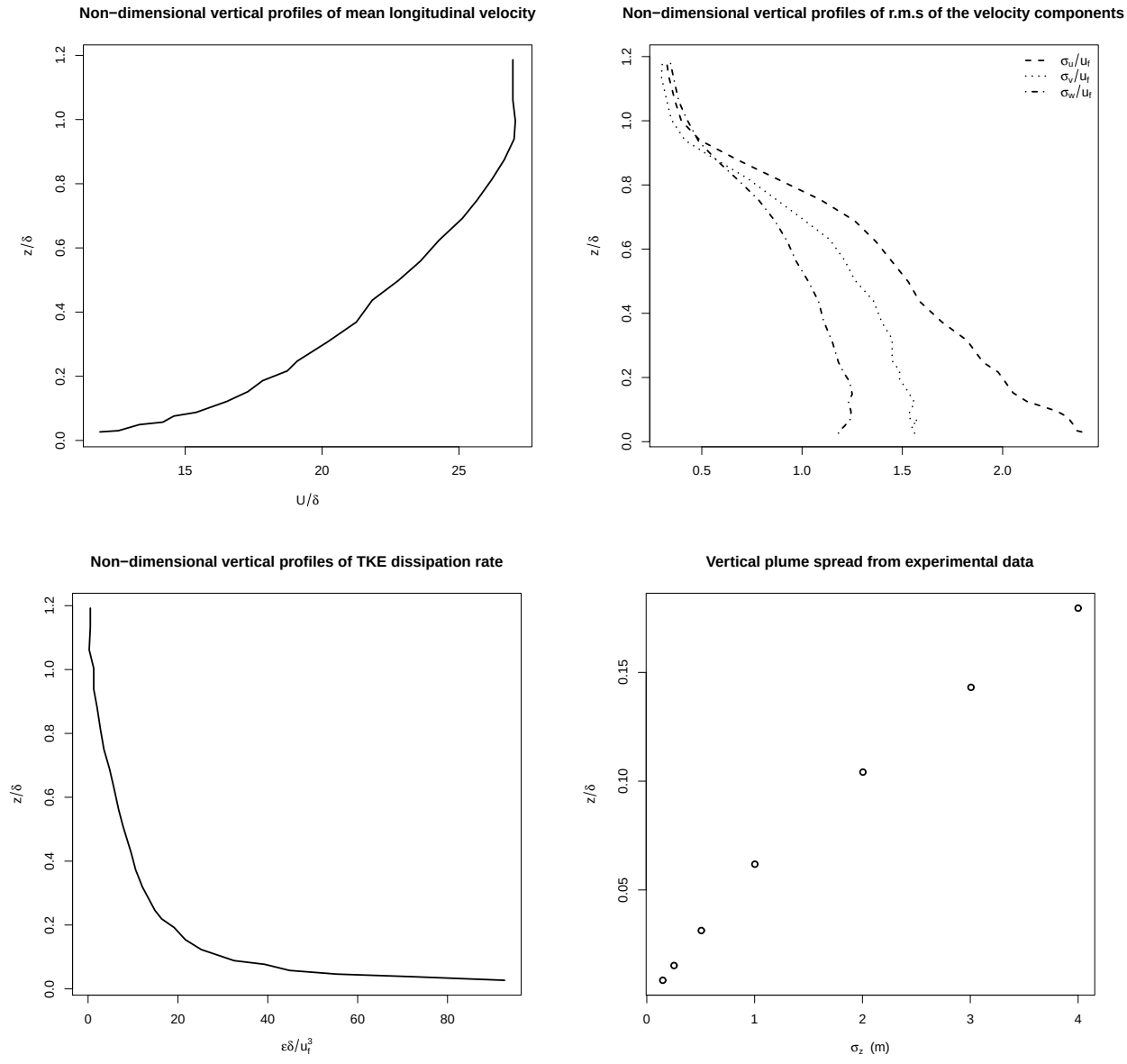

Figure 7.11: Non-dimensional vertical profiles of mean longitudinal velocity U, TKE dissipation rate ϵ, root mean square of the velocity components σ_u, σ_v and σ_w and vertical plume spread σ_z from experimental data. δ is the boundary layer depth and u_f is the friction velocity.

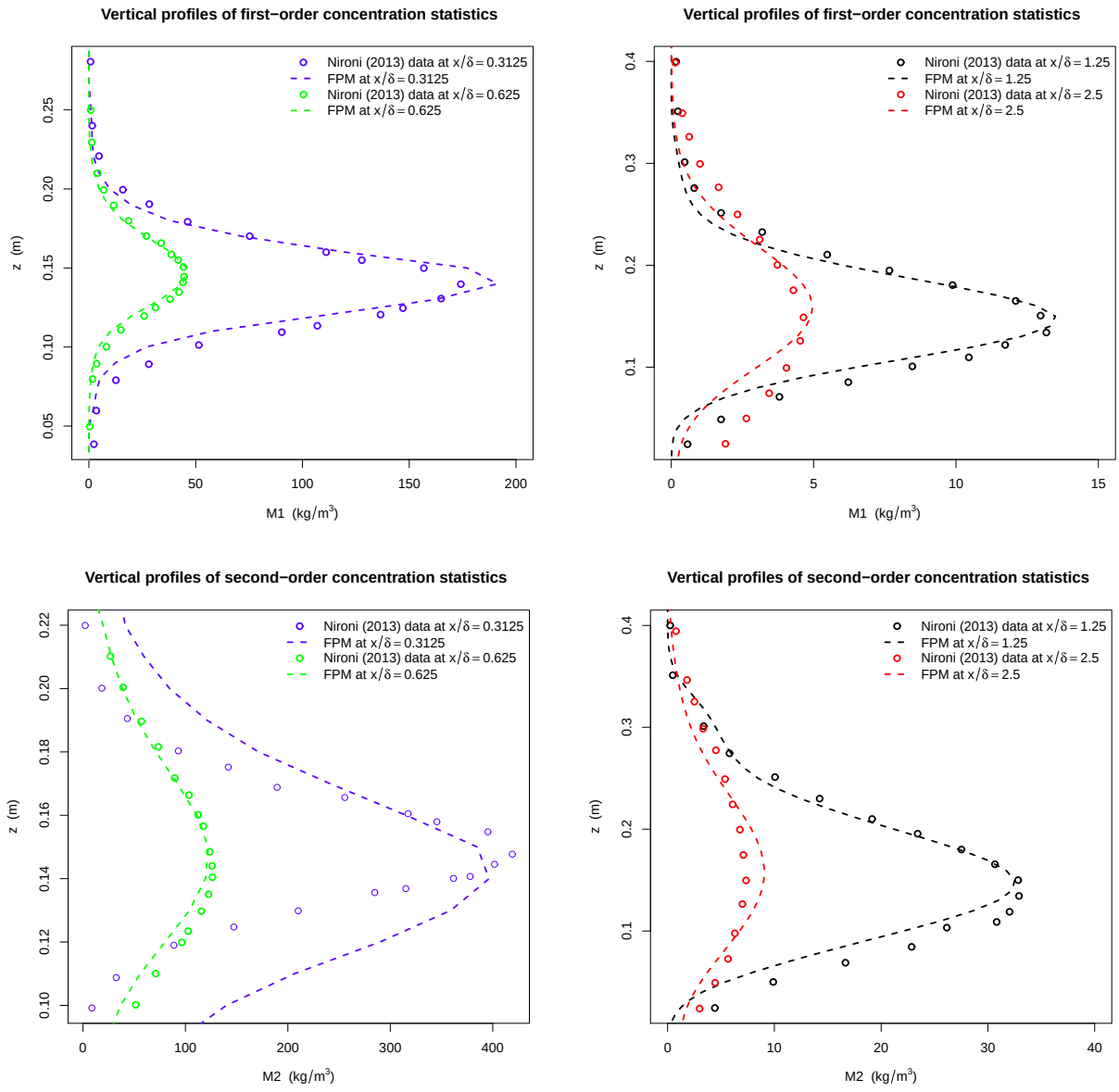

Figure 7.12: Vertical profiles of concentration mean (above) and standard deviation (below) at various distances downwind-

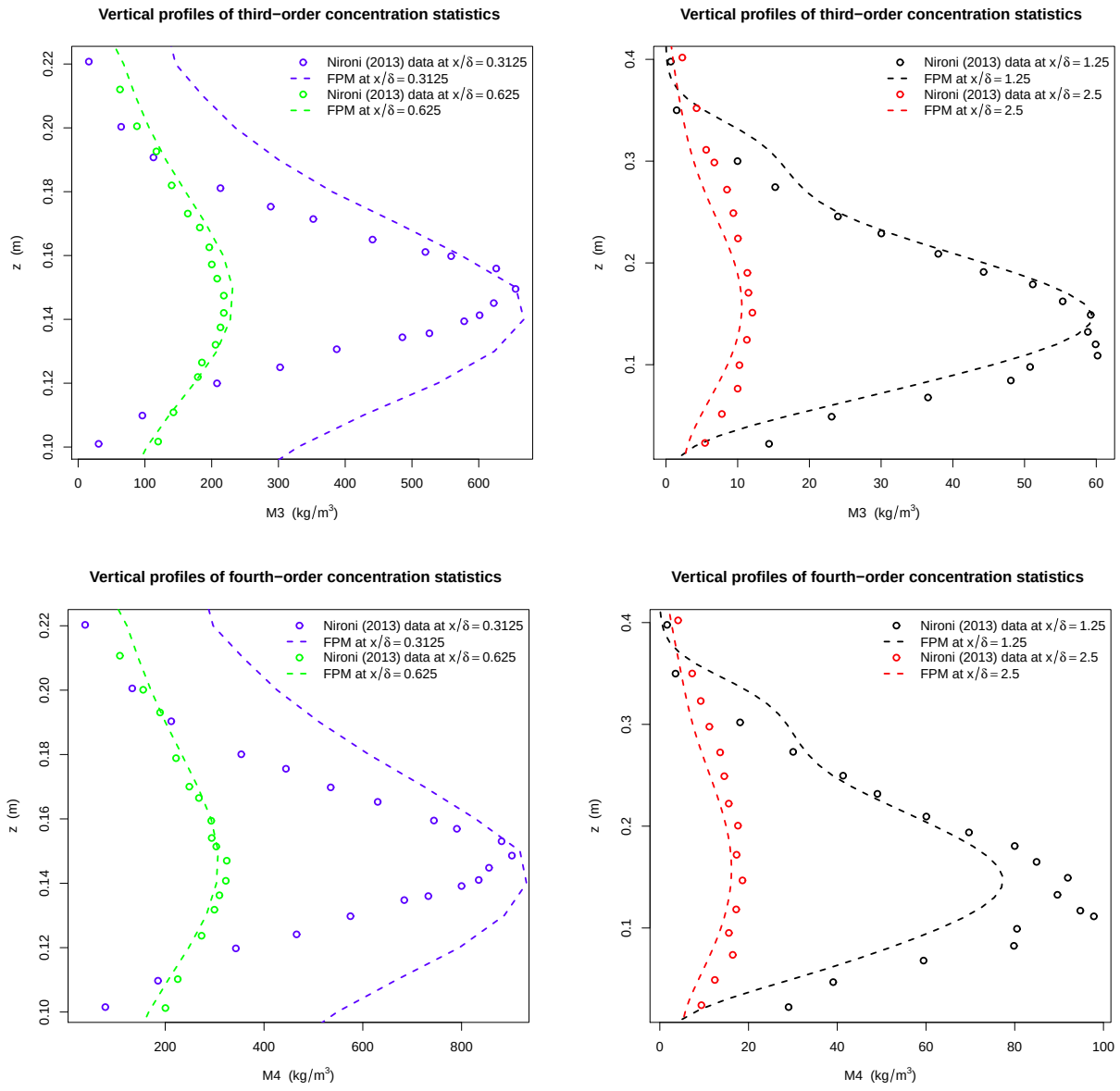

Figure 7.13: Vertical profiles of third (above) and fourth (below) moments of concentration at various distances downwind.

Conclusion

Two Lagrangian modelling approaches have been adopted to describe the role played by the fluctuations of active and passive scalar, respectively.

For the case of active scalars I introduced the effect of temperature fluctuations in a buoyant plume rise. I have constructed a hybrid Lagrangian stochastic model of buoyant plume rise that includes temperature fluctuations by combining coupled stochastic differential equations for vertical velocity and temperature with a classical plume model of buoyant plume rise in a crossflow. The model takes in account for the turbulence generated by the plume itself allowing the interaction of temperature and velocity fluctuations to generate the observed spread through the introduction of a SDE for the temperature and a $w - \vartheta$ coupling term in the SDE for w.

The model shows qualitatively a good behaviour in the idealised case of homogeneous turbulence. In particular the results suggest that the spread of the plume is much larger including temperature fluctuations and that this effect become more important as the intensity of the crossflow increases. However θ' depends weakly on the intensity of the crossflow. In fact, ϑ' doesn't depend on w or U, only on $\overline{w}$, hence ϑ' is expected to have the same order of magnitude for all the cases of intensity of the crossflow at the same height. Hence ϑ' makes a greater (relative) contribution to the SDE for w' through the coupling term $\frac{g\theta'}{\theta_0}$ than in the SDE for θ'.

Then the model is compared to the LES of [Devenish and Edwards (2009)] and [Devenish et al. (2010b)]. While some aspects of the formulation are not rigorous, results generated by the model compare reasonably well with LES results. This is true both for LES plumes in a linearly stratified environment and the realistic case of the plume generated by the explosion and fire at the Buncefield oil depot in 2005 which was previously compared with observations. In the former case, the agreement between the model and the LES results deteriorated as the ambient velocity became small ($\tilde{U} \ll 1$). The reasons for this are not clear and the behaviour of buoyant plumes in a weak crosswind merits further attention. In general, the model with temperature fluctuations exhibits a greater spread in the scalar concentration than the model without temperature fluctuations though the difference is not large. Larger differences can be observed in higher order statistics as may be expected. There is some uncertainty over the value of γ and while its range seems reasonably constrained, our results have shown that better agreement with the LES results can be obtained by varying γ within the range $0 \leq \gamma \leq 0.5$. However, arguably the best overall agreement with the LES statistics is obtained with $\gamma = 0.5$. More accurate data on buoyant plumes in a crossflow, both from experiments and numerical simulation, might help constrain the value further and elucidate any functional relationship

with wind speed that may exist.
For the case of passive scalars I developed a version completely offline of the FPM, without need for a coupled LSM, but just requiring a mean field as input. Moreover, the model is independent of the method for calculating the mean field that can be evaluated both from experiments and models. Following the fluctuating plume approaches proposed by [Luhar et al. (2000)], [Cassiani and Giostra (2002)], [Franzese (2003)] and [Mortarini et al. (2009)], I developed a method to compute the higher order concentration moments, given a mean concentration field. The evaluation of concentration fluctuations plays a crucial role in a great number of environmental issues: prediction of air pollution, simulation of chemical reactions of pollutants in the atmosphere (e.g. Nox and O3), analysis of turbulent combustion and estimation of odour threshold. In particular in recent years, considerable attention has been focused on the prediction of the PDFs of passive scalar concentration downwind a source of pollutant in the turbulent boundary layer. This is due to an increased interest in environmental problems, a more strict regulation about emissions in the atmosphere, the risk assessment of hazardous releases of toxic or flammable substances.

The presented fluctuating plume model puts together the more favourable features of the existing versions, resulting faster and simpler than the precedent methods. The choice of [Cassiani and Giostra (2002)] approach to evaluate the meandering barycentre part removes the need for the knowledge of the trajectories to compute the high order concentration fields. In fact, I underline again [Cassiani and Giostra (2002)] generalisation does not require any trajectories, but only a mean field concentration input. The requested mean concentration field can be obtained either from models or from experiments. Hence, it is possible to choice the most suitable method to evaluate the mean field, as a simple and fast model, e.g. a Gaussian model, or as a more complicated and efficient model, e.g. a single particle model, depending on the class of turbulence investigated. The parameterisation of relative motion is established on the analytical expressions producing the best agreement with the experimental data, i.e. [Gailis et al. (2007)] height-dependent formula for the relative concentration fluctuations. The model can be easily adapted to different classes of turbulence modifying the mean field input data and the parameterization of relative part. After a positive validation in homogeneous turbulence, the model is applied and compared to two neutrally stratified boundary layers, a canopy layer simulated in a

water-tunnel by [Huq and Franzese (2013)] and a new wind tunnel experiments taken by [Nironi (2013)] and [Nironi et al. (2013)]. The comparison with experimental data shows an overall good agreement both in all the cases. I presented the validation in homogeneous and isotropic turbulence and application to [Huq and Franzese (2013)] data during 15th International Conference on Harmonisation within Atmospheric Dispersion Modelling for Regulatory in Madrid (May 6-9, 2013) and results are published in [Bisignano et al. (2014)].The presented procedure is applied in the vertical direction but can be easily adapted for the crosswind meandering in the case in which it is not possible to find a simple analytical solution. I want to highlight that in the simulation of [Nironi (2013)] data I used as input the experimetal mean field provided by the author, whereas in the simulation of [Luhar et al. (2000)] data I considered a Gaussian model as input for FPM. In both the cases, the FPM is able to take in account for the turbulence inhomogenityies through the parameterisation of relative part of FPM and the low computational time demand makes the model suitable for practical applications considering that it is able to evaluate higher order concentration moments in few seconds on a standard computer.
I conclude noticing that he central thread which run through all this thesis is Lagrangian modelling. It is the natural and most powerful means to describe many interesting atmospheric processes involving both active and passive scalars. With the aid of LSM, better strategies for many environmental issues can be developed in future.

Appendix A

Although the use of the equation 7.2.9 for p_{zr} provides good overall agreement with the experiments and it is used through this thesis, a skewed PDF obtained as the sum of two reflected Gaussian PDFs ([Luhar et al. (2000)]) and especially suited for skewed turbulence can be also used, e.g. in the case of convective boundary layer (CBL) or highly asymmetrical canopies.

$$p_{zr} = \sum_{j=1}^{2} \sum_{k=-N}^{N} \frac{a_j}{\sqrt{2\pi}\sigma_j} \left[e^{\left(-\frac{z-z_m-2kz_i-\overline{z_i}}{}\right)} + e^{\left(-\frac{-z-z_m-2kz_i-\overline{z_i}}{}\right)} \right]$$

where

$$\overline{z_1} = \frac{S_r f \sigma_1}{|S_r|}$$

$$\overline{z_2} = \frac{S_r f \sigma_2}{|S_r|}$$

$$\sigma_1 = \sigma_{zr} \sqrt{a_2 / \left[a_1 (1 + f^2)\right]}$$

$$\sigma_2 = \sigma_{zr} \sqrt{a_1 / \left[a_2 (1 + f^2)\right]}$$

$$a_1 = \frac{1 - \sqrt{\frac{r}{4+r}}}{2} = 1 - a_2$$

$$r = \frac{(1 + f^2)^3 S_r^2}{1 + f^2)^2 f^2}$$

$$f = \frac{2}{3|S_r|^{\frac{1}{3}}}$$

where S_r ins the skewness of relative position. [Luhar et al. (2000)] assume that:

$$\overline{z'^3(t)} = \overline{z_m'^3(t)} + \overline{z_r'^3(t)}$$

[Dosio and de Arellano (2006)] notice that in general $\overline{z'^3} = \overline{z_m'^3 + z_r'^3}$ despite the independece between relative part and meandering centroid. Hence the correct form for S_r [Dosio and de Arellano (2006)] is given by [Dosio and de Arellano (2006)]:

$$S_r = \frac{S}{\sigma_{zr}^3}\left[\left(\overline{z'^2}\right)^{3/2} - \left(\overline{z'^2} - \overline{z_m'^2}\right)^{3/2}\right]$$

where $S = \frac{\overline{z'^3}}{\overline{z'^2}^{372}}$ is the total skewness.

Appendix B

Here I show a mathematical proof for the expression assumed for the barycentre PDF:

$$p_{zm}\Delta_{zm} = p_z\Delta_z$$

Since p_{zm} and p_z are PDFs, the previous equation represents a sort of probability distribution conservation. To proof rigorously the equation I consider that z^i_m and z^i are two stochastic processes, and at fixed times, they are two random variables. In particular, at any instant, z^i_m can be considered as the result of application of [Cassiani and Giostra (2002)] linear transformation to z^i. A basic theorem about the functions of random variable state that assuming that the equation $y = g(x)$ has n roots $y = g(x_1), y = g(x_2), ..., y = g(x_n)$ at fixed y. Now I suppose that $\hat{x}$ is a random variable with a known PDF $f_x(x)$ e $\hat{y}$ a new random variable given by the application of the real function $g(x)$ to $\hat{x}$. Then the PDF of y, $f_y(y)$ is:

$$f_y(y) = \sum_{i=1}^{n} \frac{f_x(x_i)}{|g_x(x_i)|}$$

I assume now that, for instance the equation $y = g(x)$ has three roots. Then

$$f_y(y)dy = P\{y < \hat{y} < y + dy\}$$

It is now sufficient to find the values of x for which $y < x \leq y + dy\}$ and the probability that $\hat{x}$ in contained in this set. This set consists of the three following intervals:

$$x_1 < x < x_1 + dx_1$$

$$x_2 < x < x_2 + dx_2$$

$$x_3 < x < x_3 + dx_3$$

Where I supposed that $dx_1 > 0$ and $dx_3 > 0$ but $dx_2 < 0$. Then $P\{y < \hat{y} < y + dy\}$ is given by:

$$P\{x_1 < \hat{x} < x + dx_1\} + P\{x_2 + dx_2 < \hat{x} < x_2\} + P\{x_3 < \hat{x} < x + dx_3\}$$

Now given that:

$$P\{x_1 < \hat{x} < x + dx_1\} = f_x(x_1)dx_1$$
$$P\{x_2 + dx_2 < \hat{x} < x_2\} = f_x(x_2)dx_2$$
$$P\{x_3 < \hat{x} < x + dx_3\} = f_x(x_3)dx_3$$

with

$$dx_1 = \frac{dy}{g'(x_1)}$$
$$dx_3 = \frac{dy}{g'(x_3)}$$
$$dx_3 = \frac{dy}{g'(x_3)}$$

I can conclude that

$$f_y(y)dy = \frac{f_x(x_1)}{g'(x_1)} + \frac{f_x(x_2)}{|g'(x_2)|} + \frac{f_x(x_3)}{g'(x_3)}$$

By dividing by dy I get $f_y(y) = \sum_(i = 1)^n \frac{f_x(x_i)}{|g_x(x_i)|}$ as expected.
Now I focus on the of a linear $g(x)$.

$$\hat{y} = g(\hat{x}) = a\hat{x} + b$$
$$g'(x) = a$$

The equatio has one root: $x = \frac{y-b}{a}$, hence:

$$f_y(y) = \frac{1}{|a|} f_x(fracy - ba)$$

Now I apply this result to [Cassiani and Giostra (2002)] linear transformation. In this frame z_{mi} is a linear function of z_i, and p_{zm} is the PDF of z_{mi} and p_z the PDF of z_i. Then:

$$p_{zm} = \frac{1}{|a|} p_z$$

I notice now that $dz_m = adz$ from which $a = \frac{dz_m}{dz}$. By substiting this expression for a in $p_{zm} = \frac{1}{|a|} p_z$ I get $p_{zm}\Delta_{zm} = p_z\Delta_z$, i.e. the equation of [Cassiani and Giostra (2002)] for the barycentre PDF.
A physical justification for the validity of the [Cassiani and Giostra (2002)] linear transformation can be found on [Luhar et al. (2000)].

Bibliography

[Alessandrini et al. 1993] Alessandrini S, Ferrero E (2009) A hybrid Lagrangian-Eulerian particle model for reacting pollutant dispersion in non-homogeneous non- isotropic turbulence. Physica A 388:1375-1387.

[Alessandrini et al. (2013)] Alessandrini S, Ferrero E, Anfossi D (2013) A new Lagrangian method for modelling the buoyant plume rise. Atmos Environ 77:239-249.

[Anfossi et al. 1993] Anfossi D, Ferrero E, Brusasca G, Marzorati A, Tinarelli G (1993) A simple way to of computing buoyant plume rise in Lagrangian stochastic dispersion model. Atmos Environ 27A:1443-1451.

[Anfossi 2000] Anfossi D (2000) Jet plume rise description in Lagrangian stochastic models. ICFG Rapp Int No 414/2000 9 pp.

[Batchelor (1952)] Batchelor GK (1952) Diffusion in a field of homogeneous turbulence. The relative motion of particles. Proc Cam Phil Soc 48:345362.

[Biltoft (2001)] Biltoft CA (2001) Customer report for Mock Urban Setting Test. Report No. WDTC-FR-01-121 US Army Dugway Proving Ground,Dugway UT.

[Bisignano et al. (2014)] Bisignano A, Mortarini L, Ferrero E, Alessandrini S (2014) Analytical offline approach for concentration fluctuations and higher order concentration moments. Int J of Environment and Pollution Vol.55:58-66 No 1/2/3/4..

[Bisignano and Devenish (2015)] Bisignano A, Devenish B (2015) The effect of temperature fluctuations on the spread of a buoyant plume. Submitted to Boundary-Layer Meteorol

[Boffetta and Sokolov (2002)] Boffetta G, Sokolov IM (2002) Statistics of two-particle dispersion in two dimensional turbulence. Phys Rev Lett 88.

[Borgas and Sawford (1994)] Borgas MS, Sawford BL (1994) A family of stochastic models for particle dispersion in isotropic homogeneous stationary turbulence. J Fluid Mech 279:6999.

[Briggs (1975)] Briggs GA (1975) Plume rise predictions. In: Lectures on air pollution and environmental impact analyses, Workshop Proceedings, Boston Mass, American Meteorological Society.

[Briggs (1984)] Briggs GA (1984) Plume rise and buoyancy effects. In: Randerson D (ed), Atmospheric science and power production, Office of Research, US Department of Energy, Washington, 327-366.

[Cassiani and Giostra (2002)] Cassiani M, Giostra U (2002) A simple and fast model to compute concentration moments in a convective boundary layer. Atmos Environ 36(30):47174724.

[Cassiani et al (2005a)] Cassiani M, Franzese P, Giostra U (2005a) A PDF micromixing model of dispersion for atmospheric flow Part I: development of the model, application to homogeneous turbulence and to neutral boundary layer. Atmos Environ 39(8):14571469

[Cassiani et al (2005b)] Cassiani M, Franzese P, Giostra U (2005b) A PDF micromixing model of dispersion for atmospheric flow. Part II: application to convective boundary layer. Atmos Environ 39(8):14711479

[Cassiani et al (2005c)] Cassiani M,RadicchicA,GiostracU (2005c) Probability density functionmodelling of concentration fluctuation in and above a canopy layer. Agric For Meteorol 133:153165

[Cassiani (2012)] Cassiani M. (2012) The volumetric particle approach for concentration fluctuations and chemical reactions in lagrangian particle and particle-grid models. Boundary-Layer Meteorology, 146:207233.

[Cogan (1985)] Cogan JL (1985) Monte Carlo simulation of a buoyant dispersion. Atmos Environ 19:867:878

[Das and Durbin (2005)] Das SK, Durbin PA (2005) A Lagrangian stochastic model for dispersion in stratified turbulence. Phys Fluids 17:025109

[Das and Durbin (2007)] Das SK, Durbin PA (2007) Prediction of atmospheric dispersion of pollutants in an airport environment. Atmos Env 41:1328-1341

[Devenish and Edwards (2009)] Devenish BJ, Edwards JM (2009) Large-eddy simulation of the plume generated by the fire at the Buncefield oil depot in December 2005. Proc R Soc A 465:397-419

[Devenish et al. (2010a)] Devenish BJ, Rooney GG, Thomson DJ (2010a) Large-eddy simulation of a buoyant plume in uniform and stably stratified environments. J Fluid Mech 652:75-103

[Devenish et al. (2010b)] Devenish BJ, Rooney GG, Webster HN, Thomson DJ (2010b) The entrainment rate for buoyant plumes in a crossflow. Boundary-Layer Meteorol 134:411-439

[Dosio and de Arellano (2006)] Dosio A, JVG de Arellano (2006) Statistics of absolute and relative dispersion in the atmospheric convective boundary layer: A large eddy simulation study. Journal of Atmospheric Science 63:12531272.

[Durbin (1980)] Durbin PA (1980) A stochastic model of two particle dispersion and concentration fluctuation in homogeneous turbulence. J Fluid Mech 100:279302.

[Fackrell and Robins (1982a)] Fackrell JE, Robins AG (1982). The effects of source size on concentration fluctuations in plumes. Boundary-Layer Meteorolo 22:335350.

[Fackrell and Robins (1982b)] Fackrell JE, Robins AG (1982). Concentration fluctuations and fluxes in plumes from point sources in a turbulent boundary layer. Journal Fluid Mechanics 117:126.

[Ferrero and Mortarini (2005)] Ferrero E, Mortarini L (2005) Concentration fluctuation and relative dispersion PDF. Atmos Env 39(11):21352143.

[Ferrero et al. (2012)] Ferrero E, Mortarini L, Alessandrini S, Lacagnina C (2012) Application of a Bivariate Gamma distribution for a chemically reacting plume in the atmosphere. Boundary-Layer Meteorol 147(1):123137.

[Finardi et al. (2001)] Finardi S, Tinarelli G, Nanni A, Anfossi D, Trini Castelli S (2001) In situ diagnostic or nested prognostic meteorological models to drive dispersion simulations in complex area: a comparison in real application. Air

Pollution Modelling and its Applications XIV, Grying SE and Schiermeier FA eds, Kluwer Academic, Plenum Press, New York, 641-649

[Franzese (2003)] Franzese, P (2003) Lagrangian stochastic modelling of a fluctuating plume in the convective boundary layer. Atmos Environ 37(12):16911701.

[Franzese and Huq (2001)] Franzese P, Huq P (2011) Urban Dispersion Modelling and Experiments in the Daytime and Nighttime Atmosphere,. Boundary-Layer Meteorology 409:139-395.

[Gailis et al. (2007)] Gailis RM, Hill A, Yee E, Hilderman T (2007) Extension of a fluctuating plume model of tracer dispersion to a sheared boundary layer and to a large array of obstacles. Boundary-Layer Meteorology 122:577-607.

[Gifford (1959)] Gifford F. (1959) Statistical properties of a fluctuating plume dispersion model. Advances in Geophysics, 6,117137

[Heinz and van Dop (1999)] Heinz S, van Dop H (1999) Buoyant plume rise described by a Lagrangian turbulence model. Atmos Environ 33:2031-2043

[Hoult et al. (1969)] Hoult DP, Fay JA, Forney LJ (1969) A theory of plume rise compared with field observations. J Air Pollut Control Assoc 19:585-590

[Hoult and Weil (1972)] Hoult DP, Weil JC (1972) Turbulent plume in a laminar cross flow. Atmos Environ 6:513-531

[Huq (2012)] Huq, P. (2012) Personal communication, 30 May 2012.

[Huq and Franzese (2013)] Huq P, Franzese P (2013) Measurements of turbulence and dispersion in three idealized urban canopies with different aspect ratios and comparisons with a Gaussian plume model. Boundary-Layer Meteorol 147(1):103121.

[Hurley and Physick (1993)] Hurley PJ, Physick W (1993) Lagrangian particle modelling of buoyant point source: plume rise and entrapment under convective conditions. Atmos Environ 27A:2579-1584.

[Hurley (1999)] Hurley PJ (1999) The Air Pollution Model (TAPM) version 1: technical description and examples. CSIRO Atmospheric Research Technical paper No 43.

[Kaplan and Dinar (1989)] Kaplan H, Dinar N (1989) Diffusion of an instantaneous cluster of particles in homogeneous turbulence field. J Fluid Mech 203:273287.

[Kaplan (2013)] (2103) Kaplan H. An estimation of a passive scalar variances using a one-particle lagrangian transport and diffusion model. Physica A: Statistical Mechanics and its applications, 393:19.

[Kolmogorov (1941)] Kolmogorov AN (1941) Dissipation of energy in a locally isotropic turbulence. C.R. Acad. Sci. URSS (in Russian), 32:141. (English translation in Proceedings of the Royal Society of London, Series A, 1991, 434:1517).

[Kurbanmuradov and Sabelfeld (1995)] Kurbanmuradov OA, Sabelfeld KK (1995) Stochastic Lagrangian models of relative dispersion of a pair of fluid particles in turbulent flows. Monte Carlo Meth Applic 1:101136.

[Monin and Yaglom (1971)] Monin A, Yaglom A (1971) Statistical fluid mechanics. Volume 1. MIT Press, Cambridge.

[Monin and Yaglom (1975)] Monin A, Yaglom A (1975) Statistical fluid mechanics. Volume 2. MIT Press, Cambridge.

[Luhar et al. (2000)] Luhar AK, Hibberd MF and Borgas M (2000) A skewed meandering-plume model for concentration statistics in the convective boundary layer. Atmospheric Environment 34:35993616.

[Luhar and Britter (1992)] Luhar AK, Britter RE (1992) Random walk modelling of buoyant-plume dispersion in the convective boundary layer. Atmos Environ 26A:1283-1298

[Macdonald and Ejim (2002)] Macdonald RW, Ejim CE (2002) Flow and Dispersion Data from a Hydraulic Simulation of the MUST Array. Thermal Fluids Report 20022003, University of Waterloo, Waterloo.

[Manor (2014)] Manor A. (2014) A stochastic single particle lagrangian model for the concentration fluctuation in a plume dispersing inside an urban canopy. Boundary-Layer Meteorology 150:327340.

[Marro et al. (2014)] Massimo M, Nironi C, Salizzoni P, Soulhac L (2014) A Lagrangian stochastic model for estimating the high order statistics of a fluctuating plume in the neutral boundary layer Int J of Environment and Pollution 54(2/3/4):233 - 241.

[Marro et al. (2014)] Marro M, Salizzoni P, Cierco FX, Korsakissok I, Danzi E, Soulhac L (2014) Plume rise and spread in buoyant releases from elevated sources in the lower atmosphere. Environ Fluid Mech (2014) 14:201-219,

[McCaffrey (1979)] McCaffrey BJ (1979) Purely buoyant diffusion flames: some experimental results. National Bureau of Standards NBSIR 79-1910.

[Monin and Yaglom (1975)] Monin AS, Yaglom AM (1975) Statistical Fluid Mechanics

[Mortarini et al. (2009)] Mortarini L, Franzese P, Ferrero E (2009) A fluctuating plume model for concentration fluctuations in a plant canopy. Atmos Env 43(4):921927.

[Morton et al. (1956)] Morton BR, Taylor G, Turner JS (1956) Turbulent gravitational convection from maintained and instantaneous sources. Proc R Soc A 234:1-23.

[Nironi (2013)] Nironi C (2013). Concentration fluctuations of a passive scalar in a turbulent boundary layer. PhD THESIS. Ecole Centrale de Lyon.

[Nironi et al. (2013)] Nironi C, Salizzoni P, Mjean P, Marro M, Soulhac L (2013) Pollutant concentration fluctuations in a neutral atmospheric boundary layer: a new detailed data set for the validation of dispersion models. 15th conference on Harmonisation within Atmospheric Dispersion Modelling for Regulatory Purposes, Madrid, Spain. In: Proceedings of the 15th International Conference on Harmonisation within Atmospheric Dispersion Modelling for Regulatory Purposes, Aarhus University Denmark H15-130.

[Pearson et al. (1983)] Pearson HJ, Puttock JS, Hunt JCR (1983) A statistical model of fluid-element motions and vertical diffusion in a homogeneous stratified turbulent flow. J Fluid Mech 129:219.

[Pope (2000)] Pope SB (2000) Turbulent flows. CUP, Cambridge, 771pp

[Priestley (1956)] Priestley CHB (1956) A working theory of the bent-over plume of hot gas. Quart J Roy Met Soc 89:165-176.

[Shimanuki and Nomura (1991)] Shimaunki A, Nomura Y (1991) Numerical simulation on instantaneous images of the smoke released from a chimney. J Met Soc Japan 69:187-196.

[Souto et al. (2001)] Souto MJ, Souto JA, Perez-Munuzuri V, Casares JJ, Bermudez JL (2001) A comparison of operational Lagrangian particle and adaptive puff models for plume dispersion forecasting. Atmos Environ 35:2349:2360.

[Sreenivasan (1996)] Sreenivasan KR (1996) The passive scalar spectrum and the Obukhov-Corrsin constant. Phys Fluids 8:189-196.

[Taylor (1921)] Taylor GI (1921) Diffusion by continuous movements. Proc London Math Soc, 20:196-211.

[Thomson (1987)] Thomson DJ (1987) Criteria for the selection of stochastic models of particle trajectories in turbulent flows. J Fluid Mech 180:529-556.

[Thomson (1990)] Thomson DJ (1990) A stochastic model for the motion of particle pairs in isotropic high-Reynolds number and its application to the problem of concentration variance. J Fluid Mech 210:113153.

[Tinarelli et al. (2000)] Tinarelli G, Anfossi D, Bider M, Trini Castelli S (2000) A new high performance version of the Lagrangian particle dispersion model SPRAY, some case studies. Air Pollution Modelling and its Applications XIII, Grying SE and Batchvarova E eds, Kluwer Academic, Plenum Press, New York, 499-507.

[van Dop (1992)] Van Dop D (1992) Buoyant plume rise in a Lagrangian framework. Atmos Env 26A:1335-1346.

[Webster and Thomson (2002)] Webster HN, Thomson DJ (2002) Validation of a Lagrangian model plume rise scheme using the Kincaid data set. Atmos Environ 36:5051-5062.

[Weil (1988)] Weil JC (1988) Plume rise. In: Venkatram A, Wyngaard JC (eds), Lectures on Air Pollution Modelling, American Meteorological Society, Boston, pp 119-166.

[Weil (1994)] Weil JC (1994) A hybrid Lagrangian dispersion model for elevated source in the convective boundary layer. Atmos Environ 28:3433-3448.

[Yee et al. (1994)] Yee E, Chan R, Kosteniuk PR, Chandler GM, Biltoft CA, Bowers JF (1994) Incorporation of internal fluctuations in a meandering plume model of concentration fluctuations. Boundary-Layer Meteorology 67:11-39.

[Yee and Wilson (2000)] Yee E, Wilson D (2000) A comparison of the detailed structure in dispersing tracer plumes measured in grid-generated turbulence with a meandering plume model incorporating internal fluctuations. Bound Layer Meteorol 94:253296.

[Yeung (2002)] Yeung PK (2002) Lagrangian investigations of turbulence. Ann Rev Fluid Mech 34:115-142.

[Zannetti and Al-Madani (1984)] Zannetti P, Al-Madani N (1984) Simulation of transformation, buoyancy and removal processes by Lagrangian particle methods. Proc of the 14th International Technical Meeting on Air Pollution Modelling and its Application, New York 733-744.

[1] Ecole Centrale de Lyon website, http://www.ec-lyon.fr/.

[2] Metoffice website, http://www.metoffice.gov.uk/.